MASTER'S THESIS

EXACT ZERO MODES IN COUPLED CHIRAL SYSTEMS

Author:
Adam Mielke

Supervisor:
Ass. Prof. Kim Splittorff

Submited:
July 29, 2016

NIELS BOHR INSTITUTE
FACULTY OF SCIENCE
UNIVERSITY OF COPENHAGEN

Abstract

We investigate the microscopic eigenvalue spectrum of two quenched chiral systems coupled in such a way that we preserve a common chiral symmetry. The coupling gives rise to a unique term in the lowest order effective Lagrangian and also links the topology of the two systems, which allows exact zero modes to cancel each other if they are of opposite chirality. The would-be zero modes spread out on either side of the origin as near-zero modes. For small coupling, the near-zero modes are distributed according to a finite size chiral random matrix model where the width scales as the inverse square root of the volume.

This is done for both the chiral unitary ensemble and the chiral orthogonal ensemble, and we consider the two coupled flavours in both two separate gauge fields and in the same gauge field.

We also introduce a random two-matrix model with the same coupled chiral symmetry. It agrees with the effective theory in the microscopic limit, both analytically and numerically, for all considered cases.

Acknowledgements

First and foremost, I would like to thank my supervisor, Ass. Prof. Kim Splittorff, with whom I have had many intriguing discussions, professional as well as personal. Thank you for the genuine interest you show your students in all aspects of life, and especially thank you for always making me feel welcome at your office, even at your most busy.

Credit is also due to Prof. Poul Henrik Damgaard, Prof. Karsten Flensberg, Esben Bork Hansen, and Jeroen Danon, who helped conceive the idea of a p-wave superconductors as coupled chOE random matrices, upon which this thesis is built.

A large thank you and a beer of equal size is in order for Anine Laura Borger, Carsten Fritzner Frøstrup, Gorm Ole Steffensen, Asbjørn Rasmussen, and Lucca Weis Kalckar for feedback on my manuscript.

I thank my fellow physicists at the office, Carsten Fritzner Frøstrup, Isak Buhl-Mortensen, and Kasper Engel Vardinghus for the times you helped me with my work and for the times you kept me from it. Both are needed in life.

I would also like to thank family and friends, who have very patiently listened to me explain the importance of symmetry. The interested questions were especially appreciated. I thank them for understanding my absence, even when present.

Adam Mielke
Niels Bohr Institute
University of Copenhagen
July 29, 2016

Contents

Chapter 1

Introduction

Because the Hamiltonian of a p-wave superconductor carrying Majorana fermions belongs to the symmetry class BDI (chiral orthogonal) [1, 2], it is possible that interactions between these Majorana fermions may be described as the coupling of two quenched chiral orthogonal ensembles, provided that coupling preserves a combined chiral symmetry.

The chiral orthogonal ensemble is well-described both in mathematical and high energy physics [3, 4, 7, 5, 8], which opens up the possibility of calculating any property uniquely determined by the symmetries of the solid state system with high energy techniques. This proposed connection between high energy and solid state physics was the motivation for considering the consequences of applying such a coupling to two chiral systems.

In this thesis, we lay the groundwork for treatment of coupled chiral ensembles by considering the effect of the coupling on the small eigenvalues and especially the topological eigenvalues in exact zero.

Chiral theories and chiral symmetry breaking has been studied in great detail in the low-energy regime of QCD [9, 10, 11, 12, 13]. The massless Lagrangian of QCD allows for separate transformations of left- and right-handed quark fields. The spontaneous breaking of this symmetry

$$SU_{\text{Left}}(N_f) \times SU_{\text{Right}}(N_f) \to SU_{\text{Vector}}(N_f) \tag{1.1}$$

where N_f is the number of quark flavours, gives rise to Goldstone modes [13]. As the symmetry is also broken explicitly, these modes are light rather than massless and therefore technically pseudo-Goldstone particles rather than proper ones. They are, however, significantly lighter than the rest of the composite particles, and this mass gap allows us to set up a low-energy effective theory in terms of these light pseudo-Goldstone modes only, see Figure 2.2 in Chapter 2.

In a quenched ensemble we have added a bosonic determinant with the same mass to cancel each fermionic determinant in the QCD partition function. In QCD, this approximation suppresses virtual quark loops [14], but still allows us to derive many aspects of QCD. In solid state physics, this is not an approximation, because the entries of the Hamiltonian, unlike the massless Dirac operator, are not weighted with the determinant of the entire operator. The quenched ensemble is also significantly simpler to treat numerically. For further discussion of the quenched approximation, see [14, 15, 16].

Our primary concern is the eigenvalue spectrum in and around zero, which is universal for any system that displays a spontaneous breaking of chiral symmetry [4, 7, 8, 10, 11, 12, 13, 17,

18, 19]. Because of this universality, we may calculate the spectrum in an effective low-energy theory if it breaks chiral symmetry the same way as the underlying theory.

In QCD, this study of chiral symmetry breaking through effective Lagrangians has also lead to calculation of propagators and loop diagrams of the aforementioned pseudo-Goldstone modes [9] and a greater understanding of the QCD chemical potential [20, 21, 22, 23], apart from the derivation of the microscopic eigenvalue spectrum. This microscopic is in turn connected to the spontaneous breaking of chiral symmetry [24].

The spectrum is obtained as follows: We start with the full, partially quenched partition function

$$Z(m,m') \quad = \quad \int dA \, \frac{\det\Big(-i\not{D}+m\Big)}{\det\Big(-i\not{D}+m'\Big)} \, e^{-S_{YM}(A)} \tag{1.2}$$

where $\not{D} = \gamma^\mu(\partial_\mu + A_\mu)$ is the massless Dirac operator, m and m' are the masses of quark and the bosonic ghost field respectively, $S_{YM}(A)$ is the Yang-Mills action, and A is the gauge field we integrate over. We may use this as a generating function for the quenched chiral condensate

$$\Sigma(m) = \frac{1}{V}\partial_m \ln Z(m,m')\big|_{m=m'} = \Big\langle \frac{1}{-i\not{D}+m} \Big\rangle. \tag{1.3}$$

The eigenvalue spectrum is finally obtained as the discontinuity across the imaginary axis of the quenched chiral condensate [11, 12]

$$\lim_{\epsilon\to 0}\big[\Sigma(i\lambda+\epsilon)-\Sigma(i\lambda-\epsilon)\big] = \Big\langle \delta(-i\not{D}+i\lambda)\Big\rangle = \sum_k \Big\langle \delta(\lambda-\lambda_k)\Big\rangle \equiv \rho(\lambda), \tag{1.4}$$

where λ_k are the eigenvalues of $\not{D}$. Calculating (1.2) is the challenging part, and this is where we use the effective field theory. Once we have an expression for (1.2), the rest is a straightforward calculation, although not necessarily simple. Note that we in QCD are interested in the eigenvalues of the massless Dirac operator $i\not{D}$, whereas we in solid state physics want the spectrum of the Hamiltonian H. The procedure is, however, the same.

The coupling should preserve a combined chiral symmetry of the two systems, so we construct an effective Lagrangian containing all possible terms that link left- and right-handed fields respectively of the two ensembles. There are of course an infinite amount of these terms, but, by establishing a counting scheme, we can consider the lowest order terms only, where there is a unique term to describe the chiral coupling. We work in a counting scheme that favours the light pseudo-Goldstone modes, which corresponds to the low-energy regime where the generating function can be calculated in its entirety [10, 12].

The numerical counterpart to these analytical techniques is random matrix theory. The study of random matrices and their eigenvalues originates in mathematical statistics, but has since found its applications in physics [5]. As with effective field theory, the basis of random matrix theory is the symmetries of the underlying theory. By creating a large amount of matrices with the given symmetries, we may find the universal part of the eigenvalue spectrum. The partition function of a chiral random matrix theory takes the form [5, 17, 25, 26, 27, 28]

$$Z^{n,\nu}(m) = \int dW P(WW^\dagger) \, \det{}^{N_f} \begin{pmatrix} m & iW \\ iW^\dagger & m \end{pmatrix} \tag{1.5}$$

where W are general $(n+\nu)\times n$ matrices, and ν is the number of exact zero modes. The choice of weight $P(WW^\dagger)$ is arbitrary in the microscopic limit $n\to\infty$ as long as it supports a non-zero density of eigenvalues around the origin [18].

As the microscopic eigenvalue density depends on the symmetries only, we can make a two-fold investigation of it; numerical and analytical. The chiral orthogonal ensemble (chOE), of which we wish to create a coupled version, corresponds to real entries in (1.5). In the language of effective field theory, complex entries (called the chiral unitary ensemble or chUE) correspond to the standard chiral symmetry break of QCD, seen in (2.17). The chiral orthogonal ensemble follows the pattern [7]

$$U(2N_f)\to Sp(2N_f) \tag{1.6}$$

where Sp is the symplectic group. This gives the orthogonal ensemble a larger broken group, which makes integration over the Goldstone manifold more complicated. We therefore develop much of our framework in the more simple case of the unitary ensemble, before we turn to the orthogonal one.

The main focus of this thesis is to analyse the effect on the exact zero modes of coupling two chiral ensembles to lowest order. The amount of these exact zero modes are equal to the absolute value of a topological invariant called the winding number [29], so, by analysing the zero modes, we implicitly see the combined topology of the coupled system. The eigenvalue density of two coupled unitary ensemble can be seen in Figure 6.2 in Chapter 6, where we run through different coupling strengths of the corresponding random matrix ensemble.

We there see what we show throughout this thesis: For zero coupling, the total density is merely the sum of the two single ensembles with the amount of exact zero modes preserved. For small, but non-zero, coupling, the exact modes are smeared out as near-zero modes if the zero modes are of opposite chirality. These would-be zero modes follow a well known distribution, namely that of finite size chiral random matrix ensemble (1.5) with a Gaussian weight. This may come as a surprise, as the finite ensemble, unlike the full coupled partition function, is not universal because of the arbitrary weight. The Gaussian weight is, however, a direct consequence of the quadratic nature of the unique coupling term and is therefore universal.

As the coupling strength increases, the topological modes become part of the bulk eigenvalues. In the strong coupling limit the coupled system behaves as a single, uncoupled system, but with $\lambda\to 2\lambda$. The most important result to take from this is that the total amount of exact zero modes is counted with sign, and, even to lowest order, any coupling of chiral systems that preserves a combined chiral symmetry will couple the topology of the two systems.

We apply the coupling to two very distinct cases. First we consider two separate single-flavour ensembles that are completely independent before the coupling, by which we mean that the partition function factorises. This also implies that they interact with two different gauge fields, and so they may have different topologies. Otherwise the ensembles are taken to be identical when averaged over gauge configurations.

We then consider an ensemble with an inbuilt two-flavour structure. Here we have the option of rotating the flavour basis, which gives rise to an extra symmetry that is only partially broken by coupling the two flavours. These two flavours are born in the same gauge field, which forces them to have the same topological charge. The aforementioned cancellation of topological zero modes can therefore only occur if we couple the left part of one flavour to the right part of the other. Although these two cases have different physical interpretations, the effect of the coupling on the microscopic eigenvalue spectrum is to a large extend the same.

Some differences between coupled chiral orthogonal ensembles and the superconductors carrying Majorana modes are still present. The most important distinction is that, in the superconductor, only the zero modes are Majorana modes, whereas as the bulk modes are regular Dirac modes [30]. This is not the case for the chiral orthogonal ensemble where all modes are Majorana. We therefore require a different approach. We briefly discuss alternative ways of treating the superconductor system in random matrix theory by adding a substructure to the matrices.

The thesis is organised as follows: First, in Chapter 2 we examine the relevant mathematics, including effective field theory, random matrices, and topological zero modes. In Chapter 3 we introduce the coupling and derive its properties from symmetry considerations. This is the groundwork for the calculation of the eigenvalue spectrum in Chapters 4 and 5. We finally compare these analytical results to numerics in Chapter 6 and summarise our conclusions in Chapter 7.

The chapter on the mathematical framework should be considered a review, while the new contribution is the treatment of coupled chiral systems with a coupling that preserves a combined chiral symmetry. The main results of this thesis have also been published in [31].

Chapter 2

Mathematical Framework

Let us begin by reviewing the relevant mathematics. This chapter should be considered a toolbox, which we in Chapter 3 and onwards apply to the coupled system.

We start out by going through the terminology and properties of symmetry. We then introduce low-energy effective field theory and discuss the role of exact zero modes. During most of the thesis, we will treat topology and the amount of exact zero modes as two sides of the same coin, but in Section 2.3 we give a short introduction to topology in QCD to show some of its origin. We then elaborate on the partition function's role as a generating function of the eigenvalue spectrum, which shall be our analytical stepping stone.

We also need the understanding of topology before turning to chiral random matrix theory, as we will calculate one topological sector at a time. These chiral random matrix ensembles also have a close relation to the ensembles of effective field theory, which we return to in Chapter 3. We use random matrices as the backbone of our numerical analysis in Chapter 6.

We finally compare Majorana modes in high energy physics and solid state physics with the intention of establishing a working model of the superconductor system that first inspired this coupled chiral system.

2.1 Symmetry

For the purpose of later discussions, let us begin by briefly reminding ourselves of the terminology and properties of symmetry. Similar discussions can be found in [32] or any other book on the subject (or on Wikipedia).

A symmetry is a transformation that leaves some quantity invariant. Since parts of a system are uniquely determined by symmetries and the breaking thereof, we can gain a lot of information through this analysis. We will consider invariances of the Lagrangian and partition function, and how they affect the microscopic eigenvalue spectrum.

Breaking of Symmetry

Let us consider two classic examples: The charged particle in a uniform magnetic field and the so-called Mexican hat potential. We look at these two systems, because they are good examples of explicit and spontaneous breaking of symmetry respectively.

Explicit Break: Consider the Hamiltonian of a 2D free particle with charge q

$$H_{free} = \frac{p^2}{2m}. \tag{2.1}$$

This is invariant under rotation

$$\begin{pmatrix} p_x \\ p_y \end{pmatrix} \to \begin{pmatrix} \cos(\phi) & -\sin(\phi) \\ \sin(\phi) & \cos(\phi) \end{pmatrix} \begin{pmatrix} p_x \\ p_y \end{pmatrix}. \tag{2.2}$$

If we apply a magnetic field

$$H_{mag} = \frac{p^2}{2m} + q\frac{\vec{p}}{m} \times \vec{B}, \tag{2.3}$$

we break this invariance. This is called an explicit break, because it changes the equations of motion. The explicit break will often remove degeneracies of the system. In this case, the spin degeneracy will be lifted. (We have not included the spin-part in (2.3), but it would be a term proportional to $\vec{S} \cdot \vec{B}$.)

Spontaneous Break: Consider a system, whose equations of motion have a symmetry that the ground state does not. This could be a ball sitting atop a rotationally invariant potential with a ground state further downhill, see Figure 2.1. This is called a spontaneous break, because the equations of motion are left unchanged. To investigate this mathematically, we make a small perturbation of the system and see if the ball remains stationary.

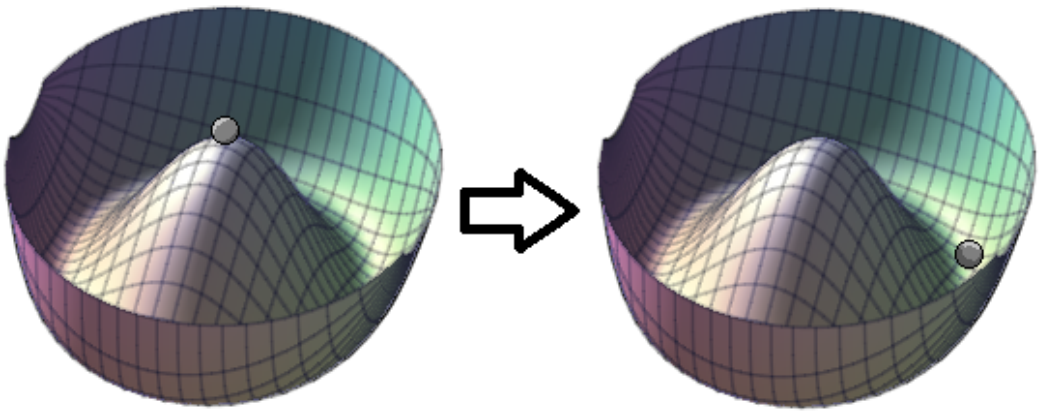

Figure 2.1: Example of a spontaneously broken symmetry. A ball in the Mexican hat potential where the midpoint is an unstable equilibrium. The equations of motion are rotationally invariant, but the ground state at the bottom of the well breaks this symmetry.

Nambu-Goldstone Theorem

The Nambu-Goldstone theorem states that if a system has a spontaneously broken continuous symmetry, there exists a massless mode for each broken generator [13]. By writing our theory in terms of these Goldstone modes, we may calculate results otherwise impossible in QCD.

The Goldstone modes can be viewed intuitively as the freedom to move along the bottom of the potential well in Figure 2.1. Mathematically speaking, this potential corresponds to a Lagrangian of the form[1]

$$\mathcal{L} = -\partial^\mu \phi^\dagger \partial_\mu \phi - \frac{1}{2} m^2 \phi^\dagger \phi - \frac{1}{4} g (\phi^\dagger \phi)^2 \tag{2.4}$$

where ϕ is a complex scalar field. This has an obvious global $U(1)$-symmetry

$$\phi \to e^{i\alpha} \phi. \tag{2.5}$$

Assuming m^2 to be negative, we have the right potential. The potential has the minimum

$$\phi(x) = \frac{1}{\sqrt{2}} v e^{i\theta} \quad , \quad v = \sqrt{\frac{4|m|^2}{g}} \tag{2.6}$$

where θ is an arbitrary phase.

If we use the parametrisation [33]

$$\phi(x) = \frac{1}{\sqrt{2}} (v + \rho(x)) e^{i\chi(x)/v}, \tag{2.7}$$

where ρ and χ are real fields, we get the Lagrangian

$$\mathcal{L} = -\partial^\mu \rho \partial_\mu \rho - \left(1 + \frac{\rho}{v}\right)^2 \partial^\mu \chi \partial_\mu \chi - \frac{1}{4} m^2 (v + \rho)^2 - \frac{1}{16} g (v + \rho)^4. \tag{2.8}$$

Notice that a $U(1)$-transformation of ϕ corresponds to a shift in χ and that χ has no mass term. We can interpret this as a massless field along the broken symmetry. Note that we have only shown this for a broken $U(1)$-symmetry. To show that this holds for all symmetries is beyond the scope of this work, see [32] for more details or [34] for the original article.

2.2 Effective Field Theory

Now that we understand symmetry and the consequences of a spontaneous break, let us apply it to effective field theory (EFT). EFT was first introduced in [35], and the idea is to construct a Lagrangian containing all terms that satisfy the symmetries of a given system and, by establishing a counting scheme, take the terms of lowest order. With this, we can express the world in terms of the lightest composite particles, which allows us to access the non-perturbative regimes of a theory like QCD.

The basic principle is as follows:

The effective Lagrangian must satisfy the same symmetries as the original theory, but must also break any broken symmetries the same way. Which terms are picked is based on the chosen counting scheme. This approach defines the effective theory up to constants that must be determined by experiments.

EFT based on the chiral symmetry breaking in QCD is often called chiral perturbation theory (chPT) and is used to describe the low-energy limit of QCD, because the full partition function of QCD cannot be solved perturbatively in this regime. Instead of expressing our theory in terms of the quark fields, we express it in terms of the light Goldstone modes, which dominate the spectrum at low energy.

[1] This derivation follows chapter 32 of [33] quite closely.

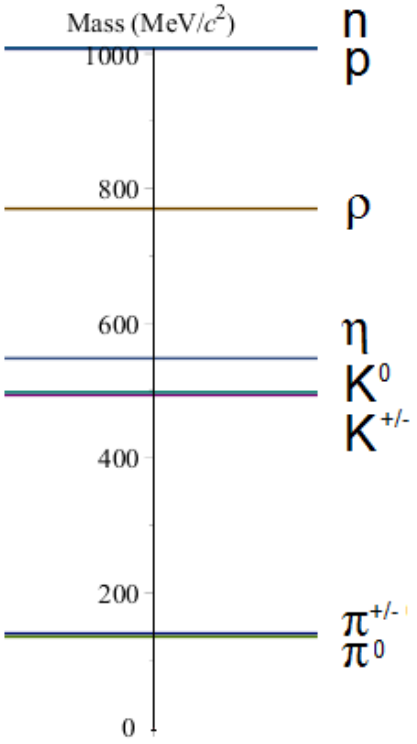

Figure 2.2: Mass spectrum of the lightest composite particles of QCD. The mass gap between the pions and the rest is what allows us to express the low-energy theory in terms of the pions only. The masses are taken from [36].

For it to be meaningful to make a cut-off at low energy, a well defined mass gap is necessary. This is also the case: The kaons, the lightest hadrons after the pions, are roughly a factor of 3.6 heavier than the pions [36], see Figure 2.2. Because the quarks only appear in deeply bound states, we need only consider them in terms of pions. Note that kaons and η-mesons are pseudo-Goldstone modes as well, so our approximation is really that only the two lightest flavours exist and that they can form pions only.

In this case, we require the quark mass to break chiral symmetry in the effective Lagrangian the same way as it does in QCD.

Counting Schemes

Taking the low-energy limit corresponds to taking the two limits $m_q \to 0$ and $V \to \infty$. A counting scheme is introduced to control the relation between m_q and V while taking these limits. There are two common choices here: [10, 13]

- p-counting:

$$\frac{1}{\beta} = \mathcal{O}(p) \ , \ \frac{1}{L} = \mathcal{O}(p) \ , \ M_\pi = \mathcal{O}(p) \tag{2.9}$$

- ϵ-counting:

$$\frac{1}{\beta} = \mathcal{O}(\epsilon) \ , \ \frac{1}{L} = \mathcal{O}(\epsilon) \ , \ M_\pi = \mathcal{O}(\epsilon^2) \tag{2.10}$$

where $L^3 \times \beta$ is the 4-volume of our box and M_π is the mass of the pion. We let $\epsilon, p \to 0$.

As we can see, the difference lies in how the mass is counted. These choices are illustrated in Figure 2.3.

The choice of counting scheme is a central part of our analysis:

Because we look at zero modes and near-zero modes, the low-momentum modes dominate and we therefore work in ϵ-counting [10, 12].

This counting scheme factorises the derivatives and mass part of the partition function, so we may treat the derivatives as normalisation. This opens up the possibility of calculating the partition function in its entirety and use it as a generating function of the eigenvalue spectrum. We show this below in Equation (2.23).

Chiral Perturbation Theory

The effective field theory used to calculate the chiral coupling is an extension of chiral perturbation theory, so let us establish the principle. Because there is a large mass gap between pions and other composite particles, they dominate the spectrum at low energy. We can therefore write our theory in terms of these Goldstone modes.

Construction of the Lagrangian works as follows: Consider the chiral transformations

$$\begin{aligned} q_R \to g_R q_R \quad &, \quad g_R = e^{\frac{1}{2}i(1+\gamma_5)\theta_R} \\ q_L \to g_L q_L \quad &, \quad g_L = e^{\frac{1}{2}i(1-\gamma_5)\theta_L} \end{aligned} \tag{2.11}$$

where θ_R, θ_L are $N_f \times N_f$ hermitian, traceless matrices. These are a symmetry of the massless QCD Lagrangian

$$\mathcal{L}_{QCD} = -i\bar{q}\not{D}q + \mathcal{L}_{YM} \tag{2.12}$$

where $\mathcal{L}_{YM}$ is the gluon field part, which we will omit in the following. These would also be a symmetry of the Lagrangian with mass

$$\mathcal{L}_{QCD} = \bar{q}(-i\not{D} + m_q)q \tag{2.13}$$

if the mass transformed like

$$m_q \to g_L m_q {g_R}^\dagger \tag{2.14}$$

at the same time. (Recall that we can write out the mass term as

$$\begin{pmatrix} \bar{q}_L & \bar{q}_R \end{pmatrix} \begin{pmatrix} m_q & 0 \\ 0 & m_q^\dagger \end{pmatrix} \begin{pmatrix} q_R \\ q_L \end{pmatrix} \tag{2.15}$$

in chiral basis.) This approach is called the spurion technique and (2.14) the spurion transformation of the mass, see for instance [13].

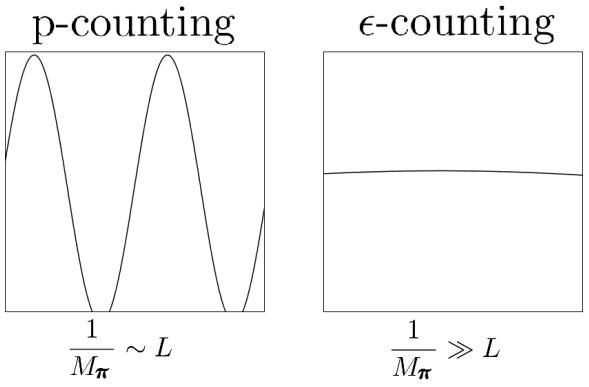

Figure 2.3: Illustration of the two counting schemes. Because the wavelength of our Goldstone mode goes as the inverse mass, taking $\mathcal{O}(M_\pi) = \mathcal{O}(L^{-1})$, the wavelength becomes the same order of magnitude as the size of the box, and the kinetic part of the Goldstone particle becomes significant. On the other hand, taking $\mathcal{O}(M_\pi) = \mathcal{O}(L^{-2})$ freezes out the dynamics of the system and allows us to consider the mass part alone.

Introducing the Goldstone field U which transforms as [13]

$$U \to g_L U {g_R}^\dagger, \tag{2.16}$$

we can construct a Lagrangian consisting of invariant Goldstone terms. The chiral symmetry breaking takes the form [13]

$$SU_R(N_f) \times SU_L(N_f) \to SU_V(N_f) \tag{2.17}$$

so the Goldstone modes live on the manifold

$$U \in SU(N_f) \times SU(N_f)/SU(N_f) \sim SU(N_f) \tag{2.18}$$

Since $\mathrm{Tr}(UU^\dagger) = N_f$, the basic building blocks are

$$\mathcal{L}_{EFT} = \frac{f^2}{4}\mathrm{Tr}[\partial_\mu U^\dagger \partial^\mu U] + \Sigma_0 \mathrm{Tr}[m_q^\dagger U + m_q U^\dagger] \tag{2.19}$$

where f and Σ_0 are the aforementioned constants that cannot be determined by symmetries. (In QCD, f can be found through scattering experiments [13]. Σ_0 is related to the spontaneous breaking of chiral symmetry.[2])

To identify how the quark mass should be counted, we must first find the relation between it and the pion mass. With the parametrisation $U = e^{i\sqrt{2}\Pi/f}$ [13], where Π is the pion field, we can expand the last term to

$$\Sigma_0 \mathrm{Tr}[m_q^\dagger U + m_q U^\dagger] \approx \Sigma_0 \mathrm{Tr}[2m_q - \frac{2m_q}{f^2}\Pi^2], \tag{2.20}$$

making the pion mass $M_\pi = \frac{\sqrt{4m_q\Sigma_0}}{f}$ [10, 37, 38]. The important part of the result is of course $m_q = \mathcal{O}({M_\pi}^2)$.

To see the factorisation of derivatives and low-momentum modes, let us now split U into a local and a global part [10]

$$U \;=\; u e^{i\xi(x)} u \tag{2.21}$$

with $uu^\dagger = 1$. Inserting this, we can expand (2.19) to

$$\begin{aligned}\mathcal{L}_{EFT} &= \frac{f^2}{4}\mathrm{Tr}[u\partial_\mu\xi(x)e^{i\xi(x)}uu^\dagger\partial^\mu\xi(x)e^{-i\xi(x)}u^\dagger] + \frac{\Sigma_0 m_q}{2}\mathrm{Tr}\left[u^2 + {u^\dagger}^2 - \frac{u\xi^2(x)u}{2} - \frac{u^\dagger\xi^2(x)u^\dagger}{2}\right] \\ &= \frac{f^2}{4}\mathrm{Tr}[\partial_\mu\xi(x)\partial^\mu\xi(x)] + \frac{\Sigma_0 m_q}{2}\mathrm{Tr}\left[U_0 + U_0^\dagger\right] - \frac{\Sigma_0 m_q\xi^2(x)}{4}\mathrm{Tr}\left[U_0 + {U_0}^\dagger\right]\end{aligned} \tag{2.22}$$

where $U_0 = u^2$.[3] The action is

$$\begin{aligned}S_{EFT} &= \int d^4x \mathcal{L}_{EFT} \\ &= \frac{f^2}{4}\int d^4x \mathrm{Tr}[\partial_\mu\xi(x)\partial_\mu\xi(x)] + \frac{V\Sigma_0 m_q}{2}\mathrm{Tr}\left[U_0 + U_0^\dagger\right] \\ &\quad -\frac{\Sigma_0 m_q}{4}\int d^4x\xi^2(x)\mathrm{Tr}\left[U_0 + {U_0}^\dagger\right].\end{aligned} \tag{2.23}$$

Since $f = \mathcal{O}(1), \Sigma_0 = \mathcal{O}(1), \int dx = \mathcal{O}(\epsilon^{-1}), \partial_\mu = \mathcal{O}(\epsilon)$, and $m_q = \mathcal{O}(\epsilon^4)$, the first term forces $\xi = \mathcal{O}(\epsilon)$ if the action should stay convergent for $\epsilon \to 0$. Knowing this, the first two terms are both $\mathcal{O}(1)$ and the last is $\mathcal{O}(\epsilon^2)$. So for $\epsilon \to 0$, the last term is suppressed. If we only care about the low-momentum modes, we can treat the first term as normalisation.

From here on we omit the subscript on U_0. We let $V \to \infty$ and $m_q \to 0$, while keeping $V\Sigma_0 m_q \equiv m$ constant. So our EFT partition function is

$$Z_{EFT}(m) = \int_{SU(N_f)} dU \exp\left\{\frac{1}{2}\mathrm{Tr}[M^\dagger U + MU^\dagger]\right\} \tag{2.24}$$

[2]This can be realised by considering the chiral condensate $\Sigma(m) = \delta_m \ln Z$, where $\Sigma(0)$ is a measure of the strength of the spontaneous chiral break. The derivative pulls out a Σ_0 in front, for $\Sigma(0) \neq 0$, the scale of the break is determined by Σ_0.

[3]It is not completely obvious that the first order terms cancel in the last trace of the first line, but because $U + U^\dagger = 2\Re[U]$, the imaginary terms must cancel.

where we have introduced the mass matrix $M = m\mathbf{1}_{N_f}$. Notice this change of variables to the dimensionless variable m. We work in these dimensionless variables throughout this work. We later find the numerical equivalent.

Let us generalise this result. Given a Lagrangian of the form

$$\mathcal{L}_{QCD} = \mathcal{L}^0_{QCD} + \bar{q}\gamma^\mu(v_\mu + \gamma_5 a_\mu)q - \bar{q}(s - i\gamma_5 p)q \tag{2.25}$$

where $\bar{q}, q$ are the quark fields, and v_μ, a_μ, s, p are external hermitian fields, we can write up the most general effective theory in p-counting [13]

$$\mathcal{L}_{EFT} = \frac{f^2}{4}\mathrm{Tr}\left[D_\mu U^\dagger D^\mu U + U^\dagger\chi + \chi^\dagger U\right] \tag{2.26}$$

where

$$\begin{aligned} D_\mu U &= \partial_\mu U - i(v_\mu + a_\mu)U + iU(v_\mu - a_\mu) \\ D_\mu U^\dagger &= \partial_\mu U^\dagger + iU^\dagger(v_\mu + a_\mu) - i(v_\mu - a_\mu)U^\dagger \\ \chi &= 2B_0(s + ip) \end{aligned} \tag{2.27}$$

and f and B_0 are constants that are not determined by symmetries (f is the same as in (2.19)).

We can obtain the same result in ϵ-counting by simply setting the derivatives to 0. We can quickly verify that considering a source of the kind $\bar{q}m_q q$ leads us to (2.24) with $B_0 = \frac{V\Sigma_0}{f^2}$.

2.3 Topology and Zero-modes

The exact zero modes play a crucial role in our system, so let us start by illustrating why they are special. A chiral operator Ω anti-commutes with some operator η that squares to unity

$$\{\Omega, \eta\} = 0 \quad , \quad \eta^2 = 1. \tag{2.28}$$

This means we can rewrite the eigenvalue equation $\Omega\,|\psi\rangle = \lambda\,|\psi\rangle$ as

$$\eta\Omega\,|\psi\rangle = \eta\lambda\,|\psi\rangle \Rightarrow -\Omega\eta\,|\psi\rangle = \lambda\eta\,|\psi\rangle \Rightarrow \Omega\,|\psi'\rangle = -\lambda\,|\psi'\rangle \tag{2.29}$$

where $|\psi'\rangle = \eta\,|\psi\rangle$. So all eigenvalues λ appear in pairs, symmetric around zero, unless $\lambda = 0$, which is why the topological zero modes stand out. In QCD, the chiral operator is the massless Dirac operator $\Omega = \not{D}$, which anti-commutes with $\eta = \gamma_5$.

The number of exact zero modes in a given system is equal to the absolute value of the winding number ν, which is a topological invariant [28, 29, 33]. This is why we can treat the number of zero modes and topology on equal footing. Because the topology of a system is not easily changed, it is often fruitful to consider topological quantities. We shall briefly discuss the role of topology in QCD, but our main focus will be zero modes.[4]

[4]For a thorough treatment of the winding number in QCD, [29] is highly recommended.

2.3.1 Topology in QCD: Winding Number and Vacuum Angle

In QCD, the winding number stems from the $U(1)$-axial anomaly as follows: The massless QCD Lagrangian

$$\mathcal{L} = -i\bar{q}\not{D}q - \frac{1}{4}G^a_{\alpha\beta}G^a_{\alpha\beta} \tag{2.30}$$

has a classical axial symmetry

$$\begin{aligned} \bar{q} &\rightarrow \bar{q}e^{i\theta\gamma_5} \\ q &\rightarrow e^{i\theta\gamma_5}q, \end{aligned} \tag{2.31}$$

by which we mean that the Lagrangian is invariant under this transformation. For now, θ is just a transformation parameter. However, a change of variables shows that this is not a true symmetry of the theory, because the partition function is not invariant. This is what we call an anomaly. Regularisation of the Jacobian leads to the term [33]

$$\Delta\mathcal{L} = \frac{\theta}{32\pi^2}\epsilon^{\alpha\beta\rho\sigma}G^a_{\alpha\beta}G^a_{\rho\sigma} \tag{2.32}$$

in the Lagrangian. Here θ is called the vacuum angle. Interestingly, this is an exact term (not subject to higher order corrections). So the full partition function with mass is

$$\begin{aligned} Z(m,\theta) = &\int D\bar{q}DqDA\ \exp\left\{i\int d^4x\bar{q}(-i\not{D}+m_q)q\right\} \\ &\times\exp\left\{-\frac{1}{4}G^a_{\alpha\beta}G^a_{\alpha\beta}+\frac{\theta}{32\pi^2}\epsilon^{\alpha\beta\rho\sigma}G^a_{\alpha\beta}G^a_{\rho\sigma}\right\}. \end{aligned} \tag{2.33}$$

Because the additional term can be rewritten as

$$\frac{\theta}{32\pi^2}\epsilon^{\alpha\beta\rho\sigma}G^a_{\alpha\beta}G^a_{\rho\sigma} = \frac{\theta}{16\pi^2}\partial_\mu\left(\epsilon^{\mu\nu\rho\sigma}\left(A^a_\nu\partial_\rho A^a_\sigma+\frac{1}{3}f_{abc}A^a_\nu A^b_\rho A^c_\sigma\right)\right), \tag{2.34}$$

it appears as a total derivative, and therefore a surface integral of the field in infinity. It is tempting to neglect the contribution of this term in the action, because one would expect the gauge field to be 0 at infinity, but this turns out not to be the case. The contribution to the action from this term is the aforementioned winding number [28, 29, 33]

$$\int d^4x\frac{1}{32\pi^2}\epsilon^{\alpha\beta\rho\sigma}G^a_{\alpha\beta}G^a_{\rho\sigma} = \nu, \tag{2.35}$$

which is a topological invariant and equal to the number of exact zero modes of $\not{D}$ in the given background field [28, 29, 33].

Inserting the integral over the additional term in the partition function, we find

$$Z(m_q,\theta) = \int D\bar{q}DqDA\exp\left\{i\int d^4x\bar{q}(-i\not{D}+m_q)q-\frac{1}{4}G^a_{\alpha\beta}G^a_{\alpha\beta}\right\}e^{i\theta\nu}. \tag{2.36}$$

In the full partition function, we integrate over all gauge field configurations, so we implicitly sum over all topologies. We wish to consider ensembles with a given number of zero

modes, which makes it important to understand how they appear in the partition function. Define $\int_\nu DA$ as an integral over all gauge field configurations that have ν zero modes, we may write

$$\begin{aligned} Z(m_q,\theta) &= \sum_{\nu=-\infty}^{\infty} e^{i\theta\nu}\int_\nu D\bar{q}DqDA\exp\left\{i\int d^4x\bar{q}(-i\not{D}+m_q)q-\frac{1}{4}G^a_{\alpha\beta}G^a_{\alpha\beta}\right\} \\ &\equiv \sum_{\nu=-\infty}^{\infty} e^{i\theta\nu}Z^\nu(m_q), \end{aligned} \tag{2.37}$$

which means we can switch between the full ensemble and an ensemble with a specific number of zero modes with a Fourier transformation.

Relation to the Quark Mass

As we shall see, a change in the vacuum angle θ corresponds to a $U(1)$ transformation of the quark mass.

Consider an ensemble with certain topological configuration, where we integrate out the quark fields (see Appendix A.1) and write $\not{D}$ in terms of its eigenvalues

$$Z^\nu(m_q)=\int_\nu DA\det{}^{N_f}(-i\not{D}+m_q)e^{S_{YM}}=\int_\nu DA\prod_k(-i\lambda_k+m_q)^{N_f}e^{S_{YM}} \tag{2.38}$$

where N_f is the number of flavours with equal mass, and S_{YM} is the Yang-Mills action.

Defining $\prod_k{}'$ as the product over non-zero eigenvalues and remembering that the system has $|\nu|$ zero modes, we may write

$$Z^\nu(m_q)=\int_\nu DA\prod_k{}'(\lambda_k\lambda_k^*+m_qm_q^*)^{N_f}m_q^{N_f\nu}e^{S_{YM}}. \tag{2.39}$$

For $\nu<0$ the factor $m_q^{N_f\nu}$ is replaced by $(m_q^*)^{-N_f\nu}$ [29].

Making a $U(1)$ transformation of the mass, we can see it transforms the partition function in the following way:

$$Z^\nu(m_qe^{i\theta_0}) = e^{i\theta_0\nu N_f}\int_\nu DA\prod_k{}'(\lambda_k\lambda_k^*+m_qm_q^*)^{N_f}m_q^{N_f\nu}e^{S_{YM}}=e^{i\theta_0\nu N_f}Z^\nu(m_q) \tag{2.40}$$

This makes

$$\begin{aligned} Z(m_qe^{i\theta_0},\theta) &= \sum_{\nu=-\infty}^{\infty}e^{i(\theta+N_f\theta_0)\nu}Z^\nu(m_q)=Z(m_q,\theta+N_f\theta_0) \\ \Rightarrow Z(m_q,\theta) &= Z(m_qe^{i\theta/N_f},0), \end{aligned} \tag{2.41}$$

which is why it is the sum

$$\theta+\arg(\det(M)) \tag{2.42}$$

we should consider, rather than θ alone. M is the quark mass matrix also used in the rest of this thesis [39]. Because of this relation, however, we shall refer to them collectively as θ. We will use the $U(1)$ transformation property of the mass from Equation (2.40) later to analyse the effective partition function.

2.3.2 Zero Modes in EFT

To analyse zero modes, we must incorporate them explicitly in the effective theory. The effective theory we derived in (2.24) is for all topologies. Reversing (2.37) and applying it to (2.24), we may write

$$\begin{aligned} Z^{\nu}_{EFT}(m) &= \int d\theta e^{i\theta\nu} Z_{EFT}(me^{i\theta\nu}, 0) \\ &= \int d\theta e^{iN_f\theta\nu} \int_{SU(N_f)} dU \exp\left\{\frac{1}{2}\mathrm{Tr}[M^\dagger e^{-i\theta}U + Me^{i\theta}U^\dagger]\right\} \end{aligned} \tag{2.43}$$

We can combine the two integrals to a $U(N_f)$-integral by absorbing a phase $e^{i\theta}$ into U and rewriting the exponential as $\det{}^{\nu}(U)$. (The determinant of the $SU(N_f)$ part is always 1.) Note that this changes the manifold of U. So the partition function is

$$Z^{\nu}_{EFT}(m) = \int_{U(N_f)} dU \det{}^{\nu}(U) \exp\left\{\frac{1}{2}\mathrm{Tr}[M^\dagger U + MU^\dagger]\right\}. \tag{2.44}$$

This shows that the zero modes appear as $\det{}^{\nu}(U)$, which we shall also see later.

Returning to the representation in (2.39), the zero mode part can also be written as the determinant of the mass matrix $M = m\mathbf{1}_{N_f}$

$$m_q^{N_f\nu} = \det{}^{\nu}(M) \quad , \quad \nu \geq 0 \tag{2.45}$$

This will lead to a $\nu\delta(\lambda)$ term in the spectrum of eigenvalues as wanted. For $\nu < 0$ this must be $\det{}^{-\nu}(M^\dagger)$, if the amount of zero modes is to be positive while retaining the transformation property from (2.40). We will use this relation later on to remove the zero modes from ensembles.

2.3.3 Distribution of Topologies

We mainly look at ensembles with a specific topology, but let us examine how the different topologies should be weighted in the total ensemble. This weighting depends on the vacuum angle.

Notice that $\theta = 0$ simply yields the sum of all Z^ν. Because of this, we may interpret the probability of a certain topology ν as

$$p(\nu, m_q) = \frac{Z^\nu(m_q)}{Z(m_q, \theta = 0)} \tag{2.46}$$

We can also identify the mean topology and topological susceptibility

$$\left.\frac{\partial_\theta Z(\theta, m_q)}{Z(\theta, m_q)}\right|_{\theta=0} = \left.\frac{\sum_{\nu=-\infty}^{\infty} i\nu e^{i\theta\nu} Z^\nu(m_q)}{Z(m_q,\theta)}\right|_{\theta=0} = i\langle\nu\rangle \tag{2.47}$$

$$\left.\frac{\partial^2_\theta Z(\theta, m)}{Z(\theta, m_q)}\right|_{\theta=0} = \left.\frac{\sum_{\nu=-\infty}^{\infty} -\nu^2 e^{i\theta\nu} Z^\nu(m_q)}{Z(m_q,\theta)}\right|_{\theta=0} = -\langle\nu^2\rangle. \tag{2.48}$$

Let us derive an example. Consider a single fermionic flavour with the parametrisation of the $U(1)$ Goldstone field given by $U = e^{i\alpha}$. The partition function of the single ensemble is

$$\begin{aligned} Z^{\nu}_{chUE,1}(m) &= \int_{-\pi}^{\pi} \frac{d\alpha}{2\pi} \det{}^{\nu}(e^{i\alpha}) e^{m\cos(\alpha)} \\ &= \int_{-\pi}^{\pi} \frac{d\alpha}{2\pi} e^{i\alpha\nu} e^{m\cos(\alpha)} \\ &= \int_{0}^{\pi} \frac{d\alpha}{\pi} \cos(\alpha\nu) e^{m\cos(\alpha)} \\ &= I_{\nu}(m). \end{aligned} \tag{2.49}$$

The full partition function $Z(m,\theta)$ is best found in the integral representation of $I_\nu(m)$

$$\begin{aligned} Z_{chUE,1}(m,\theta) &= \sum_{\nu=-\infty}^{\infty} e^{i\theta\nu} \int_{-\pi}^{\pi} \frac{d\alpha}{2\pi} e^{i\alpha\nu} e^{m\cos(\alpha)} = \int_{-\pi}^{\pi} \frac{d\alpha}{2\pi} \sum_{\nu=-\infty}^{\infty} e^{i(\alpha+\theta)\nu} e^{m\cos(\alpha)} \\ &= \int_{-\pi}^{\pi} d\alpha \sum_{n=-\infty}^{\infty} \delta(\alpha+\theta-2\pi n) e^{m\cos(\alpha)} = \sum_{n=-\infty}^{\infty} e^{m\cos(\theta-2\pi n)} \end{aligned} \tag{2.50}$$

where n is some integer. We can of course disregard the $2\pi n$. We can also ignore the sum, because it just appears as an overall factor (even though it is infinite). So

$$Z_{chUE,1}(m,\theta) = e^{m\cos(\theta)} \tag{2.51}$$

$$\Rightarrow p_1(\nu) = I_\nu(m) e^{-m} \tag{2.52}$$

with

$$\langle \nu \rangle = 0 \quad , \quad \langle \nu^2 \rangle = m \tag{2.53}$$

This discussion of topology is highly relevant because we want to consider the fate of the topological zero modes, when we couple two systems. It is also necessary to understand zero modes before we move on to random matrix theory, because these matrix theories have a fixed amount of zero modes (and therefore also a fixed topological charge).

2.4 Supersymmetric Ensemble as Generating Functional

The primary goal of our analysis is to calculate the quenched microscopic eigenvalue spectrum of the Dirac operator with the given terms in our effective Lagrangian.

Because the spectrum is prohibitively difficult to calculate analytically from first principle, we instead calculate it from the effective theory of a partially quenched ensemble. This is done for uncoupled chUE in [12].

The eigenvalue spectrum is obtained as follows: Consider first the full theory of a partially quenched ensemble

$$Z^{\nu}_{1|1}(m,m') = \int DA \frac{\det(-i\not{D}+m)}{\det(-i\not{D}+m')} e^{-S_{YM}}. \tag{2.54}$$

For $m = m'$, this can be normalised to 1. We can find the quenched chiral condensate by deriving with respect to one of the masses and setting $m = m'$.

$$\Sigma(m) = \frac{1}{V}\partial_m \ln(Z(m,m'))\Big|_{m=m'}. \tag{2.55}$$

Because

$$\partial_m \det(-i\not{D} + m) = \mathrm{Tr}\left(\frac{1}{-i\not{D}+m}\right)\det(-i\not{D}+m), \tag{2.56}$$

we can write the chiral condensate in the eigenvalue representation as

$$\begin{aligned}\Sigma(m) &= \frac{1}{V}\left\langle \sum_k \frac{1}{-i\lambda_k + m}\right\rangle \\ &= \frac{1}{V}\int d\lambda \frac{\rho(\lambda)}{-i\lambda+m},\end{aligned} \tag{2.57}$$

where λ_k are the eigenvalues of $\not{D}$, and $\rho(\lambda)$ is the density of eigenvalues.

We isolate the eigenvalue spectrum by considering the discontinuity across the imaginary axis

$$\begin{aligned}\frac{1}{V}\lim_{\epsilon\to 0}\left[\Sigma(i\lambda+\epsilon) - \Sigma(i\lambda-\epsilon)\right] &= \frac{1}{V}\lim_{\epsilon\to 0}\sum_k \left\langle \frac{1}{-i\lambda_k + i\lambda + \epsilon} - \frac{1}{-i\lambda_k + i\lambda - \epsilon}\right\rangle \\ &= \frac{1}{V}\lim_{\epsilon\to 0}\sum_k \left\langle \frac{\epsilon^2}{(\lambda_k-\lambda)^2+\epsilon^2}\right\rangle \\ &= 2\pi\sum_k \langle\delta(\lambda_k - \lambda)\rangle \\ &= 2\pi\rho(\lambda).\end{aligned} \tag{2.58}$$

The challenge is to calculate (2.54), which we do in the effective theory. The structure of the partially quenched ensemble is very similar to (2.44), except we will integrate over a different group.

2.4.1 Symmetry Group of Graded Partition Function

The Goldstone manifold of (2.54) involves the possibility of both fermionic and bosonic Goldstone modes, so we write our EFT as a supersymmetric ensemble. Let us outline the consequences of this for the group integration. This section follows Section 2 of [12] quite closely.[5]

Since our fields are not a priori related by complex conjugation, we no longer have the identity $\bar{q} = q^\dagger\gamma_0$. So our theory is no longer unitary, and symmetry group of the massless Lagrangian is extended to general linear symmetry [16]

$$q_{R,L} \to G_{R,L}q_{R,L} \quad , \quad \bar{q}_{R,L} \to \bar{q}_{R,L}G^{-1}_{R,L} \tag{2.59}$$

[5]Further discussion of the nature of the supersymmetric group integrals is beyond the scope of this work. It is discussed in details in [12] and [16].

with $G \in Gl(N_f|N_b)$, where N_f and N_b are the number of fermionic and bosonic flavours respectively.

This is not necessarily a symmetry of the partition function. Like before, we lose the possibility of making the left and right transformation independently of each other for non-zero mass. Convergence of the bosonic integrations reduces this symmetry breaking to [12]

$$Sl_R(N_f|N_b) \times Sl_L(N_f|N_b) \to Sl_V(N_f|N_b), \tag{2.60}$$

which makes the Goldstone manifold $Sl(N_f|N_b)$. Including the axial break, it becomes $Sl(N_f|N_b)\otimes Gl(1)$. It turns out that this is not a super-Riemannian manifold, and that the proper domain is $Gl(N_f|N_b)$. This restricts the fermion-fermion block to the compact domain $SU(N_f)$, whereas the boson-boson block is restricted to the non-compact domain $Gl(N_b)/U(N_b)$ [12].

The important conclusion to be drawn here is that the effective theory of an ensemble with N_f fermions and N_b bosons is [12]

$$Z^{\nu}_{chUE,N_f|N_b}(M) = \int_{Gl(N_f|N_b)} dU \, \mathrm{Sdet}^{\nu}(U) \exp\left\{\frac{1}{2}\mathrm{Str}[M^{\dagger}U + MU^{-1}]\right\}. \tag{2.61}$$

We will often take M to be real and diagonal. We use this to calculate the eigenvalue spectrum of the coupled ensemble in Chapter 4.

2.5 Random Matrix Theory

In this section, we introduce random matrix theory (RMT) as a numerical tool for calculating universal properties of a given system.[6] We will for now focus on the theoretical part of RMT and save description of the practical implementation for Chapter 6.[7]

RMT has its origin in mathematical statistics, but was first applied to physics in neutron resonance [5]. It was combined with QCD in [17], [3], and [7].

The basic principle is as follows:

We construct the most general matrix possible that obeys the same symmetries as the operator we want to investigate. The universal properties of the operators eigenvalues (and eigenvectors) can then be obtained by numerically generating a (large) number matrices with of random variables that obey the given set of symmetries.

In chiral systems such as QCD, the microscopic eigenvalue spectrum is uniquely determined by the symmetries [12], which is why we can calculate it numerically this way. We can consider three different kinds of ensembles: Orthogonal, unitary, or symplectic with real, complex, and quarternion components respectively.

Let us consider the chiral unitary ensemble a with Gaussian weight to ensure convergence as an example. The partition function reads [3, 7, 17]

$$Z^{n,\nu}_{chGUE}(m_R) = \int dW \det{}^{N_f} \begin{pmatrix} m_R & iW \\ iW^{\dagger} & m_R^* \end{pmatrix} e^{-n\mathrm{Tr}[WW^{\dagger}]} \tag{2.62}$$

[6] Note that the eigenvalues of random matrices can also be calculated analytically, but that is beyond the scope of this work. We will, however, show the relation between RMT and chPT analytically.

[7] For detailed treatments, see [5] and [6] for books on the subject. Reviews can also be found in [25, 26, 27, 28].

where W are random complex $(n+\nu)\times n$ matrices for $\nu \geq 0$ ($n\times(n-\nu)$ matrices for $\nu < 0$), and m_R is a dimensionless parameter that is relatable to the physical mass by $V\Sigma_0 m_q = 2nm_R$.[8] The notation ν is intentionally suggestive. As we shall see below, (2.62) does indeed have $|\nu|$ eigenvalues equal to zero.

Comparing to the QCD partition function

$$Z_{QCD} = \int dA \det{}^{N_f}(-i\not{D}+m)e^{-S_{YM}} \tag{2.63}$$

we see that the matrix

$$\begin{pmatrix} m_R & iW \\ iW^\dagger & m_R^* \end{pmatrix} = i\begin{pmatrix} 0 & W \\ W^\dagger & 0 \end{pmatrix} + \begin{pmatrix} m_R & 0 \\ 0 & m_R^* \end{pmatrix} \tag{2.64}$$

corresponds to $-i\not{D}+m$, and the weight corresponds to the gluon part of the QCD-action. We have written the operator in chiral basis as becomes apparent below.

The structure of (2.64) incorporates three conditions:

$$\begin{aligned} (i\not{D})^\dagger &= -i\not{D} \\ \{i\not{D},\gamma_5\} &= 0 \end{aligned} \tag{2.65}$$

and that the mass should break chiral symmetry the same way as (2.17). The first two are easily realised, as $\gamma_5 = \begin{pmatrix} -1 & 0 \\ 0 & 1 \end{pmatrix}$ in chiral basis. The third can be realised by writing the determinant as a Gaussian integral

$$\det\begin{pmatrix} m_R & iW \\ iW^\dagger & m_R^* \end{pmatrix} = \exp\left\{ \begin{pmatrix} \psi \\ \phi \end{pmatrix}^\dagger \begin{pmatrix} m_R & iW \\ iW^\dagger & m_R^* \end{pmatrix} \begin{pmatrix} \psi \\ \phi \end{pmatrix} \right\} \tag{2.66}$$

and identify ψ and ϕ as left and right parts of the quark fields respectively. The mass couples left and right and so breaks chiral symmetry in the right way.[9] This identification of chiral sectors will be important later when we introduce the coupling.

For later use, we also note that (2.62) also can be written as [7, 17]

$$Z^{n,\nu}_{chGUE}(m_R) = \begin{cases} \int dA \det{}^{n+\nu}(A^\dagger + M_R)\det{}^n(A+M_R^\dagger)e^{n\mathrm{Tr}AA^\dagger} & \nu \geq 0 \\ \int dA \det{}^{n}(A^\dagger + M_R)\det{}^{n-\nu}(A+M_R^\dagger)e^{n\mathrm{Tr}AA^\dagger} & \nu < 0 \end{cases} \tag{2.67}$$

where $M_R = m_R\mathbf{1}_{N_f}$ and A is an arbitrary complex matrix of the same size.

That ν really is the amount of zero modes becomes evident when considering the transformation properties. Let us just consider $\nu \geq 0$.

$$\begin{aligned} Z^{n,\nu}_{chGUE}(m_R e^{i\theta}) &= \int dA \det{}^{n+\nu}(A^\dagger + M_R e^{i\theta})\det{}^n(A+M_R^\dagger e^{-i\theta})e^{n\mathrm{Tr}AA^\dagger} \\ &= e^{i\nu\theta}\int dA \det{}^{n+\nu}(A^\dagger e^{-i\theta} + M_R)\det{}^n(Ae^{i\theta}+M_R^\dagger)e^{n\mathrm{Tr}AA^\dagger} \\ &= e^{i\nu\theta}Z^{n,\nu}_{chGUE}(m_R). \end{aligned} \tag{2.68}$$

[8] This is derived in [7], but we also see it in Section 3.2.

[9] There is a subtlety here: It looks like the mass links the same chiral sectors to each other, which would be in violation with (2.15), but we have neglected a $\gamma_0 = \begin{pmatrix} 0 & 1 \\ 1 & 0 \end{pmatrix}$, which can be introduced at the expense of a sign in (2.62).

In the last line we have absorbed a phase into the arbitrary complex matrix A.

We can also see this directly by considering the eigenvalue equation for $m_R = 0$.

$$\begin{pmatrix} 0 & \dots & 0 & iW_{11} & \dots & iW_{1n} \\ \vdots & \ddots & \vdots & \vdots & \ddots & \vdots \\ 0 & \dots & 0 & iW_{n+\nu 1} & \dots & iW_{n+\nu n} \\ iW_{11}^* & \dots & iW_{1n+\nu}^* & 0 & \dots & 0 \\ \vdots & \ddots & \vdots & \vdots & \ddots & \vdots \\ iW_{1n} & \dots & iW_{nn+\nu} & 0 & \dots & 0 \end{pmatrix} \begin{pmatrix} v_1 \\ \vdots \\ \vdots \\ \vdots \\ v_{2n+\nu} \end{pmatrix} = \begin{pmatrix} 0 \\ \vdots \\ \vdots \\ \vdots \\ 0 \end{pmatrix} \tag{2.69}$$

If we let $v_{n+\nu+1}, \dots, v_{2n+\nu} = 0$, we obtain n equations with $n + \nu$ free parameters. This system must have at least ν solutions, making ν the number of zero modes. We shall denote the eigenvalues of the RMT model λ_R. Again, these are relatable to the physical eigenvalues by $2n\lambda_R = V\Sigma_0\lambda \equiv u$.

Let us summarise: We now know that (2.62) has the same symmetries, amount of zero modes, and transformation properties as QCD with N_f flavours, and we should therefore be able to calculate the microscopic eigenvalue spectrum from it. We have, however, neglected one thing: The Gaussian weight is not universal, which is the next step.

Universal Limit

It turns out that in the microscopic limit $n \to \infty$ the choice of weight becomes arbitrary as long as it supports a non-zero eigenvalue distribution around zero [18]. We choose a Gaussian weight because it is convenient, and we shall denote the limit $n \to \infty$ as $Z_{chUE}^{(\nu)}$.

The universality of this limit also has other consequences. Because this model has the same symmetries as QCD, it of course has the same low-energy effective theory [7, 17]. If we keep $M \equiv 2nM_R$ constant while letting $n \to \infty$, we directly regain the EFT from (2.44), because it is constructed with a specific amount of zero modes ν.

So

$$Z_{chGUE}^{n\to\infty,\nu}(m_R = \frac{m}{2n}) \equiv Z_{chUE}^{(\nu)}(M) \quad = \quad \int_{U(N_f)} dU \det{}^{\nu}(U) \exp\left\{\frac{1}{2}\mathrm{Tr}[M^\dagger U + MU^\dagger]\right\}. \tag{2.70}$$

A simulation of the quenched version of (2.62) in the microscopic limit compared to the eigenvalue spectrum of the corresponding effective theory can be found in Figure 6.1.

It turns out the unitary ensemble is the simplest to work with, so we shall develop much of the framework in chUE, before turning our attention to chOE.

2.6 A Note on Majorana Modes

The coupling of chiral systems treated in this thesis is inspired by superconductors carrying Majorana modes, so let us go through the properties of Majorana fermions in high energy and solid state physics. High energy and solid state physics have two different approaches to Majorana modes, which is also why the coupled theory of this thesis needs further improvements before it is directly applicable to the solid state system.

This section therefore stands slightly apart from the rest of the chapter in the sense that it is not necessary for the understanding of the coupled chiral system. It should more be considered the ground work needed to bridge the gap between our coupled model and the physical system.

The most notable difference is that, in the superconductor, only the zero modes are Majorana modes, whereas the bulk are Dirac modes [1, 2, 30, 40]. This will not be the case in our model, where bulk modes and zero modes are the same. This section is largely based on [30, 40, 41].

In Appendix C.1, we outline what structure a random matrix model should have to incorporate this property.

2.6.1 High Energy: Fundamental Majorana Fermions

In high energy physics, Majorana fields are found as the real solutions to the Dirac equation. Let us start from the free Dirac equation

$$(-i\gamma^\mu \partial_\mu + m)\Psi = 0, \tag{2.71}$$

and write this as a real equation. This requires a basis, where all γ-matrices are purely imaginary. We require [41]

$$\{\gamma^\mu, \gamma^\nu\} = 2g^{\mu\nu} \tag{2.72}$$

$$\gamma_0\gamma_\mu\gamma_0 = {\gamma_\mu}^\dagger. \tag{2.73}$$

A solution to these conditions, which we shall call the Majorana basis and denote by $\tilde{\gamma}_\mu$, is [41]

$$\tilde{\gamma}_1 = \begin{pmatrix} i\sigma_1 & 0 \\ 0 & i\sigma_1 \end{pmatrix} \quad , \quad \tilde{\gamma}_2 = \begin{pmatrix} 0 & \sigma_2 \\ -\sigma_2 & 0 \end{pmatrix} \quad , \quad \tilde{\gamma}_3 = \begin{pmatrix} i\sigma_3 & 0 \\ 0 & i\sigma_3 \end{pmatrix}, \tag{2.74}$$

$$\tilde{\gamma}_0 = \begin{pmatrix} 0 & \sigma_2 \\ \sigma_2 & 0 \end{pmatrix} \quad , \quad \tilde{\gamma}_5 = \begin{pmatrix} \sigma_2 & 0 \\ 0 & -\sigma_2 \end{pmatrix},$$

where σ_j are the Pauli matrices in the usual basis where σ_2 is imaginary. This choice makes (2.71) real, and we are therefore able to find real solutions to it. These solutions represent Majorana fermions, and in the Majorana basis they satisfy

$$\tilde{\Psi} = \tilde{\Psi}^*. \tag{2.75}$$

The Majorana basis is in no way unique, but if two representations of the γ-matrices both satisfy (2.72) and (2.73), they are related by a similarity transformation with a unitary matrix [41]. So a general representation of the γ-matrices can be obtained through

$$\gamma^\mu = U\tilde{\gamma}^\mu U^\dagger \tag{2.76}$$

where U is a unitary matrix. This also implies that if $\tilde{\Psi}$ is a solution to the Dirac equation, then the solution in this general representation is

$$\Psi = U\tilde{\Psi}. \tag{2.77}$$

When referring to (2.75) in any basis, we call it the Majorana condition. Let us write it in our general representation. Inserting (2.77) in (2.75) we find

$$\begin{aligned} U^\dagger \Psi &= \left(U^\dagger \Psi\right)^* \\ \Psi &= UU^T \Psi^*. \end{aligned} \tag{2.78}$$

It is customary to write this as

$$\begin{aligned} \Psi &= \gamma_0 C \Psi^* \\ &\equiv \Psi^c, \end{aligned} \tag{2.79}$$

where Ψ^c is called the charge conjugate of Ψ.

Let us examine the object $UU^T = \gamma_0 C$. It is unitary and symmetric and satisfies

$$(UU^T)^* = U^* U^\dagger = (UU^T)^\dagger = (UU^T)^{-1}. \tag{2.80}$$

In chiral basis, we know C to be [7, 42]

$$\begin{aligned} C &= i\gamma_0\gamma_2 \\ \gamma_0 C &= i\gamma_2 \\ &= \begin{pmatrix} 0 & i\sigma_2 \\ -i\sigma_2 & 0 \end{pmatrix}. \end{aligned} \tag{2.81}$$

One quickly verifies that $i\gamma_2$ has the same properties as UU^T. Notice also that since $i\gamma_2$ is real, symmetric, and unitary it must square to 1, which can also be shown explicitly. This is not at all surprising, since flipping the sign of charges twice should leave any system invariant (although any UU^T not necessarily squares to 1). That a Majorana fermion is invariant under charge conjugation also means that it must have neutral charge.

Chiral Majorana Modes

As the normal zero modes of chUE are purely left- or right-handed modes, and as the Hamiltonian of the superconductor is chiral [1, 2], one might ask the question: Can this be the case for a Majorana mode? The answer is no, as can be shown directly in chiral basis. Consider a field in chiral basis

$$\Psi = \begin{pmatrix} \psi_L \\ \psi_R \end{pmatrix}. \tag{2.82}$$

The Majorana condition reads

$$\begin{aligned} \begin{pmatrix} \psi_L \\ \psi_R \end{pmatrix} &= \begin{pmatrix} 0 & i\sigma_2 \\ -i\sigma_2 & 0 \end{pmatrix} \begin{pmatrix} \psi_L \\ \psi_R \end{pmatrix}^* \\ &= \begin{pmatrix} i\sigma_2 \psi_R^* \\ -i\sigma_2 \psi_L^* \end{pmatrix}. \end{aligned} \tag{2.83}$$

Remember that $i\sigma_2$ is real and squares to -1, so this is just one condition

$$\psi_L = i\sigma_2 \psi_R^*, \tag{2.84}$$

which means the components of ψ_L and ψ_R are related by

$$\begin{pmatrix} \psi_R^a \\ \psi_R^b \end{pmatrix} = \begin{pmatrix} 0 & -1 \\ 1 & 0 \end{pmatrix} \begin{pmatrix} \psi_L^a \\ \psi_L^b \end{pmatrix}^* = \begin{pmatrix} -\psi_L^{b\,*} \\ \psi_L^{a\,*} \end{pmatrix}. \tag{2.85}$$

If we chose a purely right- or left-handed field ($\psi_L = 0$ or $\psi_R = 0$ respectively), we would find that the Majorana condition sets both part equal to zero.

This can also be realised without choosing a basis. Considering (say) a left-handed field [41]

$$(1+\gamma_5)\Psi \;=\; 0. \tag{2.86}$$

We apply the charge conjugation operation to it, recalling that γ_5 is hermitian, so $\gamma_5^* = {\gamma_5}^T$

$$\begin{aligned} \gamma_0 C\big((1+\gamma_5)\Psi\big)^* &= 0 \\ (1+\gamma_0 C{\gamma_5}^T)\Psi^* &= 0. \end{aligned} \tag{2.87}$$

Let us briefly consider [41]

$$\begin{aligned} C^{-1}\gamma_\mu C &= U^* U^\dagger \gamma_0 \gamma_\mu \gamma_0 U U^T \\ &= U^* U^\dagger {\gamma_\mu}^\dagger U U^T \\ &= U^* \Big(U\gamma_\mu U\Big)^\dagger U^T \\ &= U^* \tilde{\gamma_\mu}^\dagger U^T \\ &= \Big(U\tilde{\gamma_\mu}^* U^\dagger\Big)^T. \end{aligned} \tag{2.88}$$

In Majorana basis, γ_μ is imaginary, so $\tilde{\gamma_\mu}^* = -\tilde{\gamma_\mu}$

$$C^{-1}\gamma_\mu C = -\Big(U\tilde{\gamma_\mu}U^\dagger\Big)^T = -{\gamma_\mu}^T \tag{2.89}$$

or equivalently

$$C{\gamma_5}^T \;=\; \gamma_5 C. \tag{2.90}$$

Inserting this in (2.87), we find

$$(1+\gamma_0\gamma_5)C\Psi^* \;=\; 0. \tag{2.91}$$

Using the anti-commutator relations for the γ-matrices, we arrive at

$$(1-\gamma_5)\Psi^c \;=\; 0. \tag{2.92}$$

So if Ψ is left-handed, then Ψ^c is right-handed. We therefore conclude that the charge conjugation exchanges the roles of the right- and left part. If we want to construct a mode that is invariant under charge conjugation (i.e. a Majorana mode), we must have both a left- and a right-handed part. Equation (2.85) comes from the spinor indices, which we have not considered in this last part.

2.6.2 Solid State: Majorana Modes as Quasi-particles

Though such a particle has yet to be found among elementary particles, Majorana quasiparticles have been used in solid state physics for many years [30, 40]. There is, however, a huge difference between the solid state and high energy versions of a Majorana fermion. The high energy Majorana particle is just a fermion with a real Dirac equation and thus obeys Fermi-Dirac statistics, whereas the solid state Majorana fermion is a non-Abelian anyon, which means it obeys non-commuting exchange-operations [30]. Anyons are particles that obtain any phase under parity (instead of just ± 1). These can only exist in 2+1 dimensions.

Let us examine the solid state case in more detail. Here, a Majorana mode is any fermionic operator γ_i that obeys [30]

$$[H, \gamma_i] = 0 \quad , \quad \{\gamma_i, \gamma_j\} = 2\delta_{ij}. \tag{2.93}$$

Note that the second condition is the usual $\{\gamma_i^\dagger, \gamma_j\} = 2\delta_{ij}$ for $\gamma_i^\dagger = \gamma_i$. It is therefore more a mode of a particle than a particle in itself.

The Majorana modes must come in pairs, because they are, in a sense, half a fermion.[10] If n pairs of Majorana operators exists, it implies the ground state is 2^n-fold degenerate [40]. Such a degenerate ground state can house quantum information [30].

That the exchange-operations are non-commuting is a very important aspect of these Majorana modes. Clockwise exchange of two operators γ_1, γ_2 is described by $\gamma_j \to B_{12}\gamma_j B_{12}^\dagger$, where

$$B_{12} \;=\; \frac{1}{\sqrt{2}}(1 + \gamma_1\gamma_2) \tag{2.94}$$

is called the braiding operator [40]. The braid analogy becomes more obvious if one considers the world-lines of two exchanging Majorana fermions. In 2+1 dimensions this is a dual helix, and for several pairs this is a braid (one pair is also a braid, but a slightly trivial one). A consequence of this is that clockwise and counter-clockwise exchange are two topological inequivalent operations (a left-handed helix cannot become right-handed without the world-lines crossing or the endpoints leaving the spacial plane). This is also reflected in the exchange relation

$$\begin{aligned} \gamma_1 &\to \mp\gamma_2 \\ \gamma_2 &\to \pm\gamma_1 \end{aligned} \tag{2.95}$$

where the top sign is clockwise exchange [40].

Note that the Majorana condition gives a Majorana field half as many degrees of freedom as a Dirac field. (A Dirac fermion is usually just referred to as a fermion.) This property means we can write the annihilation operator of a Dirac fermion as the sum of two Majorana annihilation operators [40]

$$b \;=\; \frac{1}{2}(\gamma_1 + i\gamma_2). \tag{2.96}$$

[10] The Majorana states are also not physically measurable, only a pair of them is [40].

It can be seen as analogous to Majorana fermions being real fields and Dirac fermions complex ones. The Majorana operators are hermitian, as can be seen when inverting the above[11]

$$\begin{aligned} \gamma_1 &= b^\dagger + b \\ \gamma_2 &= i(b^\dagger - b). \end{aligned} \tag{2.97}$$

This means that a Majorana fermion is its own antiparticle, which is arguably the defining aspect of them in solid state physics.

2.7 Subconclusion

We have now established the mathematical tools necessary for treating the coupled chiral system. First of all, we have have introduced symmetries, through which we will define the coupling, and the effective field theory applied to a supersymmetric ensemble, which works as our theoretical stepping stone for calculation of the eigenvalue spectrum. Secondly, we have introduced random matrix theory as the numerical counterpart and described topology and the role of exact zero modes in both effective theory and random matrices. Finally, we have compared high energy and solid state interpretations of Majorana fermions to start bridging the gap between the coupled chiral system and a physical superconductor.

Let us move on to the coupling itself. We will start out by ensuring that the coupled partition function indeed has the correct properties. This analysis will in large part be an extension of the above considerations. We then use these tools to calculate the eigenvalue density and compare it to numerics.

[11] This also follows directly from the anticommutator relation in (2.93).

Chapter 3

Universal Coupling of Flavours

Now that the necessary tools have been introduced, we return to the main problem at hand: How to calculate the effect of coupling two flavours? In this chapter, we analyse the symmetries, effective theory, and random matrix theory of the coupling. For simplicity, we show this for fermionic flavours and move directly to calculation of the microscopic spectrum in the quenched cases in Chapters 4 and 5.

We approach the coupling in two different cases: Two single-flavour ensembles that are completely independent before the coupling, by which we mean that the partition function factorises, and an ensemble with the two flavours built in, where the uncoupled partition function does not factorise.

First we must ask what characterises the coupling?

The coupling is required to preserve a locked chiral symmetry of the two flavours by coupling the two right-handed and the two left-handed fields.

Let us examine this property in the language of EFT: Expanding the notation from (2.11) in Section 2.2, we want to introduce a term in the effective Lagrangian that sets

$$g_{1R} = g_{2R} \quad , \quad g_{1L} = g_{2L}. \tag{3.1}$$

This means that it must be off-diagonal in flavour space and transform like the massless Dirac operator. (We call this a vectorial term as opposed to an axial term.) So we start out with two coupling constants c_{RR}, c_{LL} that couple right-right and left-left respectively. We set these equal to each other once we understand their transformation properties. The spurion transformation of the coupling constants is[1]

$$c_{RR} \to g_{1R} c_{RR} {g_{2R}}^{\dagger} \quad , \quad c_{LL} \to g_{1L} c_{LL} {g_{2L}}^{\dagger}. \tag{3.2}$$

This follows if we wish coupling terms between the sectors of same chirality. We will use (3.2) to construct terms similar to the chPT approach. We will also argue that there are no other possible terms. This approach used in the case of two single-flavour ensembles. This ensemble will have the uncoupled Goldstone manifold $(U(1) \times U(1))^2$ when we have fermionic flavours only, and each favour has its own topology and mass. We will elaborate on this below.

[1] As with the mass in Equation (2.14), the spurion transformation of a parameter is the transformation we would need to make in order to still have full symmetry.

We can also start from an ensemble with the two flavours, where the flavours can be rotated into each other. This ensemble will have the uncoupled Goldstone manifold $(U(2))^2$. Here we express the coupling as an anti-hermitian vectorial source of the form

$$ic\bar{q}\gamma_0\tau_1 q \tag{3.3}$$

where γ_0 is the zeroth γ-matrix working in chiral space, τ_1 is the first Pauli matrix working in flavour space, and c is a parameter that decides the strength of the coupling. This coupling parameter arises from a rescaling of c_{RR} and c_{LL}.

In both cases we will introduce a corresponding random matrix ensemble. The structure of the random matrices will reflect the structure of the source (3.3), and we will regain the effective theory in the microscopic limit. This strengthens our claim that the terms found are the only possible ones.

Although (3.2) and (3.3) are equivalent, we stress that the two ensembles are very different:

The $U(1) \times U(1)$ ensemble consists of flavours in two independent topological sectors, whereas the $U(2)$ ensemble flavours are born in the same sector. This makes the $U(2)$ case more symmetric and gives an extra degree of freedom to integrate over. For zero coupling, the flavours of the $U(1) \times U(1)$ partition function factorises, unlike $U(2)$.

In this chapter, we establish the partition function of the effective theory and the random matrix ensemble in the two cases. We also compare the $U(2)$ and $U(1)\times U(1)$ ensembles. These discussions of the coupling symmetries serve as a warm-up for calculating the eigenvalue spectrum of the coupled case for both unitary and orthogonal ensembles in Chapters 4 and 5.

3.1 Two Single-Flavour Ensembles: EFT of Flavour Coupling

Let us start with the two single-flavour ensembles, each with their own topology and mass. As mentioned above, the partition function factorises.

$$\begin{aligned} & Z^{\nu_1,\nu_2}_{chUE,1+1}(m_1,m_2) \\ = \; & Z^{\nu_1}_{chUE}(m_1) Z^{\nu_2}_{chUE}(m_2) \\ = \; & \int_{U(1)} dU_1 dU_2 \det{}^{\nu_1}(U_1) \det{}^{\nu_2}(U_2) \exp\left\{ \frac{1}{2}\mathrm{Tr}\left[M_1^\dagger U_1 + M_1 U_1^\dagger + M_2^\dagger U_2 + M_2 U_2^\dagger \right] \right\} \end{aligned} \tag{3.4}$$

The subscript is to distinguish it from the $U(2)$ theory, which we shall denote $Z_{chUE,2}$.

From the spurion transformations (3.2) we can construct the two hermitian coupling terms

$$\mathcal{L}_{coupl} \;=\; K_1 \mathrm{Tr}\left[U_1^\dagger c_{LL} U_2 c_{RR}{}^\dagger + U_1 c_{RR} U_2^\dagger c_{LL}{}^\dagger \right] + iK_2 \mathrm{Tr}\left[U_1^\dagger c_{LL} U_2 c_{RR}{}^\dagger - U_1 c_{RR} U_2^\dagger c_{LL}{}^\dagger \right] \tag{3.5}$$

where K_1 and K_2 are low-energy parameters that cannot be determined by the symmetries.

If we make a $U(1)$ transformation of U_2, we may absorb the K_2-term into the K_1-term

$$\begin{aligned}
& K_1\mathrm{Tr}\left[U_1^\dagger c_{LL} U_2 c_{RR}{}^\dagger + U_1 c_{RR} U_2^\dagger c_{LL}{}^\dagger\right] + iK_2\mathrm{Tr}\left[U_1^\dagger c_{LL} U_2 c_{RR}{}^\dagger - U_1 c_{RR} U_2^\dagger c_{LL}{}^\dagger\right] \\
\to\ & K_1\mathrm{Tr}\left[U_1^\dagger c_{LL} U_2 e^{i\alpha} c_{RR}{}^\dagger + U_1 c_{RR} U_2^\dagger e^{-i\alpha} c_{LL}{}^\dagger\right] + iK_2\mathrm{Tr}\left[U_1^\dagger c_{LL} U_2 e^{i\alpha} c_{RR}{}^\dagger - U_1 c_{RR} U_2^\dagger e^{-i\alpha} c_{LL}{}^\dagger\right] \\
=\ & K_1\mathrm{Tr}\left[(\cos(\alpha)+i\sin(\alpha))U_1^\dagger c_{LL} U_2 c_{RR}{}^\dagger + (\cos(\alpha)-i\sin(\alpha))U_1 c_{RR} U_2^\dagger c_{LL}{}^\dagger\right] \\
& + iK_2\mathrm{Tr}\left[(\cos(\alpha)+i\sin(\alpha))U_1^\dagger c_{LL} U_2 c_{RR}{}^\dagger - (\cos(\alpha)-i\sin(\alpha))U_1 c_{RR} U_2^\dagger c_{LL}{}^\dagger\right] \\
=\ & \mathrm{Tr}\Big[(K_1\cos(\alpha)-K_2\sin(\alpha))U_1^\dagger c_{LL} U_2 c_{RR}{}^\dagger + (K_1\cos(\alpha)-K_2\sin(\alpha))U_1 c_{RR} U_2^\dagger c_{LL}{}^\dagger \\
& + i(K_2\cos(\alpha)+K_1\sin(\alpha))U_1^\dagger c_{LL} U_2 c_{RR}{}^\dagger - i(K_2\cos(\alpha)+K_1\sin(\alpha))U_1 c_{RR} U_2^\dagger c_{LL}{}^\dagger\Big].
\end{aligned} \tag{3.6}$$

For

$$\alpha = -\arctan\left(\frac{K_2}{K_1}\right) \quad , \quad \big(K_1\cos(\alpha) - K_2\sin(\alpha)\big) \to K_1 \tag{3.7}$$

the K_2-term disappears.

In the full partition function, such a transformation corresponds to a difference in phase of the masses if we absorb an overall constant in the partition function. Because we want to examine the case where the masses of the two flavours are the same, we will set $K_2 = 0$ and $m_1 = m_2 = m$ in the following. We will also define $\tilde{c} \equiv \sqrt{c_{LL}c_{RR}}$ as we no longer need the individual transformation properties.

If we expand our counting to $\tilde{c}^2 V K_1 \equiv c^2 = \mathcal{O}(1)$, we may write

$$\begin{aligned}
Z^{\nu_1,\nu_2}_{chUE,1+1}(M,c) &= \int_{U(1)} dU_1 dU_2 \det{}^{\nu_1}(U_1)\det{}^{\nu_2}(U_2) \\
&\quad \times \exp\left\{\frac{1}{2}\mathrm{Tr}\left[M^\dagger U_1 + M U_1^\dagger + M^\dagger U_2 + M U_2^\dagger\right] + c^2\mathrm{Tr}\left[U_1{}^\dagger U_2 + U_2{}^\dagger U_1\right]\right\}.
\end{aligned} \tag{3.8}$$

This is can be considered the basic coupled EFT, to which we shall return numerous times. The structure of other ensembles will be the same, although the relevant group will change.

3.2 Two Single-Flavour Ensembles: EFT of Coupled RMT

In this section we introduce the random matrix ensemble corresponding to 3.8 and show that they agree in the microscopic limit.

To construct a random matrix model with the symmetries of the coupling, we expand the standard chiral RMT (2.62) by placing each single flavour in the diagonal blocks of a larger matrix. These blocks correspond to flavour space. Off-diagonal matrices with off-diagonal substructure are added to couple the two flavours. Note the structure from (3.3). The τ_1 in flavour space places us in the off-diagonal sub-matrices, and, because $\gamma_0 = \begin{pmatrix} 0 & 1 \\ 1 & 0 \end{pmatrix}$ in chiral basis, the coupling parameter is placed on the off-diagonal part of these. This takes the form

$$Z^{n,\nu_1,\nu_2}_{chGUE,1+1} = \int dW_1 dW_2 \det \begin{pmatrix} m_R & iW_1 & 0 & ic_R \\ iW_1^\dagger & m_R & ic_R & 0 \\ 0 & ic_R & m_R & iW_2 \\ ic_R & 0 & iW_2^\dagger & m_R \end{pmatrix} e^{-n\mathrm{Tr}\left(W_1 W_1^\dagger + W_2 W_2^\dagger\right)} \tag{3.9}$$

where W_1, W_2 are complex $(n+\nu_1)\times n$ and $(n+\nu_2)\times n$ matrices respectively, and m_R, c_R are dimensionless parameters we shall later relate to physical ones. There are implicit identity matrices of appropriate sizes padded with zeros where necessary.

For instance, in the case $\nu_1 = 0, \nu_2 = 1$, and $n = 2$, the upper right-hand block is

$$\begin{pmatrix} 0 & 0 & 0 & ic_R & 0 \\ 0 & 0 & 0 & 0 & ic_R \\ ic_R & 0 & 0 & 0 & 0 \\ 0 & ic_R & 0 & 0 & 0 \end{pmatrix} \tag{3.10}$$

and the lower left-hand block is the transposed of this.

We shall return to the symmetries of this ensemble in chapter 3.3, where we will see that this is indeed the correct random matrices to consider. (This is also evident from the following derivation, where we show that it has the right low-energy effective theory, but we will show it directly from the symmetries.)

Let us derive low-energy effective theory. The following will be analogous to the derivation from [7] and [17], but with the extra off-diagonal terms. First, we express the determinant as fermionic integrals:

$$\begin{aligned} Z^{n,\nu_1,\nu_2}_{chGUE,1+1} &= \int dW_1 dW_2 d\phi^1 d\phi^2 d\psi^1 d\psi^2 e^{-n\mathrm{Tr}\left(W_1W_1^\dagger + W_2W_2^\dagger\right)} \\ &\times \exp\left\{ \begin{pmatrix}\psi^1\\ \phi^1\\ \psi^2\\ \phi^2\end{pmatrix}^\dagger \begin{pmatrix} m_R & iW_1 & 0 & ic_R \\ iW_1^\dagger & m_R & ic_R & 0 \\ 0 & ic_R & m_R & iW_2 \\ ic_R & 0 & iW_2^\dagger & m_R \end{pmatrix} \begin{pmatrix}\psi^1\\ \phi^1\\ \psi^2\\ \phi^2\end{pmatrix} \right\}. \end{aligned} \tag{3.11}$$

We then write W_j as $a_j + ib_j$ and perform the integrals over these.

$$\begin{aligned} Z^{n,\nu_1,\nu_2}_{chGUE,1+1} &= \int da_1 da_2 db_1 db_2 d\phi^1 d\phi^2 d\psi^1 d\psi^2 \exp\Big\{ -n\left(a^2_{1ij} + b^2_{1ij} + a^2_{2ij} + b^2_{2ij}\right) \\ &+ia_{1ij}(\psi_i^{1^*}\phi_j^1 - \psi_i^1\phi_j^{1^*}) + ia_{2ij}(\psi_i^{2^*}\phi_j^2 - \psi_i^2\phi_j^{2^*}) \\ &-b_{1ij}(\psi_i^{1^*}\phi_j^1 + \psi_i^1\phi_j^{1^*}) - b_{2ij}(\psi_i^{2^*}\phi_j^2 + \psi_i^2\phi_j^{2^*}) \\ &+m_R\big(\psi_i^{1^*}\psi_i^1 + \phi_i^{1^*}\phi_i^1 + \psi_i^{2^*}\psi_i^2 + \phi_i^{2^*}\phi_i^2\big) \\ &+ic_R(\phi_i^{1^*}\psi_i^2 + \psi_i^{1^*}\phi_i^2 + \phi_i^{2^*}\psi_i^1 + \psi_i^{2^*}\phi_i^1)\Big\} \\ &= \int d\phi^1 d\phi^2 d\psi^1 d\psi^2 \exp\Big\{ \frac{1}{n}\left(\psi_i^{1^*}\psi_i^1\phi_j^{1^*}\phi_j^1 + \psi_i^{2^*}\psi_i^2\phi_j^{2^*}\phi_j^2\right) \\ &+m_R\big(\psi_i^{1^*}\psi_i^1 + \phi_i^{1^*}\phi_i^1 + \psi_i^{2^*}\psi_i^2 + \phi_i^{2^*}\phi_i^2\big) \\ &+ic_R(\phi_i^{1^*}\psi_i^2 + \psi_i^{1^*}\phi_i^2 + \phi_i^{2^*}\psi_i^1 + \psi_i^{2^*}\phi_i^1)\Big\} \\ &= \int d\phi^1 d\phi^2 d\psi^1 d\psi^2 \exp\Big\{ \frac{1}{4n}\Big(\\ &(\psi_i^{1^*}\psi_i^1 + \phi_i^{1^*}\phi_i^1)(\psi_j^{1^*}\psi_j^1 + \phi_j^{1^*}\phi_j^1) - (\psi_i^{1^*}\psi_i^1 - \phi_i^{1^*}\phi_i^1)(\psi_j^{1^*}\psi_j^1 - \phi_j^{1^*}\phi_j^1) \\ &+(\psi_i^{2^*}\psi_i^2 + \phi_i^{2^*}\phi_i^2)(\psi_j^{2^*}\psi_j^2 + \phi_j^{2^*}\phi_j^2) - (\psi_i^{2^*}\psi_i^2 - \phi_i^{2^*}\phi_i^2)(\psi_j^{2^*}\psi_j^2 - \phi_j^{2^*}\phi_j^2)\Big) \\ &+m_R\big(\psi_i^{1^*}\psi_i^1 + \phi_i^{1^*}\phi_i^1 + \psi_i^{2^*}\psi_i^2 + \phi_i^{2^*}\phi_i^2\big) \\ &+ic_R(\phi_i^{1^*}\psi_i^2 + \psi_i^{1^*}\phi_i^2 + \phi_i^{2^*}\psi_i^1 + \psi_i^{2^*}\phi_i^1)\Big\}. \end{aligned} \tag{3.12}$$

This is a slight abuse of notation, so one should be careful here. Because c_R is not necessarily square, the vectors ϕ^1 and ψ^2 are not necessarily the same length. Since c_R is an identity matrix padded with zeros, it is implied that the spare entries of each vector has been removed in the coupling terms. We make four Hubbard-Stratanovitch transformations

$$\begin{aligned} Z^{n,\nu_1,\nu_2}_{chGUE,1+1} &= \int d\sigma_1 d\sigma_2 d\bar{\sigma}_1 d\bar{\sigma}_2 d\phi^1 d\phi^2 d\psi^1 d\psi^2 \exp\Big\{ -n\mathrm{Tr}(\sigma_1\sigma_1^T + \sigma_2\sigma_2^T + \bar{\sigma}_1\bar{\sigma}_1^T + \bar{\sigma}_2\bar{\sigma}_2^T) \\ &+\sigma_1(\psi_i^{1^*}\psi_i^1 + \phi_j^{1^*}\phi_j^1) + i\bar{\sigma}_1(\psi_i^{1^*}\psi_i^1 - \phi_j^{1^*}\phi_j^1) \\ &+\sigma_2(\psi_i^{2^*}\psi_i^2 + \phi_j^{2^*}\phi_j^2) + i\bar{\sigma}_2(\psi_i^{2^*}\psi_i^2 - \phi_j^{2^*}\phi_j^2) \\ &+m_R\big(\psi_i^{1^*}\psi_i^1 + \phi_i^{1^*}\phi_i^1 + \psi_i^{2^*}\psi_i^2 + \phi_i^{2^*}\phi_i^2\big) \\ &+ic_R(\phi_i^{1^*}\psi_i^2 + \psi_i^{1^*}\phi_i^2 + \phi_i^{2^*}\psi_i^1 + \psi_i^{2^*}\phi_i^1)\Big\}, \end{aligned} \tag{3.13}$$

where $\sigma_j, \bar{\sigma}_j$ are arbitrary real matrices [7]. See Appendix B.1 for an introduction to the Hubbard-Stratanovitch transformation. Defining $A_j = \sigma_j + i\bar{\sigma}_j$ and $A_j^\dagger = \sigma_j - i\bar{\sigma}_j$, we find

$$\begin{aligned} Z^{n,\nu_1,\nu_2}_{chGUE,1+1} &= \int dA_1 dA_2 d\phi^1 d\phi^2 d\psi^1 d\psi^2 \exp\Big\{ -n\mathrm{Tr}(A_1A_1^\dagger + A_2A_2^\dagger) \\ &+\psi_i^{1^*}(A_1 + m_R)\psi_i^1 + \phi_j^{1^*}(A_1^\dagger + m_R)\phi_j^1 \\ &+\psi_i^{2^*}(A_2 + m_R)\psi_i^2 + \phi_j^{2^*}(A_2^\dagger + m_R)\phi_j^2 \\ &+ic_R(\phi_i^{1^*}\psi_i^2 + \psi_i^{1^*}\phi_i^2 + \phi_i^{2^*}\psi_i^1 + \psi_i^{2^*}\phi_i^1)\Big\}. \end{aligned} \tag{3.14}$$

We first do the $n+\nu_1$ and $n+\nu_2$ integrals over ψ^1 and ψ^2 respectively, and thereafter the n integrals over ϕ^1 and ϕ^2, keeping in mind that the c_R-part only has n integrals for each

$$\begin{aligned} Z^{n,\nu_1,\nu_2}_{chGUE,1+1} &= \int dA_1 dA_2 d\phi^1 d\phi^2 \det{}^{n+\nu_1}(A_1 + m_R)\det{}^{n+\nu_2}(A_2 + m_R)\exp\Big\{ -n\mathrm{Tr}(A_1A_1^\dagger + A_2A_2^\dagger) \\ &+c_R^2\phi_i^{2^*}(A_1 + m_R)^{-1}\phi_i^2 + \phi_j^{1^*}(A_1^\dagger + m_R)\phi_j^1 \\ &+c_R^2\phi_i^{2^*}(A_2 + m_R)^{-1}\phi_i^2 + \phi_j^{2^*}(A_2^\dagger + m_R)\phi_j^2\Big\} \\ &= \int dA_1 dA_2 \exp\Big\{ -n\mathrm{Tr}(A_1A_1^\dagger + A_2A_2^\dagger)\Big\}\det{}^{n+\nu_1}(A_1 + m_R)\det{}^{n+\nu_2}(A_2 + m_R) \\ &\times\det{}^n\big(A_1^\dagger + m_R + c_R^2(A_2 + m_R)^{-1}\big)\det{}^n\big(A_2^\dagger + m_R + c_R^2(A_1 + m_R)^{-1}\big) \\ &= \int dA_1 dA_2 \exp\Big\{ -n\mathrm{Tr}(A_1A_1^\dagger + A_2A_2^\dagger)\Big\}\det{}^{\nu_1}(A_1 + m_R)\det{}^{\nu_2}(A_2 + m_R) \\ &\times\det{}^n\big((A_2 + m_R)(A_1^\dagger + m_R) + c_R^2\big)\det{}^n\big((A_1 + m_R)(A_2^\dagger + m_R) + c_R^2\big) \\ &= \int dA_1 dA_2 \exp\Big\{ -n\mathrm{Tr}(A_1A_1^\dagger + A_2A_2^\dagger)\Big\}\det{}^{\nu_1}(A_1 + m_R)\det{}^{\nu_2}(A_2 + m_R) \\ &\times\det{}^n\Big(\big(m_RA_2 + m_RA_1^\dagger + A_2A_1^\dagger + c_R^2\big)\big(m_RA_1 + m_RA_2^\dagger + A_1A_2^\dagger + c_R^2\big)\Big). \end{aligned} \tag{3.15}$$

We have ignored terms of $\mathcal{O}(m_R^2)$. In the following, we also ignore terms of the kind $c_R^2 m_R$ and

c_R^4, as these are $\mathcal{O}(n^{-2})$

$$\begin{aligned} Z^{n,\nu_1,\nu_2}_{chGUE,1+1} &= \int dA_1 dA_2 \exp\Big\{ -n\mathrm{Tr}(A_1A_1^\dagger + A_2A_2^\dagger)\Big\}\det{}^{\nu_1}(A_1+m_R)\det{}^{\nu_2}(A_2+m_R) \\ &\quad \times\det{}^n\Big(m_RA_2A_1A_2^\dagger + m_RA_2A_1^\dagger A_2^\dagger + m_RA_2 + m_RA_2^\dagger + c_R^2(A_2A_1^\dagger + A_1A_2^\dagger) + 1\Big) \\ &= \int dA_1 dA_2 \exp\Big\{ -n\mathrm{Tr}(A_1A_1^\dagger + A_2A_2^\dagger)\Big\}\det{}^{\nu_1}(A_1+m_R)\det{}^{\nu_2}(A_2+m_R) \\ &\quad \times \exp\Big\{n\mathrm{Tr}\Big[\ln\Big(m_RA_2A_1A_2^\dagger + m_RA_2A_1^\dagger A_2^\dagger + m_RA_2 + m_RA_2^\dagger + c_R^2(A_2A_1^\dagger + A_1A_2^\dagger) + 1\Big)\Big]\Big\}. \end{aligned} \tag{3.16}$$

We diagonalise with the unitary matrices $A_j = U_j\Lambda_j V_j$. Using a saddle point approximation we find that the Gaussian term sets $\Lambda \propto \mathbf{1}$, see Appendix B.2. The Gaussian term is dominant since it is $\mathcal{O}(n)$, whereas all other terms are no higher than $\mathcal{O}(1)$. We then absorb V in U and expand the logarithm.

$$\begin{aligned} Z^{n,\nu_1,\nu_2}_{chGUE,1+1} &= \int dU_1 dU_2 \det{}^{\nu_1}(U_1+m_R)\det{}^{\nu_2}(U_2+m_R) \\ &\quad \times \exp\Big\{n\mathrm{Tr}\Big[\ln\Big(m_RU_2U_1U_2^\dagger + m_RU_2U_1^\dagger U_2^\dagger + m_RU_2 + m_RU_2^\dagger + c_R^2(U_2U_1^\dagger + U_1U_2^\dagger) + 1\Big)\Big]\Big\} \\ &= \int dU_1 dU_2 \det{}^{\nu_1}(U_1+m_R)\det{}^{\nu_2}(U_2+m_R) \\ &\quad \times \exp\Big\{n\mathrm{Tr}\Big[m_RU_2U_1U_2^\dagger + m_RU_2U_1^\dagger U_2^\dagger + m_RU_2 + m_RU_2^\dagger + c_R^2(U_2U_1^\dagger + U_1U_2^\dagger)\Big]\Big\} \\ &= \int dU_1 dU_2 \det{}^{\nu_1}(U_1+m_R)\det{}^{\nu_2}(U_2+m_R) \\ &\quad \exp\Big\{n\mathrm{Tr}\Big[m_RU_1 + m_RU_1^\dagger + m_RU_2 + m_RU_2^\dagger + c_R^2(U_2U_1^\dagger + U_1U_2^\dagger)\Big]\Big\}. \end{aligned} \tag{3.17}$$

Letting $n \to \infty$ while keeping $m = 2nm_R$ and $c^2 = nc_R^2$ constant yields our final effective partition function.

$$\begin{aligned} Z^{\nu_1,\nu_2}_{chUE,1+1} &= \int dU_1 dU_2 \det{}^{\nu_1}(U_1)\det{}^{\nu_2}(U_2) \\ &\quad \times \exp\Big\{\frac{m}{2}\mathrm{Tr}\Big[U_1 + U_1^\dagger + U_2 + U_2^\dagger\Big] + c^2\mathrm{Tr}\Big[U_2U_1^\dagger + U_1U_2^\dagger\Big]\Big\} \end{aligned} \tag{3.18}$$

This is also where we see the relations for chUE

$$\begin{aligned} m_qV\Sigma_0 &= 2nm_R \equiv m \\ \lambda V\Sigma_0 &= 2n\lambda_R \equiv u \\ \tilde{c}^2VK_1 &= nc_R^2 \equiv c^2 \end{aligned} \tag{3.19}$$

that become especially important in the numerical verification in Chapter 6. The eigenvalues must be scaled the same way as the mass, which leads to the second line. These relations were first calculated (although not explicitly stated) in [7]. We refer to (3.19) as the correspondence scheme between chPT and RMT. Note that this scheme is not the same for the unitary and orthogonal ensembles. The correspondence scheme for the chiral orthogonal ensemble may be found in (3.68).

3.3 Two Single-Flavour Ensembles: Symmetries

Let us review the symmetries of the coupled ensemble more explicitly. We know the massless QCD-Lagrangian has a $U(N_f) \times U(N_f)$-symmetry in flavour space for a fixed topology, which is broken to $U(N_f)$ for non-zero mass. We want the coupled system to share this property. Let us approach this through the random matrix ensemble. Since we have just shown that the theory

$$\begin{aligned} Z^{\nu_1,\nu_2}_{chUE,1+1} &= \int dW_1 dW_2 d\phi^1 d\phi^2 d\psi^1 d\psi^2 e^{-n\mathrm{Tr}\left(W_1 W_1^\dagger + W_2 W_2^\dagger\right)} \\ &\times \exp\left\{ \begin{pmatrix} \psi^1 \\ \phi^1 \\ \psi^2 \\ \phi^2 \end{pmatrix}^\dagger \begin{pmatrix} m_R & iW_1 & 0 & ic_R \\ iW_1^\dagger & m_R & ic_R & 0 \\ 0 & ic_R & m_R & iW_2 \\ ic_R & 0 & iW_2^\dagger & m_R \end{pmatrix} \begin{pmatrix} \psi^1 \\ \phi^1 \\ \psi^2 \\ \phi^2 \end{pmatrix} \right\} \end{aligned} \tag{3.20}$$

has the desired effective theory, any symmetry we can show here, will also be a symmetry of the effective theory. Since the weight is invariant under any unitary transformation, we will only look at

$$\begin{pmatrix} \psi^1 \\ \phi^1 \\ \psi^2 \\ \phi^2 \end{pmatrix}^\dagger \begin{pmatrix} m_R & iW_1 & 0 & ic_R \\ iW_1^\dagger & m_R & ic_R & 0 \\ 0 & ic_R & m_R & iW_2 \\ ic_R & 0 & iW_2^\dagger & m \end{pmatrix} \begin{pmatrix} \psi^1 \\ \phi^1 \\ \psi^2 \\ \phi^2 \end{pmatrix}, \tag{3.21}$$

which may be directly interpreted as the quark part of the action.

It is worth repeating that each section of the matrix has a well defined interpretation. If viewed as the outer product of two 2×2 matrices, the large structure corresponds to flavour space and the small structure to chiral space.

Let us consider the following transformations: Vectorial $U(1)$, axial $U(1)$ for both $m_R = 0$ and $m_R \neq 0$, vectorial $U(1) \times U(1)$, and vectorial $U(2)$.

The vectorial $U(1)$-symmetry is merely the addition of a phase to all quark fields, so it follows quite easily for both $m_R = 0$ and $m_R \neq 0$.

Let us instead look closer at the breaking of the axial symmetry for non-zero mass. For $m = 0$ we can make the axial $U(1)$-transformation

$$\begin{pmatrix} \psi^1 \\ \phi^1 \\ \psi^2 \\ \phi^2 \end{pmatrix} \to e^{i\theta_5\gamma_5} \begin{pmatrix} \psi^1 \\ \phi^1 \\ \psi^2 \\ \phi^2 \end{pmatrix} = \left(\cos(\theta_5)\mathbf{1}_2 + i\sin(\theta_5)\gamma_5\right) \otimes \begin{pmatrix} 1 & 0 \\ 0 & 1 \end{pmatrix} \begin{pmatrix} \psi^1 \\ \phi^1 \\ \psi^2 \\ \phi^2 \end{pmatrix} \tag{3.22}$$

where γ_5 works in chiral space. In chiral basis $\gamma_5 = \begin{pmatrix} -1 & 0 \\ 0 & 1 \end{pmatrix}$.

Note that we have neglected a $\mathbf{1}_2\gamma_0$ in the theory, because the massless Dirac operator is $\bar{q}\not{D}q$ rather than $q^\dagger \not{D} q$. It disappears in the determinant, but if we are to identify the left and right fields as we have written them in our Grassmann integral, the transformation of the hermitian

conjugated fields must be

$$\begin{pmatrix}\psi^1\\ \phi^1\\ \psi^2\\ \phi^2\end{pmatrix}^\dagger \rightarrow \begin{pmatrix}\psi^1\\ \phi^1\\ \psi^2\\ \phi^2\end{pmatrix} e^{i\theta_5\gamma_5} = \begin{pmatrix}\psi^1\\ \phi^1\\ \psi^2\\ \phi^2\end{pmatrix} \big(\cos(\theta_5)\mathbf{1}_2 + i\sin(\theta_5)\gamma_5\big) \otimes \begin{pmatrix}1 & 0\\ 0 & 1\end{pmatrix} \tag{3.23}$$

because γ_5 anticommutes with γ_0.

We apply this transformation to equation 3.21 for $m = 0$ and neglect the vectors for compact notation:

$$\begin{aligned}
&\big(\cos(\theta_5)\mathbf{1}_2 + i\sin(\theta_5)\gamma_5\big) \otimes \begin{pmatrix}1 & 0\\ 0 & 1\end{pmatrix} \begin{pmatrix} 0 & iW_1 & 0 & ic_R \\ iW_1^\dagger & 0 & ic_R & 0 \\ 0 & ic_R & 0 & iW_2 \\ ic_R & 0 & iW_2^\dagger & 0 \end{pmatrix} \big(\cos(\theta_5)\mathbf{1}_2 + i\sin(\theta_5)\gamma_5\big) \otimes \begin{pmatrix}1 & 0\\ 0 & 1\end{pmatrix} \\
= \;& \cos^2(\theta_5) \begin{pmatrix} 0 & iW_1 & 0 & ic_R \\ iW_1^\dagger & 0 & ic_R & 0 \\ 0 & ic_R & 0 & iW_2 \\ ic_R & 0 & iW_2^\dagger & 0 \end{pmatrix} - \sin^2(\theta_5) \begin{pmatrix} 0 & -iW_1 & 0 & -ic_R \\ -iW_1^\dagger & 0 & -ic_R & 0 \\ 0 & -ic_R & 0 & -iW_2 \\ -ic_R & 0 & -iW_2^\dagger & 0 \end{pmatrix} \\
& +i\cos(\theta_5)\sin(\theta_5) \left(\begin{pmatrix} 0 & iW_1 & 0 & ic_R \\ -iW_1^\dagger & 0 & -ic_R & 0 \\ 0 & ic_R & 0 & iW_2 \\ -ic_R & 0 & -iW_2^\dagger & 0 \end{pmatrix} + \begin{pmatrix} 0 & -iW_1 & 0 & -ic_R \\ iW_1^\dagger & 0 & ic_R & 0 \\ 0 & -ic_R & 0 & -iW_2 \\ ic_R & 0 & iW_2^\dagger & 0 \end{pmatrix} \right) \\
= \;& \begin{pmatrix} 0 & iW_1 & 0 & ic_R \\ iW_1^\dagger & 0 & ic_R & 0 \\ 0 & ic_R & 0 & iW_2 \\ ic_R & 0 & iW_2^\dagger & 0 \end{pmatrix}
\end{aligned} \tag{3.24}$$

Expressed in words, the transformation leaves the matrix unchanged.

For $m \neq 0$, this symmetry is broken

$$\begin{aligned}
&\left(\cos(\theta_5)\mathbf{1}_2 + i\sin(\theta_5)\gamma_5\right)\begin{pmatrix}1 & 0\\ 0 & 1\end{pmatrix}\begin{pmatrix} m_R & iW_1 & 0 & ic_R \\ iW_1^\dagger & m_R & ic_R & 0 \\ 0 & ic_R & m_R & iW_2 \\ ic_R & 0 & iW_2^\dagger & m_R\end{pmatrix}\left(\cos(\theta_5)\mathbf{1}_2 + i\sin(\theta_5)\gamma_5\right)\begin{pmatrix}1 & 0\\ 0 & 1\end{pmatrix} \\
= \;& \cos^2(\theta_5)\begin{pmatrix} m_R & iW_1 & 0 & ic_R \\ iW_1^\dagger & m_R & ic_R & 0 \\ 0 & ic_R & m_R & iW_2 \\ ic_R & 0 & iW_2^\dagger & m_R\end{pmatrix} - \sin^2(\theta_5)\begin{pmatrix} m_R & -iW_1 & 0 & -ic_R \\ -iW_1^\dagger & m_R & -ic_R & 0 \\ 0 & -ic_R & m_R & -iW_2 \\ -ic_R & 0 & -iW_2^\dagger & m_R\end{pmatrix} \\
& +i\cos(\theta_5)\sin(\theta_5)\left(\begin{pmatrix} m_R & iW_1 & 0 & ic_R \\ -iW_1^\dagger & -m_R & -ic_R & 0 \\ 0 & ic_R & m_R & iW_2 \\ -ic_R & 0 & -iW_2^\dagger & -m_R\end{pmatrix} + \begin{pmatrix} m_R & -iW_1 & 0 & -ic_R \\ iW_1^\dagger & -m_R & ic_R & 0 \\ 0 & -ic_R & m_R & -iW_2 \\ ic_R & 0 & iW_2^\dagger & -m_R\end{pmatrix}\right) \\
= \;& \begin{pmatrix} 2m_R & 0 & 0 & 0 \\ 0^\dagger & -2m_R & 0 & 0 \\ 0 & 0 & 2m_R & 0 \\ 0 & 0 & 0 & -2m_R\end{pmatrix} \neq \begin{pmatrix} m_R & iW_1 & 0 & ic_R \\ iW_1^\dagger & m_R & ic_R & 0 \\ 0 & ic_R & m_R & iW_2 \\ ic_R & 0 & iW_2^\dagger & m_R\end{pmatrix},
\end{aligned} \tag{3.25}$$

which shows that the coupling breaks symmetry in the right way. Note that a coupling matrix of the kind $\begin{pmatrix} m_R & ic_R \\ ic_R & m_R\end{pmatrix}$ would also break symmetry in the same way, but would gives rise to a higher order term of m in the effective theory.

The coupling should force any chiral transformation to be the same for the two flavours. We have already seen how the axial part behaves in chiral space, so let us just look at the breaking of individual vectorial symmetry $U(1) \times U(1) \to U(1)$

$$\begin{aligned}
&\begin{pmatrix} e^{-i\theta_1} & 0 & 0 & 0 \\ 0 & e^{-i\theta_1} & 0 & 0 \\ 0 & 0 & e^{-i\theta_2} & 0 \\ 0 & 0 & 0 & e^{-i\theta_2}\end{pmatrix}\begin{pmatrix} m_R & iW_1 & 0 & ic_R \\ iW_1^\dagger & m_R & ic_R & 0 \\ 0 & ic_R & m_R & iW_2 \\ ic_R & 0 & iW_2^\dagger & m_R\end{pmatrix}\begin{pmatrix} e^{i\theta_1} & 0 & 0 & 0 \\ 0 & e^{i\theta_1} & 0 & 0 \\ 0 & 0 & e^{i\theta_2} & 0 \\ 0 & 0 & 0 & e^{i\theta_2}\end{pmatrix} \\
= \;& \begin{pmatrix} m_R & iW_1 & 0 & ic_R e^{i(\theta_2-\theta_1)} \\ iW_1^\dagger & m_R & ic_R e^{i(\theta_2-\theta_1)} & 0 \\ 0 & ic_R e^{i(\theta_1-\theta_2)} & m_R & iW_2 \\ ic_R e^{i(\theta_1-\theta_2)} & 0 & iW_2^\dagger & m_R\end{pmatrix}
\end{aligned} \tag{3.26}$$

So for $c \neq 0$ we require $\theta_1 = \theta_2$.

Let us finally consider the larger symmetry group $U(2)$. Remember that two single flavours do not have this symmetry. Only if the flavours are part of the same theory are they invariant. This is also reflected in the RMT: As long as $W_1 \neq W_2$ the theory does not have this symmetry.

The vectorial $U(2)$-transformation can be parametrised by $\exp\left\{\sum_{k=0}^{3} i\theta_k\tau_k\right\}$, where the Pauli matrices work in flavour space. We can consider one generator at a time. See for instance

the $k = 1$ part:

$$\begin{aligned}
& \mathbf{1}_2 \left(\cos(\theta_1) \begin{pmatrix} 1 & 0 \\ 0 & 1 \end{pmatrix} - i \sin(\theta_1) \begin{pmatrix} 0 & 1 \\ 1 & 0 \end{pmatrix} \right) \begin{pmatrix} 0 & iW_1 & 0 & 0 \\ iW_1^\dagger & 0 & 0 & 0 \\ 0 & 0 & 0 & iW_2 \\ 0 & 0 & iW_2^\dagger & 0 \end{pmatrix} \\
& \times \mathbf{1}_2 \left(\cos(\theta_1) \begin{pmatrix} 1 & 0 \\ 0 & 1 \end{pmatrix} + i \sin(\theta_1) \begin{pmatrix} 0 & 1 \\ 1 & 0 \end{pmatrix} \right) \\
= \; & \cos^2(\theta_1) \begin{pmatrix} 0 & iW_1 & 0 & 0 \\ iW_1^\dagger & 0 & 0 & 0 \\ 0 & 0 & 0 & iW_2 \\ 0 & 0 & iW_2^\dagger & 0 \end{pmatrix} + \sin^2(\theta_1) \begin{pmatrix} 0 & iW_2 & 0 & 0 \\ iW_2^\dagger & 0 & 0 & 0 \\ 0 & 0 & 0 & iW_1 \\ 0 & 0 & iW_1^\dagger & 0 \end{pmatrix} \\
& + i \cos(\theta_1) \sin(\theta_1) \left(\begin{pmatrix} 0 & 0 & 0 & iW_1 \\ 0 & 0 & iW_1^\dagger & 0 \\ 0 & iW_2 & 0 & 0 \\ iW_2^\dagger & 0 & 0 & 0 \end{pmatrix} - \begin{pmatrix} 0 & 0 & 0 & iW_2 \\ 0 & 0 & iW_2^\dagger & 0 \\ 0 & iW_1 & 0 & 0 \\ iW_1^\dagger & 0 & 0 & 0 \end{pmatrix} \right) \\
\neq \; & \begin{pmatrix} 0 & iW_1 & 0 & 0 \\ iW_1^\dagger & 0 & 0 & 0 \\ 0 & 0 & 0 & iW_2 \\ 0 & 0 & iW_2^\dagger & 0 \end{pmatrix}.
\end{aligned} \tag{3.27}$$

The other generators fail in similar fashion.

The $W_1 = W_2$ case corresponds to having the two flavours in the same gauge field configuration, which is the next case we consider.

3.4 Two-Flavour Ensemble: EFT of Flavour Coupling

Let us now turn to the case of two coupled flavours, where the flavours can be rotated into each other, because they interact with the same gauge field. As for the two single-flavour ensembles, we analyse its properties for fermionic flavours for the sake of simplicity.

Using the source from (3.3) we can adapt the general solution of the Lagrangian from (2.26) to the lowest order ϵ-counting. We ignore the mass terms in the following.

$$\begin{aligned}
\mathcal{L}_{EFT} &= \frac{f^2}{4} \mathrm{Tr} \left(\left(\partial_\mu U^\dagger - c U^\dagger \delta_{0\mu} \tau_1 + c \delta_{0\mu} \tau_1 U^\dagger \right) \left(\partial_\mu U + \delta_{0\mu} \tau_1 U - U \delta_{0\mu} \tau_1 \right) \right) \\
&= \frac{f^2}{4} \mathrm{Tr} \left(\partial_\mu U^\dagger \partial_\mu U + 2c^2 \left(\tau_1 U \tau_1 U^\dagger - 1 \right) + c \left(\partial_0 U^\dagger \tau_1 U + U^\dagger \partial_0 U \tau_1 - \partial_0 U^\dagger U \tau_1 - U^\dagger \tau_1 \partial_0 U \right) \right)
\end{aligned} \tag{3.28}$$

We use the parametrisation from before $U = u e^{i\xi(x)} u$. We remind ourselves that $\xi = \mathcal{O}(\epsilon)$, so we can ignore the higher order terms when expanding the exponential. The remaining terms are

$$\mathcal{L}_{EFT} = \frac{f^2}{4} \mathrm{Tr} \left(\partial_\mu \xi \partial_\mu \xi + 2c^2 \left(\tau_1 u^2 \tau_1 {u^\dagger}^2 - 1 \right) + 2c \left(i \partial_0 \xi u \tau_1 u^\dagger - i \partial_0 \xi u^\dagger \tau_1 u \right) \right) \tag{3.29}$$

Although the last two terms are the same order as first two, they appear as a total derivative of the field ξ. They therefore disappear when we integrate over the four volume, if the field is well behaved at the border.

Absorbing a constant into c, our effective partition function becomes

$$Z_{chUE,2}(M) = \int_{SU(2)} dU e^{\frac{1}{2}\mathrm{Tr}\left(MU+MU^\dagger\right)+c^2\mathrm{Tr}\left(\tau_1 U\tau_1 U^\dagger-1\right)}. \tag{3.30}$$

This is for all topologies. The individual topological sectors can be found through a Fourier transform of $Z(M,\theta) = Z(Me^{i\theta/N_f},0) \equiv Z(Me^{i\theta/N_f})$ as discussed in (2.37). In this case $N_f = 2$

$$Z^\nu_{chUE,2}(M) \;=\; \int d\theta e^{-i\nu\theta}\int_{SU(2)} dU e^{\frac{1}{2}\mathrm{Tr}\left(M^\dagger e^{-i\theta/2}U+Me^{i\theta/2}U^\dagger\right)+c^2\mathrm{Tr}\left(\tau_1 U\tau_1 U^\dagger-1\right)}. \tag{3.31}$$

Let us now interpret the factors of $e^{i\theta/2}$ as belonging to U. Such a phase disappears in the coupling term, and the factor in front is written as a determinant. This means we extend the integral to be over $U(2)$ rather than $SU(2)$

$$Z^\nu_{chUE,2}(M) \;=\; \int_{U(2)} dU \det{}^\nu(U) e^{\frac{1}{2}\mathrm{Tr}\left(MU+MU^\dagger\right)+c^2\mathrm{Tr}\left(\tau_1 U\tau_1 U^\dagger-1\right)}. \tag{3.32}$$

The determinant of the SU(2) part of U is always 1. One quickly verifies that the sign of θ and factors of 2 are consistent.

The vector source calculation involves a $U(2)$-integral as seen in (3.32). We would like to compare the $U(2)$-integral to the integral over $U(1)\times U(1)$ from (3.8) in Section 3.1. Adapting the parametrisation from [43] we can write the $U(2)$-matrix as

$$\begin{aligned} U &= \begin{pmatrix} u_1 & 0 \\ 0 & u_2 \end{pmatrix}\begin{pmatrix} e^{i\phi} & 0 \\ 0 & 1 \end{pmatrix}\begin{pmatrix} \sqrt{1-\mu^2} & \mu \\ \mu & -\sqrt{1-\mu^2} \end{pmatrix}\begin{pmatrix} e^{-i\phi} & 0 \\ 0 & 1 \end{pmatrix} \\ &= \begin{pmatrix} u_1\sqrt{1-\mu^2} & u_1\mu e^{i\phi} \\ u_2\mu e^{-i\phi} & -u_2\sqrt{1-\mu^2} \end{pmatrix} \end{aligned} \tag{3.33}$$

where $u_1, u_2 \in U(1)$, $\phi \in [0, 2\pi]$, and $\mu \in [-1, 1]$. The Jacobian is [43]

$$J = 2\sqrt{1-\mu^2} \tag{3.34}$$

The determinant part of partition function reduces to

$$\det{}^\nu\big(U\big) = \det{}^\nu(u_1)\det{}^\nu(u_2), \tag{3.35}$$

the mass term is

$$\frac{1}{2}\mathrm{Tr}\left(MU+MU^\dagger\right) = \frac{\sqrt{1-\mu^2}}{2}\mathrm{Tr}\big(mu_1+mu_1^\dagger-mu_2-mu_2^\dagger\big), \tag{3.36}$$

and the coupling term is

$$\begin{aligned} c^2\mathrm{Tr}\big(\tau_1 U\tau_1 U^\dagger-1\big) &= c^2\mathrm{Tr}\left(\begin{pmatrix} -u_2\sqrt{1-\mu^2} & u_2\mu e^{-i\phi} \\ u_1\mu e^{i\phi} & u_1\sqrt{1-\mu^2} \end{pmatrix}\begin{pmatrix} u_1^\dagger\sqrt{1-\mu^2} & u_2^\dagger\mu e^{i\phi} \\ u_1^\dagger\mu e^{-i\phi} & -u_2^\dagger\sqrt{1-\mu^2} \end{pmatrix}-1\right) \\ &= c^2\Big(\mu^2(u_1u_2^\dagger e^{2i\phi}+u_2u_1^\dagger e^{-2i\phi})-(1-\mu^2)(u_1u_2^\dagger+u_2u_1^\dagger)-2\Big) \\ &= c^2\Big(\mu^2\cos(2\phi)(u_1u_2^\dagger+u_2u_1^\dagger)+i\mu^2\sin(2\phi)(u_1u_2^\dagger-u_2u_1^\dagger) \\ &\quad -(1-\mu^2)(u_1u_2^\dagger+u_2u_1^\dagger)-2\Big) \end{aligned} \tag{3.37}$$

So the partition function can be written as

$$\begin{aligned} Z^{\nu}_{chUE,2}(M) &= \int_0^{2\pi} d\phi \int_{-1}^{1} d\mu \int_{U(1)} du_1 du_2 \sqrt{1-\mu^2}\, \det{}^{\nu}(u_1 u_2) \\ &\quad \times \exp\Big\{ \frac{\sqrt{1-\mu^2}}{2}\big(m u_1 + m u_1^\dagger - m u_2 - m u_2^\dagger\big) \\ &\quad + c^2\Big(\mu^2 \cos(2\phi)(u_1 u_2^\dagger + u_2 u_1^\dagger) + i\mu^2 \sin(2\phi)(u_1 u_2^\dagger - u_2 u_1^\dagger) \\ &\quad - (1-\mu^2)(u_1 u_2^\dagger + u_2 u_1^\dagger) - 2\Big)\Big\}. \end{aligned} \tag{3.38}$$

The integral over ϕ is known. We use an analytical continuation of an integral in [44]. The limits are not the same, but the periodicity makes the difference an overall factor, which we absorb in Z.

$$\begin{aligned} Z^{\nu}_{chUE,2}(M) &= \int_{-1}^{1} d\mu \int_{U(1)} du_1 du_2 \sqrt{1-\mu^2} \det{}^{\nu}(u_1 u_2) J_0\Big(- i c^2 \mu^2 \sqrt{(u_1 u_2^\dagger + u_2 u_1^\dagger)^2 - (u_1 u_2^\dagger - u_2 u_1^\dagger)^2}\Big) \\ &\quad \times \exp\Big\{ \frac{\sqrt{1-\mu^2}}{2}\big(m u_1 + m u_1^\dagger - m u_2 - m u_2^\dagger\big) - c^2\Big((1-\mu^2)(u_1 u_2^\dagger + u_2 u_1^\dagger) + 2\Big)\Big\} \\ &= \int_{-1}^{1} d\mu \int_{U(1)} du_1 du_2 \sqrt{1-\mu^2} \det{}^{\nu}(u_1 u_2) I_0\big(2c^2\mu^2\big) \\ &\quad \times \exp\Big\{ \frac{\sqrt{1-\mu^2}}{2}\big(m u_1 + m u_1^\dagger - m u_2 - m u_2^\dagger\big) - c^2\Big((1-\mu^2)(u_1 u_2^\dagger + u_2 u_1^\dagger) + 2\Big)\Big\} \end{aligned} \tag{3.39}$$

Numerics confirm this. If we want to regain a form similar to (3.8), we must let $u_2 \to -u_2$

$$\begin{aligned} Z^{\nu}_{chUE,2}(M) &= \int_{-1}^{1} d\mu \int_{U(1)} du_1 du_2 \sqrt{1-\mu^2} \det{}^{\nu}(u_1 u_2) I_0\big(2c^2\mu^2\big) \\ &\quad \times \exp\Big\{ \frac{\sqrt{1-\mu^2}}{2}\big(m u_1 + m u_1^\dagger + m u_2 + m u_2^\dagger\big) + c^2\Big((1-\mu^2)(u_1 u_2^\dagger + u_2 u_1^\dagger) - 2\Big)\Big\} \end{aligned} \tag{3.40}$$

The μ-integral can then be interpreted as an integral over mass and coupling scales. For $\mu = 0$ (3.40) is equal to (3.8). Numerics suggest that, while the maximum of the integrand is indeed in $\mu = 0$, it does not decrease fast enough for a saddle-point approximation. We therefore primarily evaluate this ensemble numerically, see Chapter 6.

3.5 Two-Flavour Ensemble: EFT of Coupled RMT

The derivation of the effective theory of Z_2 from the corresponding random matrix ensemble is completely analogous to the derivation of Z_{1+1}, except that we start from the theory

$$Z^{\nu}_2 = \int dW \det \begin{pmatrix} m & iW & 0 & ic_R \\ iW^\dagger & m & ic_R & 0 \\ 0 & ic_R & m & iW \\ ic_R & 0 & iW^\dagger & m \end{pmatrix} e^{-N\mathrm{Tr}(WW^\dagger)} \tag{3.41}$$

We reach the same result as in (3.32)

$$Z^{\nu}_{chUE,2}(M) = \int_{U(2)} dU \det{}^{\nu}(U) e^{\frac{1}{2}\mathrm{Tr}\left(MU + MU^\dagger\right) + c^2 \mathrm{Tr}\left(\tau_1 U \tau_1 U^\dagger\right)} \tag{3.42}$$

except that RMT cannot capture the extra factor of e^{-2c^2}, because it does not influence the symmetries. The details of the derivation can be found in Appendix C.2.

3.6 Two-Flavour Ensemble: Symmetries

Let us make the same analysis for Z_2 as we did for Z_{1+1} in Section 3.3. Now that the two flavours interact with the same gauge field, we can make a full $U(2)$-transformation for $c = 0$. We only consider the flavour transformation, because we understand the behaviour in chiral space well. Let us start from the matrix corresponding to the uncoupled ensemble

$$\begin{pmatrix} m & iW & 0 & 0 \\ iW^\dagger & m & 0 & 0 \\ 0 & 0 & m & iW \\ 0 & 0 & iW^\dagger & m \end{pmatrix}. \tag{3.43}$$

Because the matrix is proportional to identity in flavour space for $c = 0$, it follows quite trivially that it is invariant under any transformation. If we wanted to do the full calculation, we would use the same procedure as we did in Equation (3.27) for all the Pauli matrices. One finds the same result.

Let us now turn on the coupling

$$\begin{pmatrix} m & iW & 0 & ic \\ iW^\dagger & m & ic & 0 \\ 0 & ic & m & iW \\ ic & 0 & iW^\dagger & m \end{pmatrix}. \tag{3.44}$$

We can already see from the source term (3.3) that the $U(2)$-symmetry is broken, because $[\tau_i, \tau_j] \neq 0$. The first order transformations is for instance

$$\begin{aligned} ic\bar{q}\gamma_0\tau_1 q &\rightarrow ic\bar{q}\tau_2\gamma_0\tau_1\tau_2 q \\ &= -ic\bar{q}\tau_2\tau_2\gamma_0\tau_1 q \\ &= -ic\bar{q}\gamma_0\tau_1 q \end{aligned} \tag{3.45}$$

and equivalent for τ_3 and the higher order terms. This can also be seen from the matrix with the parametrisation of $U(2)$ given by $\exp\left\{\sum_{k=0}^{3} i\theta_k\tau_k\right\}$. One finds $\theta_2 = \theta_3 = 0$, because the source allows for the transformation $e^{i\theta_1\tau_1}$.

3.7 Difference Between $U(2)$ and $U(1) \times U(1)$

Let us summarise what we know of the two ensembles. The action of the two partition functions has the same kind of terms, but the greater symmetry of two flavours introduces a weighting of different choices of mass- and coupling scale up to m and c.

Two Single-Flavour Ensembles $Z_{chUE,1+1}$

$Z_{chUE,1+1}$ comprises two flavours that are completely unconnected to each other until we couple them, by which we mean that the uncoupled partition function factorises. The two flavours

interact with two different gauge fields, which allows for different topology. They can only interact through the coupling, which also couples the topology. Once we turn on the coupling, chiral transformations of the fields must to be done simultaneously, so the coupling breaks the massless Lagrangian in the pattern

$$U(1)^4 \to U(1)^2. \tag{3.46}$$

The individual axial- and vectorial transformations break into combined ones.

Two-Flavour Ensemble $Z_{chUE,2}$

$Z_{chUE,2}$ comes from a single ensemble, where the two-flavour structure of the theory is built in. We can therefore rotate the flavour basis, and the partition function does not factorise for $c = 0$. The two flavours interact with the same gauge field with a single topology, and so the zero modes cannot cancel.[2] For $c \neq 0$, the flavours cannot be rotated in the same way, but two of the generators are broken explicitly. So the coupling breaks the massless Lagrangian in the pattern

$$U(2)^2 \to U(1)^2 \times U(1)^2 \tag{3.47}$$

The full axial- and vectorial transformations break to locked chiral symmetry and exchange of the fields, which comes from the final $U(2)$ generator.

Note that in Chapters 4 and 5, we primarily look at the coupled single-flavour ensembles, which for quenched chUE is $Gl(1|1) \times Gl(1|1)$. These are the simplest to calculate, but also the only case, where we can see a coupling of topology.

The two flavour theory requires an integral over $Gl(2|2)$. A parametrisation of this is available in [45], but the partition function involves too many terms to be practical. This is briefly sketched in Section 4.3.

3.8 Topology in Coupled Systems

Since the two flavours of the $U(2)$ ensemble already are in the same topological sector, the coupling does not influence the topology, so let us just consider the topology of the two single-flavour ensembles.

We can get a sense of the common topological charge of the coupled sectors by looking at mass transformation properties. Recall the transformation properties from (2.40)

$$Z^{\nu}(me^{i\theta}) \quad = \quad e^{i\theta\nu N_f} Z^{\nu}(m). \tag{3.48}$$

Let us briefly return to the $m_1 \neq m_2$ case to see the individual transformation of the masses. Without the coupling we can rotate the masses independently of each other

$$Z^{\nu_1,\nu_2}_{chUE,1+1}(e^{i\theta_1}m_1, e^{i\theta_2}m_2, c=0) \quad = \quad e^{i\theta_1\nu_1 + i\theta_2\nu_2} Z^{\nu_1,\nu_2}_{chUE,1+1}(m_1, m_2, c=0). \tag{3.49}$$

The coupling term $\mathrm{Tr}\left[U_1U_2^\dagger + U_2U_1^\dagger\right]$ is only invariant for $\theta_1 = \theta_2$, so the couple partition function transforms as

$$Z^{\nu_1,\nu_2}_{chUE,1+1}(e^{i\theta}m_1, e^{i\theta}m_2, c) \quad = \quad e^{i\theta(\nu_1+\nu_2)} Z^{\nu_1,\nu_2}_{chUE,1+1}(m_1, m_2, c) \tag{3.50}$$

so it is natural to assume the coupled system has $\nu_1 + \nu_2$ zero modes.

[2] We can redefine left and right for one of the flavours and thus achieve cancellation. We treat this ensemble numerically in Chapter 6.

3.8.1 Distribution of Topologies in Coupled Systems

Because the uncoupled partition function of $U(1) \times U(1)$ ensemble factorises, we can express the partition function for all topologies as

$$Z_{chUE,1+1}(\theta, \theta', m_1, m_2, c = 0) = \sum_{\nu_1,\nu_2} e^{i(\theta\nu_1 + \theta'\nu_2)} Z^{\nu_1,\nu_2}_{chUE,1+1}(m_1, m_2, c = 0). \quad (3.51)$$

For $c \neq 0$ we must have $\theta = \theta'$, if the Lagrangian is to be invariant under a $U(1)$ transformation of the quark mass. This leaves us with

$$Z_{chUE,1+1}(\theta, m_1, m_2, c) = \sum_{\nu_1,\nu_2} e^{i\theta(\nu_1+\nu_2)} Z^{\nu_1,\nu_2}_{chUE,1+1}(m_1, m_2, c) \quad (3.52)$$

which is to be expected from the transformation properties of the coupled partition function.

If we want a form similar to (2.37), we must define a partition function that only depends on the common topology $\nu = \nu_1 + \nu_2$. We can rewrite (3.52) as

$$Z_{chUE,1+1}(\theta, m_1, m_2, c) = \sum_{\nu} e^{i\theta\nu} Z^{\nu}_{chUE,1+1}(m_1, m_2, c) \quad (3.53)$$

where

$$Z^{\nu}_{chUE,1+1}(m_1, m_2, c) = \sum_{\nu_1+\nu_2=\nu} Z^{\nu_1,\nu_2}_{chUE,1+1}(m_1, m_2, c). \quad (3.54)$$

Let us evaluate this as in Section 2.3.3 with the parametrisation of $U(1)$ given by $U_j = e^{i\alpha_j}$

$$Z^{\nu_1,\nu_2}_{1+1}(m_1, m_2, c) = \int_{-\pi}^{\pi} d\alpha_1 d\alpha_2 \det{}^{\nu_1}(e^{i\alpha_1}) \det{}^{\nu_2}(e^{i\alpha_2}) e^{m_1\cos(\alpha_1)+m_2\cos(\alpha_2)+2c^2\cos(\alpha_1-\alpha_2)}.$$

It is convenient to use $\sum_\nu \sum_{\nu_1+\nu_2=\nu} = \sum_{\nu_1,\nu_2}$ and simply deal with the double sum. We can then make the same transformation for each topological charge

$$\begin{aligned}
Z_{chUE,1+1}(m_1, m_2, \theta, c) &= \sum_{\nu_1,\nu_2} e^{i\theta(\nu_1+\nu_2)} \int_{-\pi}^{\pi} \frac{d\alpha_1}{2\pi}\frac{d\alpha_2}{2\pi} e^{i\alpha_1\nu_1} e^{i\alpha_2\nu_2} e^{m_1\cos(\alpha_1)+m_2\cos(\alpha_2)+2c^2\cos(\alpha_1-\alpha_2)} \\
&= \sum_{\nu_1,\nu_2} \int_{-\pi}^{\pi} \frac{d\alpha_1}{2\pi}\frac{d\alpha_2}{2\pi} e^{i(\alpha_1+\theta)\nu_1} e^{i(\alpha_2+\theta)\nu_2} e^{m_1\cos(\alpha_1)+m_2\cos(\alpha_2)+2c^2\cos(\alpha_1-\alpha_2)} \\
&= \sum_{n_1,n_2} \int_{-\pi}^{\pi} d\alpha_1 d\alpha_2 \delta(\alpha_1 + \theta - 2\pi n_1)\delta(\alpha_2 + \theta - 2\pi n_2) \\
&\quad \times e^{m_1\cos(\alpha_1)+m_2\cos(\alpha_2)+2c^2\cos(\alpha_1-\alpha_2)} \\
&= \sum_{n_1,n_2} e^{m_1\cos(\theta-2\pi n_1)+m_2\cos(\theta-2\pi n_2)+2c^2\cos(\theta-2\pi n_1-\theta+2\pi n_2))}. \quad (3.55)
\end{aligned}$$

Again we disregard the sum and $2\pi n$

$$Z_{chUE,1+1}(m_1, m_2, \theta, c) = e^{m_1\cos(\theta)+m_2\cos(\theta)+2c^2}. \quad (3.56)$$

Although not a main result, this is very interesting. We regain the case of two uncoupled systems up to a factor. This means that the distributions have the same mean and width. Numerics confirm that the two distributions are the same. Interestingly, the factor would cancel with the extra factor we get in (3.31).

3.9 Orthogonal Ensemble: EFT from RMT for Coupled chOE

Before moving on to calculation of the spectral density, let us for completeness also show the derivation of the EFT from a coupled chOE RMT. The cases are analogous, but we arrive at a slightly different correspondence scheme, which makes this derivation very important for the comparison to numerics in Chapter 6.

In analogy with [7] and Section 3.2 we start from the theory

$$Z_{chOE} = \int dW_1 dW_2 \det \begin{pmatrix} m & iW_1 & 0 & ic \\ iW_1^\dagger & m & ic & 0 \\ 0 & ic & m & iW_2 \\ ic & 0 & iW_2^\dagger & m \end{pmatrix} e^{-\frac{n}{2}\mathrm{Tr}[W_1 W_1^\dagger + W_2 W_2^\dagger]} \tag{3.57}$$

with W_j being $n \times n$ real matrices (for simplicity we assume $\nu_1 = \nu_2 = 0$).

Expressing the determinant as fermionic integrals, we find

$$\begin{aligned} Z_{chOE} = \int dW_1 dW_2 d\psi^1 d\psi^2 d\phi^1 d\phi^2 \exp\Big\{ & -\frac{n}{2}(W_{1ij}^2 + W_{2ij}^2) \\ & + iW_{1ij}(\psi_i^{1^*}\phi_j^1 - \psi_i^1\phi_j^{1^*}) + iW_{2ij}(\psi_i^{2^*}\phi_j^2 - \psi_i^2\phi_j^{2^*}) \\ & + m\big(\psi_j^{1^*}\psi_j^1 + \phi_j^{1^*}\phi_j^1 + \psi_j^{2^*}\psi_j^2 + \phi_j^{2^*}\phi_j^2\big) \\ & + ic\big(\phi_j^{1^*}\psi_j^2 + \psi_j^{1^*}\phi_j^2 + \phi_j^{2^*}\psi_j^1 + \psi_j^{2^*}\phi_j^1\big)\Big\}. \end{aligned} \tag{3.58}$$

We integrate out the W_j and define

$$I \equiv \begin{pmatrix} 0 & -1 \\ 1 & 0 \end{pmatrix}, \; M \equiv \begin{pmatrix} 0 & -m \\ m & 0 \end{pmatrix}, \; C \equiv \begin{pmatrix} 0 & -c \\ c & 0 \end{pmatrix}, \tag{3.59}$$

so we may write

$$\begin{aligned} Z_{chOE} = \int d\psi^1 d\psi^2 d\phi^1 d\phi^2 \exp\Big\{ & -\frac{1}{2n}\left(\left[\begin{pmatrix}\psi_i^1 \\ \psi_i^{1*}\end{pmatrix} I \begin{pmatrix}\phi_j^1 \\ \phi_j^{1*}\end{pmatrix}\right]^2 + \left[\begin{pmatrix}\psi_i^2 \\ \psi_i^{2*}\end{pmatrix} I \begin{pmatrix}\phi_j^2 \\ \phi_j^{2*}\end{pmatrix}\right]^2\right) \\ & + \frac{1}{2}\begin{pmatrix}\psi_i^1 \\ \psi_i^{1*}\end{pmatrix} M \begin{pmatrix}\psi_i^1 \\ \psi_i^{1*}\end{pmatrix} + \frac{1}{2}\begin{pmatrix}\phi_i^1 \\ \phi_i^{1*}\end{pmatrix} M \begin{pmatrix}\phi_i^1 \\ \phi_i^{1*}\end{pmatrix} + \frac{1}{2}\begin{pmatrix}\psi_i^2 \\ \psi_i^{2*}\end{pmatrix} M \begin{pmatrix}\psi_i^2 \\ \psi_i^{2*}\end{pmatrix} + \frac{1}{2}\begin{pmatrix}\phi_i^2 \\ \phi_i^{2*}\end{pmatrix} M \begin{pmatrix}\phi_i^2 \\ \phi_i^{2*}\end{pmatrix} \\ & + i\begin{pmatrix}\psi_i^1 \\ \psi_i^{1*}\end{pmatrix} C \begin{pmatrix}\phi_i^2 \\ \phi_i^{2*}\end{pmatrix} + i\begin{pmatrix}\psi_i^2 \\ \psi_i^{2*}\end{pmatrix} C \begin{pmatrix}\phi_i^1 \\ \phi_i^{1*}\end{pmatrix}\Big\}. \end{aligned} \tag{3.60}$$

The squared terms can be rewritten as [7]

$$
\begin{aligned}
Z_{chOE} &= \int d\psi^1 d\psi^2 d\phi^1 d\phi^2 \\
&\times \exp\Big\{ -\frac{1}{8n}\Bigg(\Bigg[\begin{pmatrix} \psi_i^1 \\ \psi_i^{1*} \end{pmatrix}_f \begin{pmatrix} \psi_j^1 \\ \psi_j^{1*} \end{pmatrix}_g + I_{gg'} \begin{pmatrix} \psi_i^1 \\ \psi_i^{1*} \end{pmatrix}_{g'} \begin{pmatrix} \psi_j^1 \\ \psi_j^{1*} \end{pmatrix}_{f'} I_{f'f} \Bigg]^2 \\
&- \Bigg[\begin{pmatrix} \psi_i^1 \\ \psi_i^{1*} \end{pmatrix}_f \begin{pmatrix} \psi_j^1 \\ \psi_j^{1*} \end{pmatrix}_g - I_{gg'} \begin{pmatrix} \psi_i^1 \\ \psi_i^{1*} \end{pmatrix}_{g'} \begin{pmatrix} \psi_j^1 \\ \psi_j^{1*} \end{pmatrix}_{f'} I_{f'f} \Bigg]^2 \Bigg) \\
&+ \frac{1}{2} \begin{pmatrix} \psi_i^1 \\ \psi_i^{1*} \end{pmatrix} M \begin{pmatrix} \psi_i^1 \\ \psi_i^{1*} \end{pmatrix} + \frac{1}{2} \begin{pmatrix} \phi_i^1 \\ \phi_i^{1*} \end{pmatrix} M \begin{pmatrix} \phi_i^1 \\ \phi_i^{1*} \end{pmatrix} + (1 \to 2) \\
&+ i \begin{pmatrix} \psi_i^1 \\ \psi_i^{1*} \end{pmatrix} C \begin{pmatrix} \phi_i^2 \\ \phi_i^{2*} \end{pmatrix} + i \begin{pmatrix} \psi_i^2 \\ \psi_i^{2*} \end{pmatrix} C \begin{pmatrix} \phi_i^1 \\ \phi_i^{1*} \end{pmatrix} \Big\}.
\end{aligned} \tag{3.61}
$$

Four Hubbard-Stratanovitch transformations lead to

$$
\begin{aligned}
Z_{chOE} &= \int dA_1 dA_2 d\psi^1 d\psi^2 d\phi^1 d\phi^2 \exp\Big\{ -2n\mathrm{Tr}\left(A_1 A_1^\dagger + A_2 A_2^\dagger \right) \\
&+ \frac{1}{2} \begin{pmatrix} \psi_i^1 \\ \psi_i^{1*} \end{pmatrix} \left(2A_1^\dagger + M \right) \begin{pmatrix} \psi_i^1 \\ \psi_i^{1*} \end{pmatrix} + \frac{1}{2} \begin{pmatrix} \phi_i^1 \\ \phi_i^{1*} \end{pmatrix} \left(2IA_1 I^T + M \right) \begin{pmatrix} \phi_i^1 \\ \phi_i^{1*} \end{pmatrix} + (1 \to 2) \\
&+ i \begin{pmatrix} \psi_i^1 \\ \psi_i^{1*} \end{pmatrix} C \begin{pmatrix} \phi_i^2 \\ \phi_i^{2*} \end{pmatrix} + i \begin{pmatrix} \psi_i^2 \\ \psi_i^{2*} \end{pmatrix} C \begin{pmatrix} \phi_i^1 \\ \phi_i^{1*} \end{pmatrix} \Big\}.
\end{aligned} \tag{3.62}
$$

We let $2A_j \to A_j$ and use the relation

$$
\int d^n\theta \exp\left\{ -\frac{1}{2}\theta^T A \theta + J^T \theta \right\} = \sqrt{\det A} \exp\left\{ \frac{1}{2} J^T A^{-1} J \right\} \tag{3.63}
$$

to do first the n integrals over ϕ^j and then ψ^j

$$
\begin{aligned}
Z_{chOE} &= \int dA_1 dA_2 d\psi^1 d\psi^2 \exp\Big\{ -\frac{n}{2}\mathrm{Tr}\left(A_1 A_1^\dagger + A_2 A_2^\dagger \right) \\
&+ \frac{1}{2} \begin{pmatrix} \psi_i^1 \\ \psi_i^{1*} \end{pmatrix} \left(A_1^\dagger + M \right) \begin{pmatrix} \psi_i^1 \\ \psi_i^{1*} \end{pmatrix} - \frac{1}{2} \begin{pmatrix} \psi_i^1 \\ \psi_i^{1*} \end{pmatrix} C \left(IA_1 I^T + M \right)^{-1} C \begin{pmatrix} \psi_i^1 \\ \psi_i^{1*} \end{pmatrix} + (1 \to 2) \Big\} \\
&\times \det{}^{\frac{n}{2}} \left((IA_1 I^T + M)(IA_2 I^T + M) \right) \\
&= \int dA_1 dA_2 \exp\Big\{ -\frac{n}{2}\mathrm{Tr}\left(A_1 A_1^\dagger + A_2 A_2^\dagger \right) \Big\} \\
&\times \det{}^{\frac{n}{2}} \Big((IA_1 I^T + M)(A_2^\dagger + M - C \left(IA_1 I^T + M \right)^{-1} C) \Big) \\
&\times \det{}^{\frac{n}{2}} \Big((IA_2 I^T + M)(A_1^\dagger + M - C \left(IA_2 I^T + M \right)^{-1} C) \Big) \\
&= \int dA_1 dA_2 \exp\Big\{ -\frac{n}{2}\mathrm{Tr}\left(A_1 A_1^\dagger + A_2 A_2^\dagger \right) \Big\} \\
&\times \det{}^{\frac{n}{2}} \Big((IA_1 I^T + M)(IA_2^\dagger I - M) - c^2 \Big) \det{}^{\frac{n}{2}} \Big((IA_2 I^T + M)(IA_1^\dagger I - M) - c^2 \Big).
\end{aligned} \tag{3.64}
$$

We make a saddle point approximation that effectively sets $A_j = U_j$, where U_j is unitary. We ignore terms that include m^2, c^4, or mc^2 as these are higher order

$$\begin{aligned} Z_{chOE} &= \int dU_1 dU_2 \det{}^{\frac{n}{2}} \Big(\big(I(U_2+M)(U_1^\dagger+M)I - c^2\big)\big(I(U_1+M)(U_2^\dagger+M)I - c^2\big)\Big) \\ &= \int dU_1 dU_2 \det{}^{\frac{n}{2}} \Big(\big(U_2U_1^\dagger + MU_1^\dagger + U_2M + c^2\big)\big(U_1U_2^\dagger + MU_2^\dagger + U_1M + c^2\big)\Big) \\ &= \int dU_1 dU_2 \det{}^{\frac{n}{2}} \Big(1 + MU_1^\dagger + U_2M + MU_2^\dagger + U_1M + c^2U_2U_1^\dagger + c^2U_1U_2^\dagger\Big). \end{aligned} \tag{3.65}$$

Expressing the determinant as the trace of a logarithm and expanding that logarithm, we find

$$Z_{chOE} = \int dU_1 dU_2 \exp\left\{ \frac{n}{2} \mathrm{Tr}\Big(MU_1^\dagger + MU_2 + MU_2^\dagger + MU_1 + c^2U_2U_1^\dagger + c^2U_1U_2^\dagger\Big)\right\}. \tag{3.66}$$

Comparing this to the effective theory of chOE

$$Z_{chOE} = \int dU_1 dU_2 \exp\left\{ \frac{1}{2} \mathrm{Tr}\Big(MU_1^\dagger + MU_2 + MU_2^\dagger + MU_1\Big) + c^2\Big(U_2U_1^\dagger + U_1U_2^\dagger\Big)\right\}, \tag{3.67}$$

we find the correspondence scheme for chOE

$$\begin{aligned} m_q V\Sigma_0 &= n m_R \equiv m \\ \lambda V\Sigma_0 &= n\lambda_R \equiv u \\ \tilde{c}^2 V K_1 &= \frac{1}{2} n c_R^2 \equiv c^2 \end{aligned} \tag{3.68}$$

which is used in the numerical verification in Chapter 6. Compared to (3.19), there is a factor of 2 in both mass and coupling constant.

3.10 Subconclusion

This concludes the analysis of the coupling properties on partition function level. We found a unique term in the effective Lagrangian

$$\mathcal{L}_{coup} = c^2 \mathrm{Tr}\left[U_1U_2^\dagger + U_2U_1^\dagger \right] \tag{3.69}$$

with the desired symmetries, which gives us the basic partition function structure

$$\begin{aligned} Z^{\nu_1,\nu_2}_{chUE,1+1}(M,c) = & \int_{U(1)} dU_1 dU_2 \det{}^{\nu_1}(U_1) \det{}^{\nu_2}(U_2) \\ & \times \exp\left\{ \frac{1}{2} \mathrm{Tr}\left[M^\dagger U_1 + MU_1^\dagger + M^\dagger U_2 + MU_2^\dagger \right] + c^2 \mathrm{Tr}\left[{U_1}^\dagger U_2 + {U_2}^\dagger U_1 \right] \right\} \end{aligned} \tag{3.70}$$

of two coupled single-flavour ensembles. The coupled two-flavour ensemble has a similar structure, but with integration over mass and coupling scales.

With this in mind we turn our attention to the calculation of the spectral densities.

Chapter 4

Spectral Density of Coupled chUE

With the partition function well understood, we turn our attention to calculation of the spectral density. In Section 2.4.1 we established that the relevant group for quenched chUE is $Gl(1|1)$, so let us directly reuse the structure from (3.8). The result is

$$\begin{aligned} & Z^{\nu_1,\nu_2}_{chUE,1|1+1|1}(m,m',c) \qquad (4.1)\\ = & \int_{Gl(1|1)} dU_1 dU_2 \ \mathrm{Sdet}^{\nu_1}(U_1)\ \mathrm{Sdet}^{\nu_2}(U_2) \\ & \times \exp\left\{\frac{1}{2}\mathrm{Str}\left[M^\dagger U_1 + M U_1^{-1} + M^\dagger U_2 + M U_2^{-1}\right] + c^2 \mathrm{Str}\left[U_1 U_2^{-1} + U_2 U_1^{-1}\right]\right\} \end{aligned}$$

where $M = \mathrm{diag}(m, m')$ and Str and Sdet are graded trace and determinant.[1]

We will make use of the parametrisation of $Gl(1|1)$ given by [12]

$$U_j = \begin{pmatrix} e^{i\theta_j} & 0 \\ 0 & e^{s_j} \end{pmatrix} \exp\begin{pmatrix} 0 & \alpha_j \\ \beta_j & 0 \end{pmatrix} = \begin{pmatrix} e^{i\theta_j}(1+\frac{1}{2}\alpha_j\beta_j) & e^{i\theta_j}\alpha_j \\ e^{s_j}\beta_j & e^{s_j}(1-\frac{1}{2}\alpha_j\beta_j) \end{pmatrix} \qquad (4.2)$$

and

$$U_j^{-1} = \begin{pmatrix} e^{-i\theta_j}(1+\frac{1}{2}\alpha_j\beta_j) & -e^{-i\theta_j}\alpha_j \\ e^{-s_j}\beta_j & e^{-s_j}(1-\frac{1}{2}\alpha_j\beta_j) \end{pmatrix}. \qquad (4.3)$$

Here α and β are Grassmann variables and the angular variable θ extends over $[-\pi : \pi]$, while $s \in [-\infty : \infty]$ is non-compact, the Berezinian (a generalisation of the Jacobian) is 1 [12]. We then evaluate the supertraces and superdeterminants and perform the integrals to find the partition function. The spectral density is then obtained using the methods introduced in Section 2.4.

For $c = 0$, the microscopic density is already known to be [12, 19]

$$\rho^{\nu}_{chUE,1|1}(u) = \frac{u}{2}\left(J_\nu(u)^2 + J_{\nu+1}(u)J_{\nu-1}(u)\right) \qquad (4.4)$$

where $u = V\Sigma_0\lambda$ like in (3.19). Numerical comparison with the random matrix ensemble can be found in Figure 6.1 in Chapter 6.

[1] See Appendix A for an introduction to these.

Direct evaluation of (4.1) with the parametrisation from (4.2) gives

$$\begin{aligned}
& Z^{\nu_1,\nu_2}_{chUE,1|1+1|1}(m,m',c) \\
= \; & \frac{1}{(2\pi)^2}\int ds_1 ds_2 d\theta_1 d\theta_2 \, e^{\nu_1(i\theta_1-s_1)}e^{\nu_2(i\theta_2-s_2)} \\
& \times \exp\Big[m\cos(\theta_1)+m\cos(\theta_2)-m'\cosh(s_1)-m'\cosh(s_2)+2c^2(\cos(\theta_1-\theta_2)-\cosh(s_1-s_2))\Big] \\
& \times\Big(1/4(m\cos(\theta_1)+m'\cosh(s_1))(m\cos(\theta_2)+m'\cosh(s_2))+c^2/2(\cos(\theta_1-\theta_2)-\cosh(s_1-s_2)) \\
& +c^2/2(\cos(\theta_1-\theta_2)+\cosh(s_1-s_2))(m\cos(\theta_1)+m\cos(\theta_2)+m'\cosh(s_1)+m'\cosh(s_2)) \\
& -c^4(\sin(\theta_1-\theta_2)+i\sinh(s_2-s_1))^2\Big).
\end{aligned} \tag{4.5}$$

The full derivation can be found in Appendix C.3. We check explicitly with numerical integration that this expression equals 1 when evaluated at $m = m'$.

Differentiation with respect to m yields the chiral condensate

$$\begin{aligned}
& \Sigma^{\nu_1,\nu_2}_{chUE,1|1+1|1}(m,c) \\
= \; & \frac{1}{(2\pi)^2}\int ds_1 ds_2 d\theta_1 d\theta_2 \, e^{\nu_1(i\theta_1-s_1)}e^{\nu_2(i\theta_2-s_2)} \\
& \times \exp\Big[m_1\cos(\theta_1)+m_2\cos(\theta_2)-m_1\cosh(s_1)-m_2\cosh(s_2)+2c^2(\cos(\theta_1-\theta_2)-\cosh(s_1-s_2))\Big] \\
& \times\Big[1/4\cos(\theta_1)(m_2\cos(\theta_2)+m_2\cosh(s_2))+1/4(m_1\cos(\theta_1)+m_1\cosh(s_1))\cos(\theta_2) \\
& +(\cos(\theta_1)+\cos(\theta_2))\Big(1/4(m_1\cos(\theta_1)+m_1\cosh(s_1))(m_2\cos(\theta_2)+m_2\cosh(s_2)) \\
& \quad +c^2\cos(\theta_1-\theta_2) \\
& \quad +c^2/2(\cos(\theta_1-\theta_2)+\cosh(s_1-s_2))(m_1\cos(\theta_1)+m_2\cos(\theta_2)+m_1\cosh(s_1)+m_2\cosh(s_2)) \\
& \quad -c^4(\sin(\theta_1-\theta_2)+i\sinh(s_2-s_1))^2\Big)\Big].
\end{aligned} \tag{4.6}$$

We can now in principle find the full eigenvalue density numerically from

$$\rho^{\nu_1,\nu_2}_{chUE,1|1+1|1}(E,c) = \frac{1}{\pi}\Re\left[\Sigma^{\nu_1,\nu_2}_{chUE,1|1+1|1}(iE,c)\right]. \tag{4.7}$$

Equation (4.6) is a main result of this thesis, but regularisation issues arise when performing the numerical integral. These are discussed in the second part of Appendix C.3. The expression is in itself also rather complicated.

We can, however, obtain analytical expressions for limiting cases $c \gg 1$ and $c \ll 1$.

4.1 Strong Coupling Approximation of chUE

In the limit of large c the generating function can be evaluated by saddle point approximation, again see Appendix B.2. We integrate out the Grassmann variables in our partition function and identify the term in the exponential related to c. From (4.5) we find

$$2(\cos(\theta_1-\theta_2)-\cosh(s_1-s_2)). \tag{4.8}$$

The maximum of this occurs at $\theta_1 = \theta_2, s_1 = s_2$, i.e. $U_1 = U_2$. From this we obtain

$$\begin{aligned} Z^{\nu_1,\nu_2}_{chUE,1|1+1|1}(M, c \gg 1) &= \int dU \ \mathrm{Sdet}^{\nu_1+\nu_2}(U) \ e^{\mathrm{Str}(M(U+U^{-1}))} \\ &= Z^{\nu_1+\nu_2}_{chUE,1|1}(2m). \end{aligned} \tag{4.9}$$

Notice that the topology of the coupled system is indeed $\nu = \nu_1 + \nu_2$ as discussed in Section 3.8 and that $U \to 2U$ compared to (2.61) Using the definitions (2.55) and (2.58) we directly obtain

$$\begin{aligned} \rho^{\nu_1,\nu_2}_{chUE,1|1+1|1}(u, c \gg 1) &= 2\rho^{\nu_1+\nu_2}_{chUE,1|1+1|1}(2u) \\ &= 2u\big(J^2_{\nu_1+\nu_2}(2u) - J_{\nu_1+\nu_2+1}(2u)J_{\nu_1+\nu_2-1}(2u)\big) \\ &\quad +|\nu_1 + \nu_2|\delta(u). \end{aligned} \tag{4.10}$$

where the prefactor of 2 comes from normalisation.

A comparison with the random matrix ensemble for $c \gg 1$ can be found in Figure 6.4 in Chapter 6. The analytical result is in agreement with the numerical one.

4.2 Weak Coupling Limit of chUE

For small coupling, the coupling only affects the exact zero modes modes, while the bulk eigenvalues are only affected at higher order in c. The coupled ensemble again displays $\nu_1 + \nu_2$ exact zero modes as discussed in Section 3.8. The remaining $|\nu_1| + |\nu_2| - |\nu_1 + \nu_2|$ would-be zero modes from the uncoupled system will be spread out as $2n$ near-zero modes (n on each side) according to a finite size chiral unitary random matrix ensemble with a Gaussian weight, where the width is determined by c. In other words, we will prove the factorisation

$$Z^{\nu_1,\nu_2}_{chUE,1|1+1|1}(M, c \ll 1) = Z^{n',\nu}_{chUE}\Big(\frac{M}{2\sqrt{n'}c}\Big) Z^{(\nu_1),bulk}_{chUE}(MM^\dagger) Z^{(\nu_2),bulk}_{chUE}(MM^\dagger) \tag{4.11}$$

where $\nu = \nu_1 + \nu_2$, $n' = \frac{|\nu_1|+|\nu_2|-|\nu_1+\nu_2|}{2}$, and the $bulk$-superscript means we stripped the partition function of its zero modes.

To save space we have suppressed the $1|1 + 1|1$ part of the subscript. Note that the zero modes are contained in the finite ensemble. As the argument of $Z^{(\nu),bulk}_{chUE}(MM^\dagger)$ suggests, the partition functions without zero modes are invariant under rotation of the mass.

To linearise the coupled partition function

$$\begin{aligned} & Z^{\nu_1,\nu_2}_{chUE,1|1+1|1}(m, m', c) \\ = & \int_{Gl(1|1)} dU_1 dU_2 \ \mathrm{Sdet}^{\nu_1}(U_1) \ \mathrm{Sdet}^{\nu_2}(U_2) \\ & \times \exp\left\{\frac{1}{2}\mathrm{Str}\left[M^\dagger U_1 + MU_1^{-1} + M^\dagger U_2 + MU_2^{-1}\right] + c^2\mathrm{Str}\left[U_1U_2^{-1} + U_2U_1^{-1}\right]\right\} \end{aligned} \tag{4.12}$$

from (4.1), we make two Hubbard-Stratanovitch transformations

$$e^{c^2\mathrm{Str}(Q^2)} \sim \int d\sigma e^{-\mathrm{Str}\frac{\sigma^2}{4c^2}+\mathrm{Str}(Q\sigma)} \tag{4.13}$$

$$e^{-c^2\mathrm{Str}(\bar{Q}^2)} \sim \int d\bar{\sigma} e^{-\mathrm{Str}\frac{\bar{\sigma}^2}{4c^2}+i\mathrm{Str}(\bar{Q}\bar{\sigma})} \tag{4.14}$$

with $Q = \frac{U_1+U_1^{-1}+U_2+U_2^{-1}}{2}$ and $\bar{Q} = \frac{U_1-U_1^{-1}+U_2-U_2^{-1}}{2}$, where

$$\sigma = \begin{pmatrix} a & \chi \\ \eta & ib \end{pmatrix} \quad , \quad \bar{\sigma} = \begin{pmatrix} \bar{a} & \bar{\chi} \\ \bar{\eta} & i\bar{b} \end{pmatrix} \tag{4.15}$$

and $a, b, \bar{a}, \bar{b} \in \mathbb{R}$, again see Appendix B.1. We ignore an overall constant and get

$$\begin{aligned} Z^{\nu_1,\nu_2}_{chUE,1|1+1|1}(M) &= \int_{Gl(1|1)} dU_1 dU_2 d\sigma d\bar{\sigma}\, \mathrm{Sdet}^{\nu_1}(U_1)\, \mathrm{Sdet}^{\nu_2}(U_2) \exp\Big[-\mathrm{Str}\Big(\frac{\sigma^2+\bar{\sigma}^2}{4c^2}\Big)\Big] \\ &\times \exp\Big[\frac{1}{2}\mathrm{Str}(M^\dagger U_1 + M U_1^{-1}) + \frac{1}{2}\mathrm{Str}(M^\dagger U_2 + M U_2^{-1})\Big] \\ &\times \exp\Big[\mathrm{Str}\Big(\frac{\sigma}{2}(U_1+U_1^{-1}+U_2+U_2^{-1})\Big) + \mathrm{Str}\Big(\frac{i\bar{\sigma}}{2}(U_1-U_1^{-1}+U_2-U_2^{-1})\Big)\Big]. \end{aligned} \tag{4.16}$$

We define $A = \sigma + i\bar{\sigma}$ and $A^\dagger = \sigma - i\bar{\sigma}$

$$\begin{aligned} Z^{\nu_1,\nu_2}_{chUE,1|1+1|1}(M) &= \int_{Gl(1|1)} dU_1 dU_2 dA\, \mathrm{Sdet}^{\nu_1}(U_1)\mathrm{Sdet}^{\nu_2}(U_2) \exp\Big[-\mathrm{Str}\Big(\frac{AA^\dagger}{4c^2}\Big)\Big] \\ &\times \exp\Big[\frac{1}{2}\mathrm{Str}((M^\dagger + A)U_1 + (M + A^\dagger)U_1^{-1}) \\ &+\frac{1}{2}\mathrm{Str}((M^\dagger + A)U_2 + (M + A^\dagger)U_2^{-1})\Big]. \end{aligned} \tag{4.17}$$

Using the graded version of (2.70), we can write this as

$$Z^{\nu_1,\nu_2}_{chUE,1|1+1|1}(M) = \int_{Gl(1|1)} dA \exp\Big[-\mathrm{Str}\Big(\frac{AA^\dagger}{4c^2}\Big)\Big] Z^{(\nu_1)}_{chUE}(M + A^\dagger) Z^{(\nu_2)}_{chUE}(M + A^\dagger). \tag{4.18}$$

Note that by letting $A \to 2c\sqrt{n'}A$ and pulling out a factor in front, we can identify the Gaussian part of Equation (2.67) for $n = n'$ and $M_R = M$. This makes the argument $\frac{M}{2c\sqrt{n'}}$ as we have written in (4.11).

We can rewrite in terms of $Z^{(\nu),bulk}_{chUE}(MM^\dagger)$ by noting that

$$Z^{(\nu)}_{chUE}(M, c) = \begin{cases} \mathrm{Sdet}^{\nu}(M) Z^{(\nu),bulk}_{chUE}(MM^\dagger) & , \quad \nu \geq 0 \\ \mathrm{Sdet}^{-\nu}(M^\dagger) Z^{(\nu),bulk}_{chUE}(MM^\dagger) & , \quad \nu < 0 \end{cases}. \tag{4.19}$$

This follows from (2.45). The superdeterminants are then compared to (2.67). We present one case in detail and refer to Appendix C.4 for the rest.

For $\nu_1, \nu_2 \geq 0$

From Equation (4.19) we have

$$\begin{aligned} Z^{\nu_1,\nu_2}_{chUE,1|1+1|1}(M) &= \int_{Gl(1|1)} dA \exp\Big[-\mathrm{Str}\Big(\frac{AA^\dagger}{4c^2}\Big)\Big] \mathrm{Sdet}^{\nu_1+\nu_2}(M + A^\dagger) \\ &\times Z^{(\nu_1),bulk}_{chUE}([M + A^\dagger][M^\dagger + A]) Z^{(\nu_2),bulk}_{chUE}([M + A^\dagger][M^\dagger + A]). \end{aligned} \tag{4.20}$$

This next step is crucial and very non-trivial. Equation (4.20) is an integral of the form

$$\int dA f(A, c) g(A, c) \tag{4.21}$$

with

$$\begin{aligned} f(A,c) &= \mathrm{Sdet}^{\nu_1+\nu_2}(M+A^\dagger)\exp\Big[-\mathrm{Str}\Big(\frac{AA^\dagger}{4c^2}\Big)\Big] \\ g(A,c) &= Z^{(\nu_1),bulk}_{chUE}([M+A^\dagger][M^\dagger+A])Z^{(\nu_2),bulk}_{chUE}([M+A^\dagger][M^\dagger+A]). \end{aligned} \tag{4.22}$$

The Gaussian term sets $A \sim c$, so a Taylor-expansion around $c = 0$ corresponds to an expansion around $A = 0$. Remember that we seek the $c \ll 1$ behaviour.

The Gaussian part suppresses the constant term of f, whereas the rest stays finite. The leading term is then the zeroth order term from g. The leading contribution from f is the first order term. Note also that g is even in $(M + A^\dagger)$, $g'(A, 0) = 0$, which means we would have to go to even higher order to get a contribution.This is why these choices of f and g are good ones.

We thus have the approximation

$$f(A,c)g(A,c) \approx f(A,c)g(0,0), \tag{4.23}$$

which corresponds to

$$\begin{aligned} Z^{\nu_1,\nu_2}_{chUE,1|1+1|1}(M, c \ll 1) &= \int_{Gl(1|1)} dA \exp\Big[-\mathrm{Str}\Big(\frac{AA^\dagger}{4c^2}\Big)\Big]\mathrm{Sdet}^{\nu_1+\nu_2}(M+A^\dagger) \\ &\quad \times Z^{(\nu_1),bulk}_{chUE}(MM^\dagger)Z^{(\nu_2),bulk}_{chUE}(MM^\dagger) \end{aligned} \tag{4.24}$$

This step is common to all cases and is the reason for the factorisation. It is similar to the continuum limit of Wilson fermions in [8].

Since $\nu_1 + \nu_2 \geq 0$, we can directly identify $n = 0$ and $\nu = \nu_1 + \nu_2$ from Equation (2.67), which is consistent with $n' = \frac{|\nu_1|+|\nu_2|-|\nu_1+\nu_2|}{2} = 0$ since ν_1 and ν_2 has the same sign. Notice that $n = 0$ is not meaningful, which shows that there is no spreading of zero modes for $\mathrm{sign}(\nu_1) = \mathrm{sign}(\nu_2)$.

Let us recap: For low coupling, we get the factorisation

$$Z^{\nu_1,\nu_2}_{chUE,1|1+1|1}(M, c \ll 1) = Z^{n',\nu}_{chUE}\Big(\frac{M}{2\sqrt{n'}c}\Big)Z^{(\nu_1),bulk}_{chUE}(MM^\dagger)Z^{(\nu_2),bulk}_{chUE}(MM^\dagger) \tag{4.25}$$

with $n' = \frac{|\nu_1|+|\nu_2|-|\nu_1+\nu_2|}{2}$ and $\nu = \nu_1 + \nu_2$ and the width of the finite ensemble $2\sqrt{n'}c$.

This makes the chiral condensate

$$\Sigma^{\nu_1,\nu_2}_{chUE,1|1+1|1}(m, c \ll 1) = \Sigma^{N,\nu}_{chUE}\left(\frac{u}{2\sqrt{n'}c}\right) + \Sigma^{(\nu_1),bulk}_{chUE}(m) + \Sigma^{(\nu_2),bulk}_{chUE}(m) \tag{4.26}$$

The spectral density then becomes

$$\rho^{\nu_1,\nu_2}_{chUE,1|1+1|1}(u, c \ll 1) = \rho^{N,\nu}_{chUE}\left(\frac{u}{2\sqrt{n'}c}\right) + \rho^{(\nu_1),bulk}_{chUE}(u) + \rho^{(\nu_2),bulk}_{chUE}(u) \tag{4.27}$$

which is why the spectrum is unchanged far away from zero. Adapting the finite n spectral density solution from [19] and using the width calculated above, we have

$$\rho^{n',\nu}_{chUE}(\frac{u}{2\sqrt{n'}c}) = \frac{n'!}{c\Gamma(n'+\nu)}e^{-z^2}(z^2)^{\nu+1/2}\Big(L^\nu_{n'-1}(z^2)L^{\nu+1}_{n'-1}(z^2) - L^\nu_{n'}(z^2)L^{\nu+1}_{n'-2}(z^2)\Big) \tag{4.28}$$

where we have used the shorthand

$$z^2 = \frac{u^2}{2c^2} \tag{4.29}$$

We have normalised this to $2n'$. Also note that the argument is u instead of λ, because we already have taken the $n \to \infty$ limit when constructing the effective theory.

A comparison with the corresponding random matrix ensemble for $c \ll 1$ can be found in Figure 6.3 in Chapter 6. As expected, the two are in agreement. Note that, while the width of the bulk eigenvalues scale as $\frac{1}{V}$, the width of the would-be zero modes scale as $\frac{1}{\sqrt{V}}$, see the correspondence scheme (3.19).

4.3 Two Flavour Theory of chUE

In this section we investigate what would happen if we worked directly from a two flavour theory similar to the one derived in Section 3.4. If we follow (2.61), the quenched ensemble will be an integral over $Gl(2|2)$.

We may again calculate an analytical expression for the small coupling, but finding a good parametrisation is problematic, and therefore applying a saddle point approximation to the strong coupling limit is ill-defined. We sketch the problem here and refer to the numerical treatment in Section 6.3.

This theory is less interesting than the two flavours in separate backgrounds, as we do not have cancellation of topological modes. We therefore only treat the two flavour case for chUE.

The partition function is

$$\begin{aligned} & Z^{\nu}_{chUE,2|2}(m,m',c) \\ = & \int_{Gl(2|2)} dU \, \mathrm{Sdet}^{\nu}(U) \exp\left\{ \frac{1}{2}\mathrm{Str}[\mathcal{M}^{\dagger}U + \mathcal{M}U^{-1}] + c^2 \mathrm{Str}\left[U\tau_1 U^{-1}\tau_1\right] \right\}. \end{aligned} \tag{4.30}$$

In this case, the mass matrix is $\mathcal{M} = \mathrm{diag}(M, M)$, where $M = \mathrm{diag}(m, m')$.

Let us work from the parametrisation of $Gl(2|2)$ from [45].

$$\begin{aligned} U &= \begin{pmatrix} w_1 & 0 \\ 0 & w_2 \end{pmatrix} \begin{pmatrix} \sqrt{1-w\bar{w}} & w \\ -\bar{w} & \sqrt{1-\bar{w}w} \end{pmatrix} \begin{pmatrix} w_1 & 0 \\ 0 & w_2 \end{pmatrix} \\ U^{-1} &= \begin{pmatrix} w_1^{-1} & 0 \\ 0 & w_2^{-1} \end{pmatrix} \begin{pmatrix} \bar{w}^{-1}\sqrt{1-\bar{w}w}\bar{w} & -w \\ \bar{w} & w^{-1}\sqrt{1-w\bar{w}}w \end{pmatrix} \begin{pmatrix} w_1^{-1} & 0 \\ 0 & w_2^{-1} \end{pmatrix} \end{aligned} \tag{4.31}$$

where $w_1, w_2, w, \bar{w} \in Gl(1|1)$. Notice that the supermatrices do not have one block of fermion-fermion, one block of boson-boson, and two mixing blocks, but rather four blocks, each with this structure. This means we can take $\tau_1 = \begin{pmatrix} 0 & 1 \\ 1 & 0 \end{pmatrix}$, without destroying the supermatrix structure.

Inserting (4.31) in (4.30), we find

$$\begin{aligned}
\mathrm{Str}\left[\mathcal{M}U+\mathcal{M}U^{-1}\right] &= \mathrm{Str}\big[M\big(w_1\sqrt{1-w\bar{w}}w_1+w_2\sqrt{1-\bar{w}w}w_2 \qquad (4.32)\\
&\quad +w_1^{-1}\bar{w}^{-1}\sqrt{1-\bar{w}w}\bar{w}w_1^{-1}+w_2^{-1}w^{-1}\sqrt{1-w\bar{w}}ww_2^{-1}\big)\big]\\
\mathrm{Str}\left[U\tau_1U^{-1}\tau_1\right] &= \mathrm{Str}\big[w_1\sqrt{1-w\bar{w}}w_1w_2^{-1}w^{-1}\sqrt{1-w\bar{w}}ww_2^{-1} \qquad (4.33)\\
&\quad +w_2\sqrt{1-\bar{w}w}w_2w_1^{-1}\bar{w}^{-1}\sqrt{1-\bar{w}w}\bar{w}w_1^{-1}\\
&\quad -w_1^{-1}ww_2^{-1}w_1ww_2-w_2\bar{w}w_1w_2^{-1}\bar{w}w_1^{-1}\big]\\
\mathrm{Sdet}(U) &= \mathrm{Sdet}^2(w_1w_2)\mathrm{Sdet}(\sqrt{1-\bar{w}w})\mathrm{Sdet}(\sqrt{1-w\bar{w}}+w(\sqrt{1-\bar{w}w})^{-1}\bar{w}). \qquad (4.34)
\end{aligned}$$

Note that each $Gl(1|1)$ has two Grassmann integrations, which means that the full partition function will have eight. This will contribute more terms than is realistic to handle, especially with four coupled non-compact conventional integrals. We are also not guaranteed convergence, as can be seen with the following consideration.

We set all Grassmannian variables to zero to find the exponent of the partition function after all Grassmann integrations. This makes the $Gl(1|1)$-matrices

$$w = \begin{pmatrix} e^{i\phi} & 0 \\ 0 & e^{s} \end{pmatrix}, \qquad (4.35)$$

corresponding to (4.2) without Grassmann variables.

The important part for the saddle point approximation is the coupling term, which becomes

$$c^2\left(\cos\left(2(\phi_1-\phi_2)\right)\left(1-e^{i(\phi+\tilde{\phi})}\right)-\cosh\left(2(s_1-s_2)\right)\left(1-e^{s+\tilde{s}}\right)\right). \qquad (4.36)$$

This is problematic, as the bosonic part does not have a definite sign and therefore does not necessarily converge. This makes the saddle point approximation ill-defined, but may change with a different parametrisation.

Small Coupling Limit

In the small coupling limit, we may linearise the partition function with Hubbard-Stratanovitch transformations as in Section 4.2. We find

$$\begin{aligned}
& Z^{\nu}_{chUE,2|2}(\mathcal{M},\mathcal{M}^{\dagger},c)\\
= & \int_{Gl(2|2)} dU\ \mathrm{Sdet}^{\nu}(U)\exp\left\{\frac{1}{2}\mathrm{Str}[\mathcal{M}^{\dagger}U+\mathcal{M}U^{-1}]+c^2\mathrm{Str}\left[U\tau_1U^{-1}\tau_1\right]\right\}\\
= & \int_{Gl(2|2)} dUdA\ \mathrm{Sdet}^{\nu}(U)\exp\left\{-\frac{AA^{\dagger}}{4c^2}\right\}\\
& \times\exp\left\{\frac{1}{2}\mathrm{Str}[\left(\mathcal{M}^{\dagger}+\tau_1A\right)U+\left(\mathcal{M}+\tau_1A^{\dagger}\right)U^{-1}]+c^2\mathrm{Str}\left[U\tau_1U^{-1}\tau_1\right]\right\}\\
= & \int_{Gl(2|2)} dUdA\ Z^{(\nu)}_{chUE}(\mathcal{M}+\tau_1A^{\dagger},\mathcal{M}^{\dagger}+\tau_1A,c). \qquad (4.37)
\end{aligned}$$

Let us assume $\nu \geq 0$, as the cases are again analogous.

$$\begin{aligned} & \int_{Gl(2|2)} dU dA \ \exp\left\{-\frac{AA^\dagger}{4c^2}\right\} \ Z^{(\nu)}_{chUE}(\mathcal{M}+\tau_1 A^\dagger, \mathcal{M}^\dagger + \tau_1 A, c) \\ = & \int_{Gl(2|2)} dU dA \ \exp\left\{-\frac{AA^\dagger}{4c^2}\right\} \ \mathrm{Sdet}\left(\mathcal{M}+\tau_1 A^\dagger\right) \ Z^{(\nu),bulk}_{chUE}(\mathcal{M}+\tau_1 A^\dagger, \mathcal{M}^\dagger + \tau_1 A, c). \end{aligned} \tag{4.38}$$

For $c \ll 1$ we have the factorisation

$$\begin{aligned} & \int_{Gl(2|2)} dU dA \ \exp\left\{-\frac{AA^\dagger}{4c^2}\right\} \ \mathrm{Sdet}\left(\mathcal{M}+\tau_1 A^\dagger\right) \ Z^{(\nu),bulk}_{chUE}(\mathcal{M}+\tau_1 A^\dagger, \mathcal{M}^\dagger + \tau_1 A, c) \\ \approx & \int_{Gl(2|2)} dU dA \ \exp\left\{-\frac{AA^\dagger}{4c^2}\right\} \ \mathrm{Sdet}\left(\mathcal{M}+\tau_1 A^\dagger\right) \ Z^{(\nu),bulk}_{chUE}(\mathcal{M}, \mathcal{M}^\dagger, c). \end{aligned} \tag{4.39}$$

Letting $A \to A\tau_1$ we can identify $n = 0$ from (2.67). This is no surprise. Because we only have one topological index from the beginning, we do not have any cancellation of zero modes. The low coupling limit therefore has the same eigenvalue spectrum as the uncoupled case.

Chapter 5

Spectral Density of Coupled chOE

Now that we have treated the coupling of chiral unitary ensembles, we turn our attention to the orthogonal ensemble. These results follow in analogy with Chapter 4, and we are therefore somewhat briefer in this chapter.

The Goldstone manifold of chOE is larger, so, although the structure of the EFT is very similar, we integrate over $\Sigma(2|2) = U(2|2)/UOSp(2|2)$ rather than $Gl(1|1)$ [8].

The single, uncoupled, quenched system is [8]

$$Z^{\nu}_{chOE,2|2}(M) \;=\; \int_{\Sigma(2|2)} dU\ \mathrm{Sdet}^{\nu/2}(U)\ e^{\frac{1}{2}\mathrm{Str}(M^{\dagger}U+MU^{-1})} \tag{5.1}$$

with the mass matrix

$$M = \begin{pmatrix} m\mathbf{1}_2 & 0 \\ 0 & m'\mathbf{1}_2 \end{pmatrix} \tag{5.2}$$

and $\Sigma(2|2) = U(2|2)/UOSp(2|2)$. The corresponding coupled version is

$$\begin{aligned} Z^{\nu_1,\nu_2}_{chOE,2|2+2|2}(M,c) \;=\; & \int_{\Sigma(2|2)} dU_1 dU_2\ \mathrm{Sdet}^{\nu_1/2}(U_1)\ \mathrm{Sdet}^{\nu_2/2}(U_2) \\ & \times e^{\frac{1}{2}\mathrm{Str}(M^{\dagger}U_1+M{U_1}^{-1})+\frac{1}{2}\mathrm{Str}(M^{\dagger}U_2+M{U_2}^{-1})+c^2\mathrm{Str}(U_1^{-1}U_2+U_1U_2^{-1})}. \end{aligned} \tag{5.3}$$

Note that the partition function transformations just like chUE under rotation of the mass. So we expect exactly the same number of exact zero modes and same small-coupling behaviour of would-be zero modes. One can evaluate the partition function with the parametrisation [8]

$$U_j = \mathrm{diag}(\mathbf{1}_2, O_j) \begin{pmatrix} e^{i\varphi_j} & 0 & \alpha_j^* & \beta_j^* \\ 0 & e^{i\varphi_j} & -\alpha_j & -\beta_j \\ \alpha_j & \alpha_j^* & e^{s_j} & 0 \\ \beta_j & \beta_j^* & 0 & e^{t_j} \end{pmatrix} \mathrm{diag}(\mathbf{1}_2, O_j^T) \tag{5.4}$$

where $O \in O(2)$. We parametrise the orthogonal matrix by adding the possibility of reflection to the common parametrisation of $SO(2)$

$$O_j = \begin{pmatrix} \cos(\theta_j) & -\sin(\theta_j) \\ \sin(\theta_j) & \cos(\theta_j) \end{pmatrix} \begin{pmatrix} 1 & 0 \\ 0 & -1 \end{pmatrix}^{k_j} \;,\ \theta_j \in [-\pi, \pi] \;,\ k_j \in \{0, 1\}. \tag{5.5}$$

The full expression is prohibitively cumbersome because of the many combinations of Grassmann numbers, so we do not evaluate the full expression as we did for chUE in Appendix C.3. For the saddle point approximation for large c^2 we will need the action part of the partition function, which can be found as in Section 4.3 by setting all Grassmannian variables to zero. We find

$$\begin{aligned} &4\cos(\varphi_1-\varphi_2)-2\cos^2(\theta_1-\theta_2)\cosh(s_1-s_2)-2\cos^2(\theta_1-\theta_2)\cosh(t_1-t_2) \\ &\quad -2\sin^2(\theta_1-\theta_2)\cosh(s_1-t_2)-2\sin^2(\theta_1-\theta_2)\cosh(t_1-s_2), \end{aligned} \tag{5.6}$$

which brings us to the limiting cases.

5.1 Strong Coupling Approximation of chOE

Completely analogous to chUE for large c^2 in Section 4.1 we make a saddle point approximation, which corresponds to minimising (5.6). This effectively sets $\varphi_1, s_1, t_1, \theta_1 = \varphi_2, s_2, t_2, \theta_2$. We again assume this to be the same as $U_1 = U_2$. So the generating function becomes

$$Z^{\nu_1,\nu_2}_{chOE,2|2+2|2}(M, c \gg 1) \;=\; \int dU\ \mathrm{Sdet}^{(\nu_1+\nu_2)/2}(U)\ e^{\mathrm{Str}(M(U+U^{-1}))}, \tag{5.7}$$

and it follows from the definitions of the quenched chiral condensate and eigenvalue density, (2.55) and (2.58), that

$$\rho^{\nu_1,\nu_2}_{chOE,2|2+2|2}(E, c \gg 1) \;=\; 2\rho^{\nu_1+\nu_2}_{chOE}(2u) \tag{5.8}$$

where[4, 46]

$$\rho^{\nu}_{chOE}(u) \;=\; u/2\left(J^2_{|\nu|}(u) - J_{|\nu|+1}(u)J_{|\nu|-1}(u)\right) + \frac{1}{2}J_{|\nu|}(u)\left(1 - \int_0^u dx J_{|\nu|}(x)\right) \tag{5.9}$$

is the spectral density of a single ensemble. The prefactor of 2 comes from normalisation.[1]

A comparison with the orthogonal random matrix ensemble for $c^2 \gg 1$ can be seen in Figure 6.7 in Chapter 6. As expected, the are in agreement.

5.2 Weak Coupling Limit of chOE

We expect the low coupling limit to behave similar to chUE. So the partition function should factorise in the way

$$Z^{\nu_1,\nu_2}_{chOE,2|2+2|2}(M, c \ll 1) \;=\; Z^{n',\nu}_{chGOE}\Big(\frac{M}{\sqrt{2n'}c}\Big) Z^{(\nu_1),bulk}_{chGOE}(MM^\dagger) Z^{(\nu_2),bulk}_{chGOE}(MM^\dagger) \tag{5.10}$$

with $n' = \frac{|\nu_1|+|\nu_2|-|\nu|}{2}$ and $\nu = \nu_1 + \nu_2$. Like before, $bulk$ means without zero modes. These can be found from

$$Z^{(\nu)}_{chOE}(M) \;=\; \begin{cases} \mathrm{Sdet}^{\frac{\nu}{2}}(M) Z^{(\nu),bulk}_{chOE}(MM^\dagger) & ,\quad \nu \geq 0 \\ \mathrm{Sdet}^{-\frac{\nu}{2}}(M^\dagger) Z^{(\nu),bulk}_{chOE}(MM^\dagger) & ,\quad \nu < 0 \end{cases}. \tag{5.11}$$

[1] Note that [46] only considers $\nu \geq 0$, which is why we have added the absolute value. It only makes a difference in the last term.

To show this factorisation, we make two Hubbard-Stratanovitch transformations on (5.4), like we did in (4.17), except that $\sigma, \bar{\sigma} \in \tilde{\Sigma}(2|2)$, which can be parametrised as [8]

$$\sigma_j = \mathrm{diag}(\mathbf{1}_2, \tilde{O}_j) \begin{pmatrix} iu & 0 & \eta_j^* & \chi_j^* \\ 0 & iu & -\eta_j & -\chi_j \\ \eta_j & \eta_j^* & v_j & 0 \\ \chi_j & \chi_j^* & 0 & w_j \end{pmatrix} \mathrm{diag}(\mathbf{1}_2, \tilde{O}_j^T) \tag{5.12}$$

where $\tilde{O} \in O(2)$ and $u, v, w \in \mathbb{R}$.

We find

$$\begin{aligned} Z^{\nu_1,\nu_2}_{chOE,2|2+2|2}(M) &= \int_{\tilde{\Sigma}(2|2)} dA \int_{\Sigma(2|2)} dU_1 dU_2 \, \mathrm{Sdet}^{\frac{\nu_1}{2}}(U_1) \, \mathrm{Sdet}^{\frac{\nu_2}{2}}(U_2) \exp\Big[-\mathrm{Str}\Big(\frac{AA^\dagger}{4c^2}\Big)\Big] \\ &\quad \times \exp\Big[\frac{1}{2}\mathrm{Str}((M^\dagger + A)U_1 + (M + A^\dagger)U_1^{-1}) \\ &\quad + \frac{1}{2}\mathrm{Str}((M^\dagger + A)U_2 + (M + A^\dagger)U_2^{-1})\Big] \\ &= \int_{\tilde{\Sigma}(2|2)} dA \exp\Big[-\mathrm{Str}\Big(\frac{AA^\dagger}{4c^2}\Big)\Big] Z^{(\nu_1)}_{chOE}(M + A^\dagger) Z^{(\nu_2)}_{chOE}(M + A^\dagger). \end{aligned} \tag{5.13}$$

In the last line, we have used that the $n \to \infty$ limit of chGOE is [8]

$$Z^{n\to\infty,\nu}_{chGOE}(m_R = m/2n) \equiv Z^{(\nu)}_{chOE}(M) = \int dU \, \mathrm{Sdet}^{\frac{\nu}{2}}(U) e^{\frac{1}{2}\mathrm{Str}(M^\dagger U + M U^{-1})} \tag{5.14}$$

Splitting this into zero modes and non-zero modes like before, the factors of $\frac{1}{2}$ cancel and we arrive directly at

$$Z^{\nu_1,\nu_2}_{chOE,2|2+2|2}(M, c \ll 1) = Z^{n',\nu}_{chGOE}\Big(\frac{M}{\sqrt{2n'}c}\Big) Z^{(\nu_1),bulk}_{chOE}(MM^\dagger) Z^{(\nu_2),bulk}_{chOE}(MM^\dagger), \tag{5.15}$$

with $n' = \frac{|\nu_1|+|\nu_2|-|\nu_1+\nu_2|}{2}$ and $\nu = \nu_1 + \nu_2$ and the width of the finite ensemble proportional to c, by the same procedure as in Section 4.2. Note the different width, which comes from a difference of 2 in the Gaussian weights of chGUE and chGOE

$$Z^{n,\nu}_{chGOE}(m) = \int dW \, \det{}^{N_f} \begin{pmatrix} m & iW \\ iW^\dagger & m \end{pmatrix} e^{\frac{n}{2}\mathrm{Tr}(WW^\dagger)}. \tag{5.16}$$

Again, the transformation properties of the mass are contained in $Z^{n',\nu}_{chOE}(\frac{M}{\sqrt{2n'}c})$. This factorisation makes the chiral condensate

$$\Sigma^{\nu_1,\nu_2}_{chOE,2|2+2|2}(m, c \ll 1) = \Sigma^{n,\nu}_{chGOE}\left(\frac{m}{\sqrt{2n'}c}\right) + \Sigma^{(\nu_1),bulk}_{chOE}(m) + \Sigma^{(\nu_2),bulk}_{chOE}(m) \tag{5.17}$$

and the spectral density

$$\rho^{\nu_1,\nu_2}_{chOE,2|2+2|2}(u, c \ll 1) = \rho^{n',\nu}_{chGOE}\left(\frac{u}{\sqrt{2n'}c}\right) + \rho^{(\nu_1),bulk}_{chOE}(u) + \rho^{(\nu_2),bulk}_{chOE}(u). \tag{5.18}$$

The explicit results for $n' = 1, \nu = 0$ and $n' = 1, \nu = 1$ are

$$\rho_{chGOE}^{n'=1,\nu=0}(u) = \frac{1}{\sqrt{4\pi c^2}} e^{-\frac{u^2}{4c^2}} \tag{5.19}$$

and

$$\rho_{chGOE}^{n'=1,\nu=1}(u) = \frac{1}{4c^2} u\, e^{-\frac{u^2}{4c^2}}. \tag{5.20}$$

The derivation of these can be found in Appendix C.5. The full expression for even n can be found in [4].

A comparison with the corresponding random matrix ensemble for $c^2 \ll 1$ can be found in Figure 6.6 in Chapter 6. Again, the width of the bulk eigenvalues scale as $\frac{1}{V}$, while the width of the would-be zero modes scale as $\frac{1}{\sqrt{V}}$, see the correspondence scheme (3.68).

5.3 Subconclusion

This concludes the analytical part of our investigation. In Chapters 4 and 5 we have applied the coupling introduced in Chapter 3. We find a complicated expression for the full chiral condensate for chUE in (4.6), allowing numerical calculation of the eigenvalue density.

For both chUE and chOE we find simple, analytical expressions for the limiting cases $c \gg 1$ and $c \ll 1$. In the strong coupling limit the coupled system behaves as a single, uncoupled system with $\lambda \to 2\lambda$. In the weak coupling limit the partition function factorises, and the cancelled zero modes spread out on either side of the origin as a finite size chiral ensemble with a Gaussian weight. The bulk modes are unaffected to lowest order. The Gaussian weight is a direct consequence of the unique quadratic term in the effective Lagrangian found in Chapter 3 and therefore universal, although the choice of weight is usually arbitrary. In all cases we find that the total number of zero modes should be counted with sign, which allows zero modes of opposite chirality to cancel each other.

The cancellation of zero modes and factorisation of would-be zero modes for both chUE and chOE, (4.11) and (5.10) are the main analytical results of this thesis. In Chapter 6 we compare these results to numerics.

Chapter 6

Comparison to Numerics

In this chapter, we use the chiral two random matrix theory introduced in Chapter 3 to numerically calculate the eigenvalue density of the coupled system. We compare this to the spectrum obtained from the effective theory in Chapters 4 and 5.

6.1 Creating a Random Matrix Algorithm

We start with the simplest case as an example: A single, uncoupled chUE.

As we are dealing with numerics, the true microscopic limit $n \to \infty$ is of course unattainable. We therefore work from a finite size ensemble with a Gaussian weight

$$Z^{n,\nu}_{chGUE} = \int dW \det \begin{pmatrix} m & iW \\ iW^\dagger & m \end{pmatrix} e^{-n\mathrm{Tr}(WW^\dagger)} \tag{6.1}$$

where W is a general $(n+\nu) \times n$ matrix ($n \times (n-\nu)$ for $\nu < 0$) with complex entries and simply choose a sufficiently large n. In most cases, $n \geq 20$ is plenty to see the agreement between EFT and RMT.

The quenched version of (6.1) corresponds to removing the determinant, creating matrices of the form

$$\begin{pmatrix} 0 & iW \\ iW^\dagger & 0 \end{pmatrix} \tag{6.2}$$

with the components of W drawn from the weight

$$e^{-n\mathrm{Tr}(WW^\dagger)} \quad = \quad e^{-n\left({a_{ij}}^2+{b_{ij}}^2\right)} \quad , \quad W = a + ib, \tag{6.3}$$

and finding the eigenvalues λ_R of these matrices. For the distribution of these random matrices to be close to the true distribution, the number of matrices calculated should be around 10^4 or more.

Recall that the microscopic eigenvalue spectrum is a function of $u = \Sigma_0 V \lambda = 2n\lambda_R$, see Equation (3.19). We therefore rescale all eigenvalues accordingly and normalise the distribution to the number of eigenvalues $(2n + |\nu|)$.

For the most part, we use the same binning across the whole spectrum, but in the case of small coupling, we increase our resolution around the near-zero modes. The microscopic

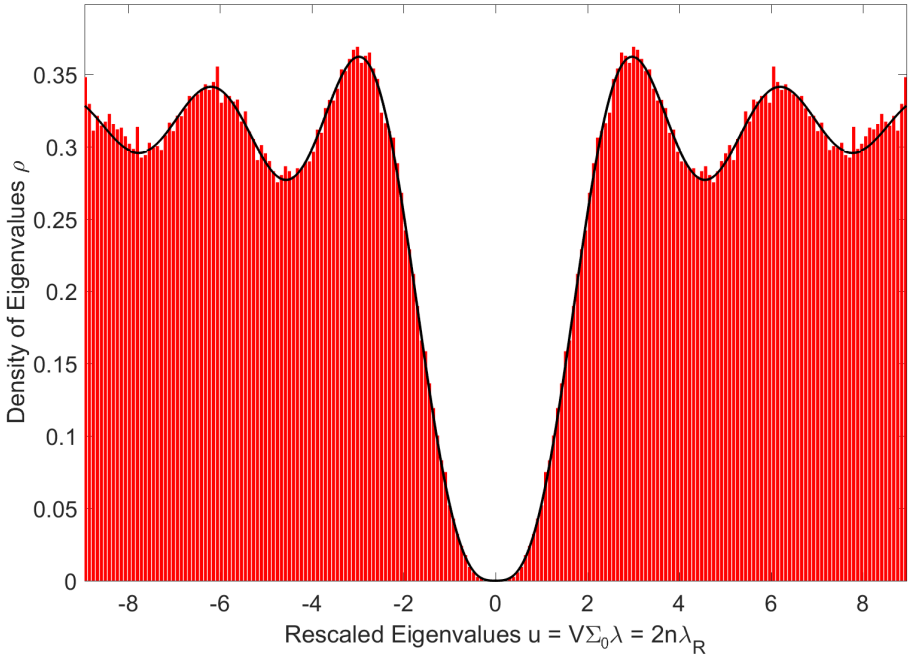

Figure 6.1: Distribution of eigenvalues for a single, uncoupled chiral unitary ensemble. Plotted is eigenvalue density as a function of $u = \Sigma_0 V\lambda = 2n\lambda_R$ of 10^5 chGUE matrices for $\nu = 1$ and $n = 40$. The theoretical curve from Equation (4.4) (black) has been plotted on top. We have zoomed in on the $\sqrt{2n}$ smallest eigenvalues.

eigenvalue spectrum from (4.4) is valid around $|u| < \sqrt{V}$ [11, 47], so we zoom in on this part. In all cases, we remove the (numerically) exact zero modes from the distribution, because it does not make sense to compare a δ-function to numerics. In other words, we only look at eigenvalues for $10^{-14} < |\lambda_R| < \frac{1}{\sqrt{2n}}$.

We make a histogram of u and plot the theoretical curve on top. The result can be seen in Figure 6.1. The numerical and theoretical distributions are compared by eye. We elaborate on the possibility of a proper statistical comparison in Appendix D.

Now that we have established that our code runs as expected, we turn to the coupled case.

Table 6.1: Parameters used in random matrix theory and chiral perturbation theory for chUE and how they correspond to each other. Notice the factor of 2 that comes from the choice of factors in the EFT.
Notice also the difference between the parameters. λ_C and $\tilde{c}$ are physical energy and coupling constant, whereas λ_R and c_R are dimensionless parameters of our random matrix model. These are relatable through the space-time volume of the system, the low-energy constants Σ_0, K_1, and the size of the matrix in RMT. We have assumed $\Sigma_0 = K_1 = 1$ and $V, n \to \infty$, while keeping $u, c \sim 1$.

chUE	chPT	RMT
u	$\Sigma_0 V\lambda$	$2n\lambda_R$
c^2	$K_1 V\tilde{c}^2$	nc_R^2

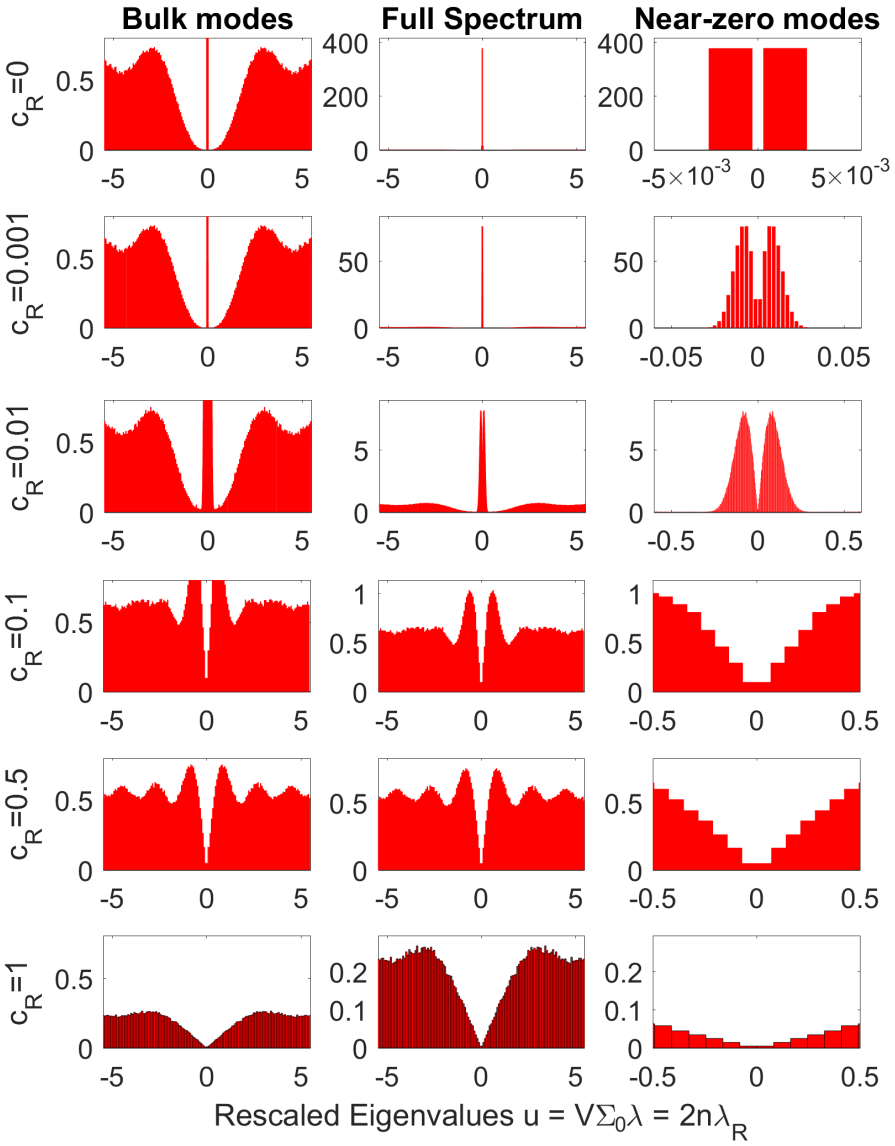

Figure 6.2: Numerical search of the coupling parameter space of two coupled chiral unitary ensembles for $\nu_1 = -\nu_2 = 1$ and $n = 30$, as can be found in (3.9). Plotted are the eigenvalues of random matrix simulations for different coupling strengths. For zero coupling, the topological modes of each ensemble are unaffected. The stronger the coupling, the more the would-be zero modes spread out on either side until they become part of the bulk. We have left the exact zero modes in the spectrum to illustrate this spreading, although numerical effects place them slightly on either side of the origin.
Centre column: The full spectrum. **Left column:** Zoom-in on the bulk modes. These are unaffected for small coupling. When the coupling becomes strong enough, the would-be zero modes become part of the bulk. **Right column:** Zoom-in on the modes close to the origin. For zero coupling, the zero modes are intact. For small, but non-zero, coupling, the would-be zero modes are distributed as discussed in Sections 4.2 and 6.2. When the would-be zero modes become part of the bulk, there are no modes near the origin.

6.2 Coupled Chiral Unitary Ensemble

The numerical set up of the two coupled matrices is completely analogous to the single matrix.

We work from the theory

$$Z_{1+1}^{\nu_1,\nu_2} = \int dW_1 dW_2 \det \begin{pmatrix} m & iW_1 & 0 & ic_R \\ iW_1^\dagger & m & ic_R & 0 \\ 0 & ic_R & m & iW_2 \\ ic_R & 0 & iW_2^\dagger & m \end{pmatrix} e^{-n\mathrm{Tr}\left(W_1W_1^\dagger + W_2W_2^\dagger\right)} \tag{6.4}$$

where W_j are $(n+\nu_j)\times n$ complex matrices. This is the same theory as in (3.9), repeated for ease of reading. c_R is a matrix that determines the coupling strength. It is proportional to unity and for $\nu_j \neq 0$, c_R is padded with zeros.

For instance, in the case $\nu_1 = 0, \nu_2 = 1$, and $n = 2$, the upper right-hand block is

$$\begin{pmatrix} 0 & 0 & 0 & ic_R & 0 \\ 0 & 0 & 0 & 0 & ic_R \\ ic_R & 0 & 0 & 0 & 0 \\ 0 & ic_R & 0 & 0 & 0 \end{pmatrix}, \tag{6.5}$$

and the low left-hand block is the transposed of this. So we create matrices of the form

$$\begin{pmatrix} 0 & iW_1 & 0 & ic_R \\ iW_1^\dagger & 0 & ic_R & 0 \\ 0 & ic_R & 0 & iW_2 \\ ic_R & 0 & iW_2^\dagger & 0 \end{pmatrix} \tag{6.6}$$

and plot the rescaled eigenvalues along the theoretical curves. An important addition in the coupled case is the relation between the coupling strength c of the effective theory and the parameter c_R of the random matrix theory. This can be found in Equation (3.19) and is repeated in Table 6.1.

We may now calculate the eigenvalue spectrum numerically for any coupling strength, see Figure 6.2. The limiting cases $c \gg 1$ and $c \ll 1$ are of special interest, because we can compare them to the analytical distributions derived in Sections 4.1 and 4.2 respectively.

Small Coupling Limit

For $c_R = 0$ the density simplifies to the sum of two single ensembles. For small, but non-zero coupling the bulk modes are still unaffected, whereas the exact zero modes spread out as near-zero modes, as can be seen in Figure 6.3. The theoretical curve for small coupling limit can be found in Equation (4.27).

Strong Coupling Limit

The large c-limit yields the spectrum

$$\rho_{chUE}^{\nu_1,\nu_2}(u, c \gg 1) \quad = \quad 2\rho_{chUE}^{(\nu_1+\nu_2)}(2u), \tag{6.7}$$

the derivation of which can be found in Section 4.1.

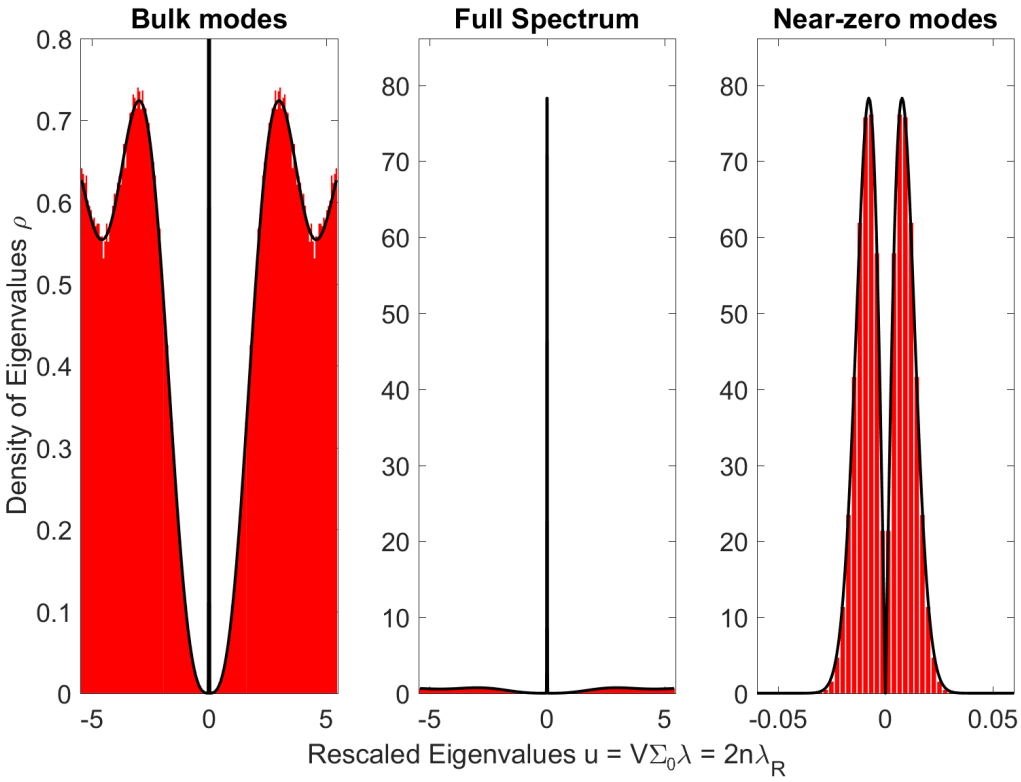

Figure 6.3: The small coupling limit of chUE, which is a main result of this thesis. The zero modes of each system is counted with sign, which allows zero modes of opposite chirality to cancel each other. For small coupling, these would-be zero modes spread out on either side of the origin as near-zero modes. The distribution follows that of a finite chiral unitary ensemble with a Gaussian weight. Plotted are the eigenvalues of a simulation of 10^5 coupled chGUE matrices with $n = 30$ and $\nu_1 = -\nu_2 = 1$ for $c_R = 10^{-4}$.
Centre: The full spectrum. **Left:** A zoom-in on the bulk modes that are left unchanged by the coupling. **Right:** A zoom-in on the would-be zero modes distributed according to a finite Gaussian ensemble. The small c-approximation of the density from (4.27) has been plotted on top (black). This figure has also been published in [31].

As we can see in our correspondence scheme (see Table 6.1), we can choose between large n or large c_R, as they both represent the strong coupling limit. Large c_R will place all eigenvalues in $\pm c_R$, and the W-matrices provide only small perturbations around this value. The limit $c_R \gg 1$ does therefore not support a distribution around the origin, which is a requirement of the universal spectrum [18]. We therefore choose large n, which in this case means $n = 1000$. Some corners can be cut by utilising numerical methods that only compute the lowest k eigenvalues, where we set $k = \sqrt{n}$. This method requires non-singular matrices, so we can only calculate $\nu_1 = -\nu_2$ this way. These methods are part of standard packages in Matlab. The result can be seen in Figure 6.4.

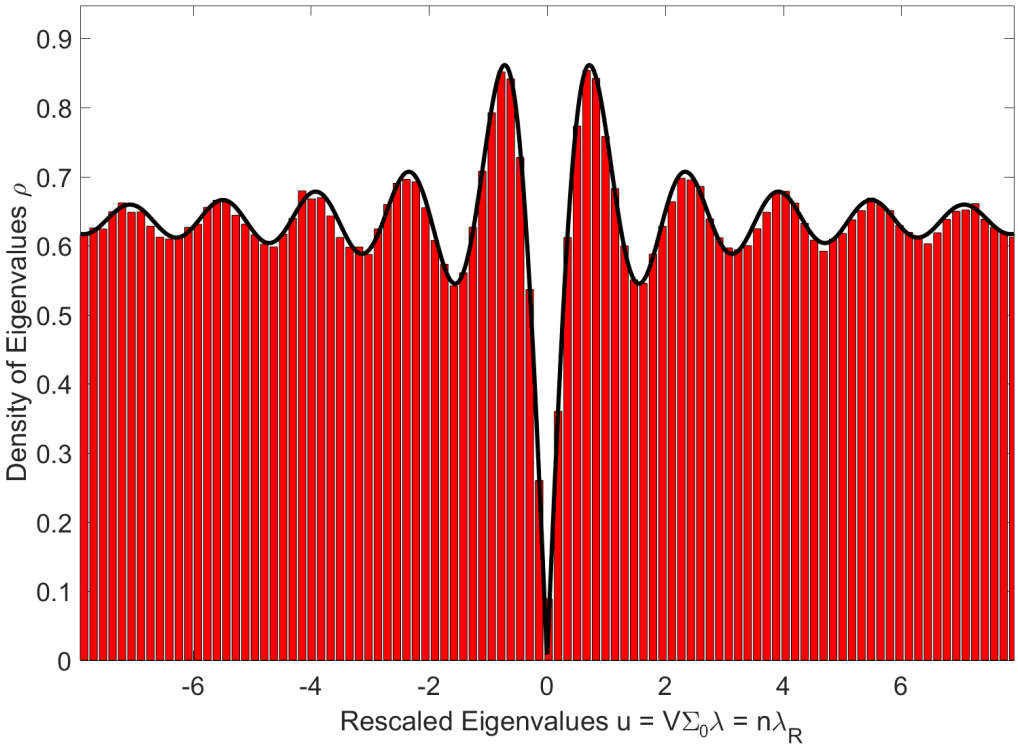

Figure 6.4: The strong coupling limit of chUE. The coupled system behaves like a single, uncoupled ensemble with $u \to 2u$. Plotted are the rescaled eigenvalues $u = 2n\lambda_R$ of a coupled chUE random matrix simulation with $n = 1000$, $\nu_1 = -\nu_2 = 1$ and $c_R = 0.1$. The large c-approximation from (4.11) has been plotted on top (black). The result is independent of the exact value of c_R. This figure has also been published in [31].

6.2.1 Two-Flavour Theory: $W_1 = W_2$

As was treated in Section 3.4, working from a theory with the two flavours built in corresponds to $W_1 = W_2$ in the random two matrix theory. This connection is seen even more clearly in Appendix C.2, where we derive the effective theory of the $W_1 = W_2$-random matrix model. So we work from the theory

$$Z_2^\nu = \int dW \det \begin{pmatrix} m & iW & 0 & ic_R \\ iW^\dagger & m & ic_R & 0 \\ 0 & ic_R & m & iW \\ ic_R & 0 & iW^\dagger & m \end{pmatrix} e^{-n\mathrm{Tr}(WW^\dagger)} \tag{6.8}$$

where W are $(n+\nu) \times n$ complex matrices. We create matrices of the form

$$\begin{pmatrix} 0 & iW & 0 & ic_R \\ iW^\dagger & 0 & ic_R & 0 \\ 0 & ic_R & 0 & iW \\ ic_R & 0 & iW^\dagger & 0 \end{pmatrix} \tag{6.9}$$

and compare the rescaled eigenvalues to the theoretical curves on top.

The spectrum of this theory is slightly trivial compared to $W_1 \neq W_2$, as there can be no cancellation of topological modes ($W_1 = W_2$ implies $\nu_1 = \nu_2$). The strong coupling limit, however, behaves slightly different for $W_1 = W_2$. Here we do not have $u \to 2u$, which we show numerically, see Figure 6.5.

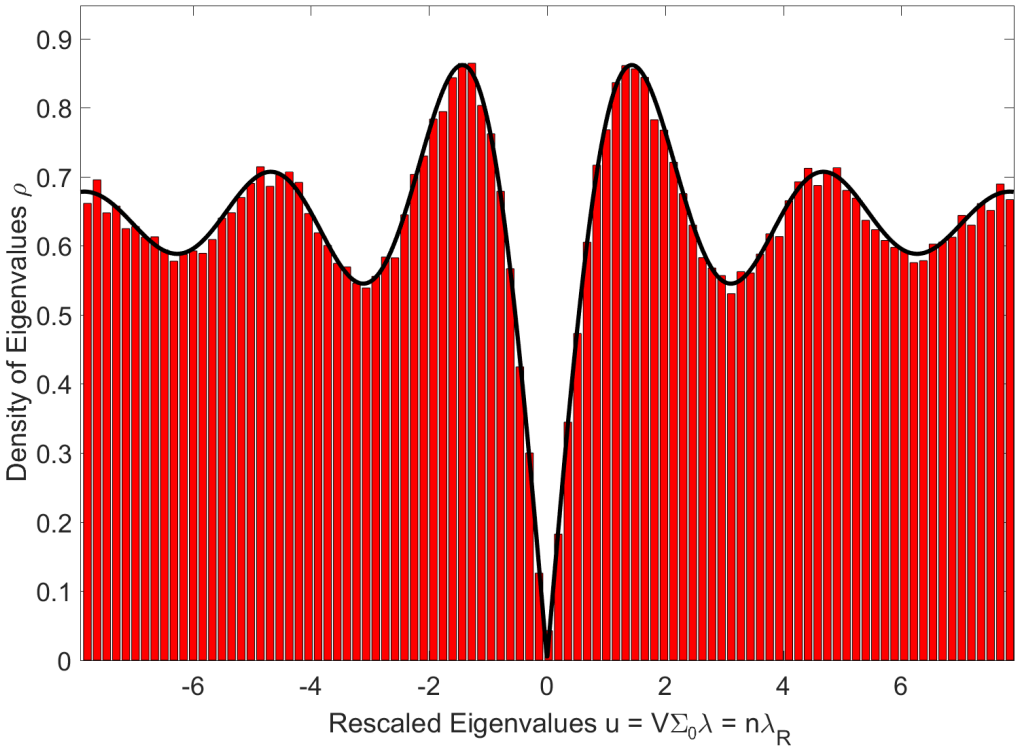

Figure 6.5: The strong coupling limit of chUE for $W_1 = W_2$. The coupled system behaves like a single, uncoupled ensemble. Compared to $W_1 \neq W_2$ we do not have $u \to 2u$. We only show this numerically. Plotted are the rescaled eigenvalues $u = 2n\lambda_R$ of a coupled chUE random matrix simulation with $n = 1000$, $\nu_1 = -\nu_2 = 1$ and $c_R = 0.1$. The distribution of a single, uncoupled ensemble (4.4) normalised to $4n$ has been plotted on top (black). The result is independent of the exact value of c.

Twisted Two-Flavour Theory: $W_1 = W_2^\dagger$

Let us examine a final case of coupled chUE. If we want cancelling of topological modes of two flavours in the same background, we may redefine right and left for one of the flavour sections. This corresponds to the theory

$$Z_2^{*\nu} = \int dW \det \begin{pmatrix} m & iW & 0 & ic_R \\ iW^\dagger & m & ic_R & 0 \\ 0 & ic_R & m & iW^\dagger \\ ic_R & 0 & iW & m \end{pmatrix} e^{-n\mathrm{Tr}\left(WW^\dagger\right)}. \tag{6.10}$$

One should be careful how to run this simulation, as a coupling matrix proportional to unity simplifies the spectrum more than intended. Consider the eigenvalue condition

$$\begin{aligned}
0 &= \det\left[\begin{pmatrix} -\lambda_R & iW & 0 & ic_R \\ iW^\dagger & -\lambda_R & ic_R & 0 \\ 0 & ic_R & -\lambda_R & iW^\dagger \\ ic_R & 0 & iW & -\lambda_R \end{pmatrix}\right] \\
&= \det\left[\begin{pmatrix} -\lambda_R & iW^\dagger \\ iW & -\lambda_R \end{pmatrix}\left(\begin{pmatrix} -\lambda_R & iW \\ iW^\dagger & -\lambda_R \end{pmatrix} - \begin{pmatrix} 0 & ic_R \\ ic_R & 0 \end{pmatrix}\begin{pmatrix} -\lambda_R & iW^\dagger \\ iW & -\lambda_R \end{pmatrix}^{-1}\begin{pmatrix} 0 & ic_R \\ ic_R & 0 \end{pmatrix}\right)\right] \\
&= \det\left[\begin{pmatrix} -\lambda_R & iW^\dagger \\ iW & -\lambda_R \end{pmatrix}\left(\begin{pmatrix} 0 & 1 \\ 1 & 0 \end{pmatrix}\begin{pmatrix} -\lambda_R & iW \\ iW^\dagger & -\lambda_R \end{pmatrix}\begin{pmatrix} 0 & 1 \\ 1 & 0 \end{pmatrix} - (ic_R)^2\begin{pmatrix} -\lambda_R & iW^\dagger \\ iW & -\lambda_R \end{pmatrix}^{-1}\right)\right] \\
&= \det\left[\begin{pmatrix} -\lambda_R & iW^\dagger \\ iW & -\lambda_R \end{pmatrix}^2 - \begin{pmatrix} ic_R & 0 \\ 0 & ic_R \end{pmatrix}^2\right] \\
&= \det\left[\begin{pmatrix} -\lambda_R & iW^\dagger \\ iW & -\lambda_R \end{pmatrix} - \begin{pmatrix} ic_R & 0 \\ 0 & ic_R \end{pmatrix}\right]\det\left[\begin{pmatrix} -\lambda_R & iW^\dagger \\ iW & -\lambda_R \end{pmatrix} + \begin{pmatrix} ic_R & 0 \\ 0 & ic_R \end{pmatrix}\right].
\end{aligned} \tag{6.11}$$

From this we see that the spectrum of this naïvely twisted coupled ensemble reduces to the spectrum of two single, uncoupled ensembles shifted in opposite direction by c_R.

The interpretation must be as follows: Although (6.10) has the right symmetries, it does not allow the two flavour sections to interact fully. If we instead of the normal choice of c_R (6.5) choose the elements randomly from a Gaussian distribution similar to W, the spectrum becomes numerically identical to the $W_1 \neq W_2$-case with $\nu_1 = \nu_2$.

One should also be careful of the $U(2)$-symmetry. An additional γ_0 in chiral space is needed in the transformation to account for the difference in chirality of the two flavours. If this is added, we preserve full $U(2)$-symmetry.

6.3 Coupled Chiral Orthogonal Ensemble

The orthogonal ensemble is in many respects completely analogous to the unitary ensemble, save factors of 2. We work from the theory

$$Z_{1+1}^{\nu_1,\nu_2} = \int dW_1 dW_2 \det\begin{pmatrix} m & iW_1 & 0 & ic_R \\ iW_1^T & m & ic_R & 0 \\ 0 & ic_R & m & iW_2 \\ ic_R & 0 & iW_2^T & m \end{pmatrix} e^{-\frac{n}{2\sigma^2}\mathrm{Tr}\left(W_1W_1^T + W_2W_2^T\right)} \tag{6.12}$$

where W_j are $(n+\nu_j)\times n$ real matrices. Note that the extra factor of $\frac{1}{2}$ in the weight compared to chGUE comes from the definition of the ensembles. So we construct matrices of the form

$$\begin{pmatrix} 0 & iW_1 & 0 & ic_R \\ iW_1^T & 0 & ic_R & 0 \\ 0 & ic_R & 0 & iW_2 \\ ic_R & 0 & iW_2^T & 0 \end{pmatrix} \tag{6.13}$$

with the entries of W_j chosen from a Gaussian distribution. The correspondence scheme is a slightly different one than for chUE and can be found in Table 6.2.

Table 6.2: Parameters used in random matrix theory and chiral perturbation theory for chOE and how they correspond to each other. This is a reprint of Equation (3.68). Notice the differences from the unitary ensemble.

chOE	chPT	RMT
u	$\Sigma_0 V\lambda$	$n\lambda_R$
c^2	$K_1 V\tilde{c}^2$	$\frac{1}{2}nc_R^2$

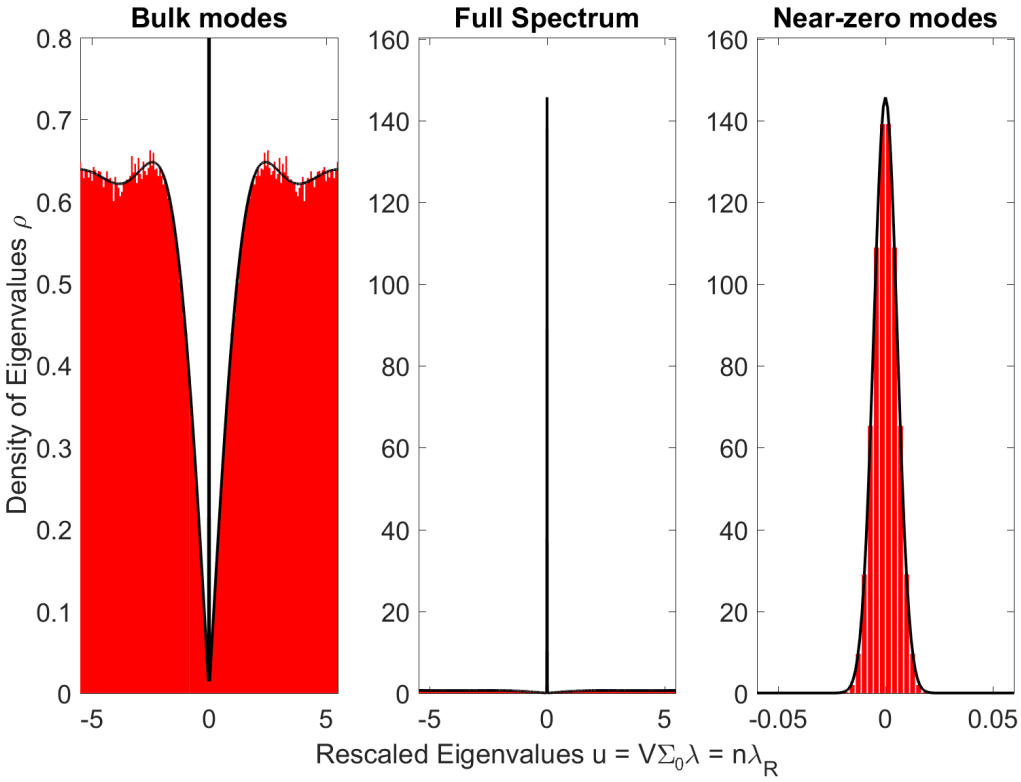

Figure 6.6: The small coupling limit of chOE, which is a main result of this thesis. For small, but non-zero coupling the would-be topological modes spread out on either side of the origin as a finite chiral ensemble with a Gaussian weight. The bulk modes are unaffected to lowest order. Plotted is the eigenvalue spectrum of a coupled random matrix simulation with $n = 30$, $\nu_1 = -\nu_2 = 1$, and $c_R = 10^{-4}$.
Centre: The full spectrum. **Left:** A zoom-in on the bulk modes that are left unchanged by the coupling. **Right:** A zoom-in on the would-be zero modes distributed according to a finite Gaussian ensemble. The small c-approximation of the density from (4.27) has been plotted on top (black). This figure has also been published in [31].

Small Coupling Limit

Like for chUE $c_R = 0$ reduces to the sum of two single ensembles. For small, but non-zero coupling we find the same spreading of topological modes. The theoretical curve for small c can be found in Equation (5.18). A plot of this can be found in Figure 6.6.

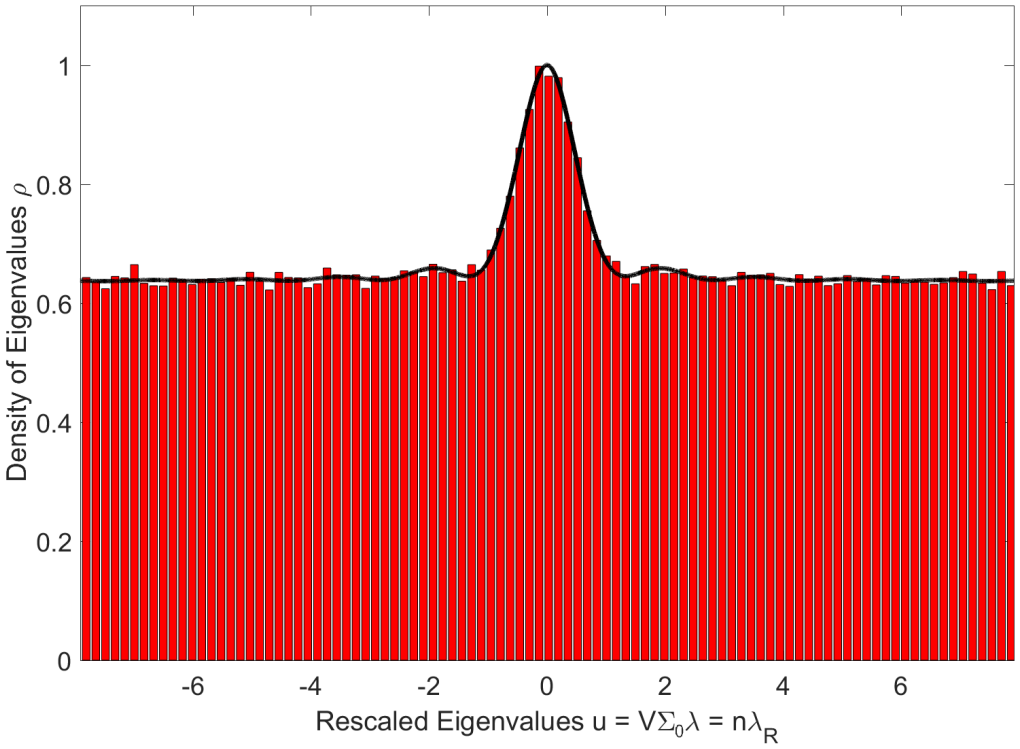

Figure 6.7: The strong coupling limit of chOE. The coupled ensemble behaves as a single, uncoupled ensemble with $u \to 2u$. Plotted is the spectral density of a coupled random matrix simulation with $c_R = 0.1$, $n = 1000$, and $\nu_1 = -\nu_2 = 1$. The large c-approximation has been plotted on top of this (black). This figure has also been published in [31].

Strong Coupling Limit

As for chUE, the strong coupling ensemble behaves like a single ensemble with $u \to 2u$. The expression can be found in Equation (5.8) and a plot of it in Figure 6.7.

Chapter 7

Concluding Remarks

7.1 Summary

In this thesis we have laid the groundwork for the treatment of two coupled chiral systems, where the coupling preserves a combined chiral symmetry. We considered the effect of such a coupling on the small eigenvalues with a special focus on the cancellation of topological modes in exact zero and the smearing of these would-be zero modes on either side of the origin.

We started out in Chapter 3 by establishing the properties of the chiral coupling and the following chapters saw the calculation of its microscopic eigenvalue spectrum in different cases.

Analytically, we set up an effective theory. We here found a unique term in the effective Lagrangian that couples the two ensembles to lowest order. The consequences of this unique term were then investigated in Chapters 4 and 5, where we derived the microscopic eigenvalue density. We found that the total number of zero modes is the sum of the individual zero modes counted with sign. We also found that, for small coupling, the $|\nu_1| + |\nu_2| - |\nu_1 + \nu_2|$ zero modes that do no survive the coupling spread out as near-zero modes according to a finite random matrix ensemble with a Gaussian weight.

Numerically, we introduced a random two-matrix model with the same symmetries as the coupled systems. This allowed us to calculate the spectrum numerically for any coupling strength. In Chapter 6 we compared the analytical and numerical results for the limiting cases and found good agreement between the eigenvalue densities. We also bridged the gap between the effective field theory and the random two-matrix theory further by showing that they have the same low-energy effective theory. This is not surprising, as they have the same symmetries, and it is therefore an important check of the analytical computations.

We did this analysis for both two coupled single-flavour theories and for two flavours in the same background. We found that the two-flavour theory is significantly more complicated to derive analytically, but numerics showed that it behaves very similar to the two single-flavour ensembles. The main difference is that zero modes cannot cancel because the winding number is tied to the gauge field background, and so the two winding numbers always have the same sign. We considered a two-flavour ensemble, where left and right was redefined for one of the flavours. This requires an additional transformation when rotating the flavours into each other, but allows zero modes to cancel. This ensemble is, according to numerics, very similar to the two single-flavour ensembles.

These results may be viewed on their own as an exercise in mathematical physics, but it is also our hope that this understanding of coupled chiral systems will help pave the way for

a full description of the superconductors carrying Majorana modes, which was the original inspiration.

7.2 Outlook

The obvious avenue to pursue is the development of a random matrix model that incorporates the Majorana condition for the zero modes only. We have already touched upon the subject in Section 2.6 and Appendix C.1, but we have yet to construct a model that fulfils this requirement. It is unclear whether such a model will be born with two interacting zero modes or whether we will have to apply the coupling as in this thesis. Whichever the case, this would make the model directly applicable to the solid state system.

In terms of mathematics, it would also be interesting to do the same calculation for the chiral symplectic ensemble, which has quaternion real entries instead of real or complex ones. We expect the limiting cases to be straightforward, because the effective theories have a very similar structure. We also expect same factorisation of near-zero modes and bulk modes for small coupling that we found in chUE and chOE.

We would very much like to investigate the generality of the factorisation into bulk modes and a finite Gaussian ensemble. We have seen the same behaviour in [8] for a theory with a term of the form

$$\mathcal{L}_{\text{Wilson}} \quad = \quad -a^2 \operatorname{Str}(U^2 + U^{-2}) \tag{7.1}$$

in the $a \ll 1$ limit, so the question remains: Does this happen for any quadratic term? One might for a start consider a term of the kind

$$\mathcal{L}_{\text{Quad}} \quad = \quad b^2 \operatorname{Str}(AUBU^{-1}) \tag{7.2}$$

in the limit $b \ll 1$, where A and B are general matrices. We expect constraints on A and B will be necessary to ensure convergence. We do not expect to be able to identify all parts of the factorised partition function as known ensembles.

If the coupling is indeed applicable to a physical system, superconductor or otherwise, identification of the parameter c as a measurable quantity is needed. So far, we would be able to measure it as the width of the near-zero eigenvalue distribution for small coupling, which should scale as $\frac{1}{\sqrt{V}}$ (the bulk modes scale as $\frac{1}{V}$). We would, however, also like to identify it elsewhere. Our suggestion here is to review the effective Lagrangian in p-counting and calculate the propagation and loop diagrams of the coupled system as in [9]. We conjecture that c will appear, possibly in combination with other observables, as a scattering amplitude, allowing us to observe it several places and compare the results.

Bibliography

[1] E. B. Hansen, "Unpaired Majorana Fermions in Disordered p-wave Superconductor and Random Matrix Theory" (Master's Thesis, available at `http://cmt.nbi.ku.dk/student_projects/msc/thesis_esben.pdf`).

[2] Esben Bork Hansen, Jeroen Danon, and Karsten Flensberg, "Phase-tunable Majorana bound states in a topological N-SNS junction," Phys. Rev. B **93**, no. 9, 094501 (2016).

[3] J. J. M. Verbaarschot, "The Spectrum of the QCD Dirac operator and chiral random matrix theory: The Threefold way," Phys. Rev. Lett. **72**, 2531 (1994) doi:10.1103/PhysRevLett.72.2531 [hep-th/9401059].

[4] J. J. M. Verbaarschot, "The Spectrum of the Dirac operator near zero virtuality for $N_c = 2$ and chiral random matrix theory," Nucl. Phys. B **426**, 559 (1994) [hep-th/9401092].

[5] Random Matrices, Madan Lal Mehta (Third Edition, Elsevier, 2004).

[6] The Oxford Handbook of Random Matrix Theory, Edited by Gernot Akemann, Jinho Baik, and Philippe Di Francesco (First Edition, Oxford University Press 2015).

[7] A. M. Halasz and J. J. M. Verbaarschot, "Effective Lagrangians and chiral random matrix theory," Phys. Rev. D **52**, 2563 (1995) doi:10.1103/PhysRevD.52.2563 [hep-th/9502096].

[8] M. Kieburg, J. J. M. Verbaarschot and S. Zafeiropoulos, "Dirac Spectrum of the Wilson Dirac Operator for QCD with Two Colors," Phys. Rev. D **92**, no. 4, 045026 (2015) doi:10.1103/PhysRevD.92.045026 [arXiv:1505.01784 [hep-lat]].

[9] J. Gasser and H. Leutwyler, "Chiral Perturbation Theory to One Loop," Annals Phys. **158**, 142 (1984). doi:10.1016/0003-4916(84)90242-2

[10] J. Gasser and H. Leutwyler, "Thermodynamics of Chiral Symmetry," Phys. Lett. B **188**, 477 (1987). doi:10.1016/0370-2693(87)91652-2

[11] J. C. Osborn, D. Toublan and J. J. M. Verbaarschot, "From chiral random matrix theory to chiral perturbation theory," Nucl. Phys. B **540**, 317 (1999) doi:10.1016/S0550-3213(98)00716-0 [hep-th/9806110].

[12] P. H. Damgaard, J. C. Osborn, D. Toublan and J. J. M. Verbaarschot, "The microscopic spectral density of the QCD Dirac operator," Nucl. Phys. B **547**, 305 (1999) doi:10.1016/S0550-3213(99)00094-2 [hep-th/9811212].

[13] A. Pich, "Effective field theory: Course," hep-ph/9806303.

[14] C. W. Bernard and M. F. L. Golterman, "Chiral perturbation theory for the quenched approximation of QCD," Phys. Rev. D **46**, 853 (1992) doi:10.1103/PhysRevD.46.853 [hep-lat/9204007].

[15] C. W. Bernard and M. Golterman, "The Quenched approximation in health and in sickness," Nucl. Phys. Proc. Suppl. **30**, 217 (1993) doi:10.1016/0920-5632(93)90193-A [hep-lat/9211017].

[16] S. R. Sharpe and N. Shoresh, "Partially quenched chiral perturbation theory without Φ_0," Phys. Rev. D **64**, 114510 (2001) doi:10.1103/PhysRevD.64.114510 [hep-lat/0108003].

[17] E. V. Shuryak and J. J. M. Verbaarschot, "Random matrix theory and spectral sum rules for the Dirac operator in QCD," Nucl. Phys. A **560**, 306 (1993) doi:10.1016/0375-9474(93)90098-I [hep-th/9212088].

[18] G. Akemann, P. H. Damgaard, U. Magnea and S. Nishigaki, "Universality of random matrices in the microscopic limit and the Dirac operator spectrum," Nucl. Phys. B **487**, 721 (1997) doi:10.1016/S0550-3213(96)00713-4 [hep-th/9609174].

[19] J. J. M. Verbaarschot and I. Zahed, "Spectral density of the QCD Dirac operator near zero virtuality," Phys. Rev. Lett. **70**, 3852 (1993) doi:10.1103/PhysRevLett.70.3852 [hep-th/9303012].

[20] J. B. Kogut, M. A. Stephanov, D. Toublan, J. J. M. Verbaarschot and A. Zhitnitsky, "QCD-like theories at finite baryon density," Nucl. Phys. B **582**, 477 (2000) [hep-ph/0001171].

[21] D. T. Son and M. A. Stephanov, "QCD at finite isospin density," Phys. Rev. Lett. **86**, 592 (2001) [hep-ph/0005225].

[22] K. Splittorff, D. T. Son and M. A. Stephanov, "QCD-like theories at finite baryon and isospin density," Phys. Rev. D **64**, 016003 (2001) [hep-ph/0012274].

[23] P. H. Damgaard, U. M. Heller, K. Splittorff, B. Svetitsky and D. Toublan, "Microscopic eigenvalue correlations in QCD with imaginary isospin chemical potential," Phys. Rev. D **73**, 105016 (2006).

[24] T. Banks and A. Casher, Nucl. Phys. B **169**, 103 (1980). doi:10.1016/0550-3213(80)90255-2

[25] J. J. M. Verbaarschot and T. Wettig, "Random matrix theory and chiral symmetry in QCD," Ann. Rev. Nucl. Part. Sci. **50**, 343 (2000) [hep-ph/0003017].

[26] J. J. M. Verbaarschot, "QCD, chiral random matrix theory and integrability," hep-th/0502029.

[27] P. H. Damgaard, "Chiral Random Matrix Theory and Chiral Perturbation Theory," J. Phys. Conf. Ser. **287**, 012004 (2011) [arXiv:1102.1295 [hep-ph]].

[28] G. Akemann, "Random Matrix Theory and Quantum Chromodynamics," arXiv:1603.06011 [math-ph].

[29] H. Leutwyler and A. V. Smilga, "Spectrum of Dirac operator and role of winding number in QCD," Phys. Rev. D **46**, 5607 (1992). doi:10.1103/PhysRevD.46.5607

[30] Sankar Das Sarma, Michael Freedman, Chetan Nayak, "Majorana zero modes and topological quantum computation," Npj Quantum Information **1**, Article number: 15001 (2015)

[31] Adam Mielke and K. Splittorff, "Universal Distribution of Would-be Topological Zero Modes in Coupled Chiral Systems," To be published.

[32] M. E. Peskin and D. V. Schroeder, "An Introduction to Quantum Field Theory," Westview Press (1995) 842 p

[33] M. Srednicki, "Quantum field theory," Cambridge University Press (2007) 660 p

[34] Y. Nambu, "Quasiparticles and Gauge Invariance in the Theory of Superconductivity," Phys. Rev. **117**, 648 (1960). doi:10.1103/PhysRev.117.648

[35] S. Weinberg, "Phenomenological Lagrangians," Physica A **96**, 327 (1979).

[36] Particle Data Group: `http://pdg.lbl.gov/`

[37] M. Gell-Mann, R. J. Oakes and B. Renner, Phys. Rev. **175**, 2195 (1968). doi:10.1103/PhysRev.175.2195

[38] J. Gasser and H. Leutwyler, "Spontaneously Broken Symmetries: Effective Lagrangians at Finite Volume," Nucl. Phys. B **307**, 763 (1988). doi:10.1016/0550-3213(88)90107-1

[39] A. Pich and E. de Rafael, "Strong CP violation in an effective chiral Lagrangian approach," Nucl. Phys. B **367**, 313 (1991). doi:10.1016/0550-3213(91)90019-T

[40] Martin Leijnse and Karsten Flensberg, "Introduction to topological superconductivity and Majorana fermions," Semiconductor Science and Technology, Volume 27, Number 12.

[41] P. B. Pal, "Dirac, Majorana and Weyl fermions," Am. J. Phys. **79**, 485 (2011) doi:10.1119/1.3549729 [arXiv:1006.1718 [hep-ph]].

[42] `https://www.ippp.dur.ac.uk/~krauss/Lectures/QuarksLeptons/Dirac/DiracSolutions_1.html`

[43] K. Splittorff and J. J. M. Verbaarschot, "Factorization of Correlation Functions and the Replica Limit of the Toda Lattice Equation," Nucl. Phys. B **683**, 467 (2004) doi:10.1016/j.nuclphysb.2004.01.031 [hep-th/0310271].

[44] G. Akemann, P. H. Damgaard, K. Splittorff and J. J. M. Verbaarschot, "Spectrum of the Wilson Dirac Operator at Finite Lattice Spacings," Phys. Rev. D **83**, 085014 (2011) doi:10.1103/PhysRevD.83.085014 [arXiv:1012.0752 [hep-lat]].

[45] P. H. Damgaard, U. M. Heller, K. Splittorff, B. Svetitsky and D. Toublan, "Microscopic eigenvalue correlations in QCD with imaginary isospin chemical potential," Phys. Rev. D **73**, 105016 (2006) doi:10.1103/PhysRevD.73.105016 [hep-th/0604054].

[46] D. A. Ivanov, "The supersymmetric technique for random-matrix ensembles with zero eigenvalues," arXiv:cond-mat/0103137

[47] J. C. Osborn and J. J. M. Verbaarschot, "Thouless energy and correlations of QCD Dirac eigenvalues," Nucl. Phys. B **525**, 738 (1998) doi:10.1016/S0550-3213(98)00424-6 [hep-ph/9803419].

[48] Chapter 2 of Supersymmetry in Disorder and Chaos, Konstantin Efetov (Cambridge University Press, 1997).

[49] Handbook of Mathematical Functions, M. Abramowitz and I. A. Stegun (Martino Publishing, 2014).

[50] `http://bolvan.ph.utexas.edu/~vadim/Classes/2011f/saddle.pdf`

[51] R. J. Barlow: "Statistics - A Guide to the Use of Statistical Methods in the Physical Sciences," (Wiley 1989)

Appendix A

Grassmann Variables and Supermathematics

As Grassmann variables (or Grassmann numbers) are used in our calculations of supersymmetric ensembles, we shall here endeavour to give a short introduction. For a more thorough treatment, the reader is referred to [48], upon which this section is also based.

A Grassmann number is a variable that anticommutes with other Grassmann numbers[1]

$$\{\alpha_i, \alpha_j\} \quad = \quad 0. \tag{A.1}$$

The case $i = j$ shows that all Grassmann variables square to 0

$$\alpha^2 \quad = \quad 0. \tag{A.2}$$

They commute with conventional numbers

$$[x, \alpha] \quad = \quad 0. \tag{A.3}$$

Functions of Grassmann variables are defined as Taylor expansions

$$f(\alpha) \quad = \quad f(0) + f'(0)\,\alpha. \tag{A.4}$$

Notice that no higher than linear order contributes. We may generalise this to functions of multiple variables, where cross-terms also appear.

Differentiation is defined as

$$\partial_\alpha 1 = 0 \ , \ \partial_\alpha \alpha = 1 \tag{A.5}$$

as usual. Again, definitions of higher orders are unnecessary. Integration is defined the same way as differentiation

$$\int d\alpha 1 = 0 \ , \ \int d\alpha\, \alpha = 1 \tag{A.6}$$

which may be surprising to unfamiliar readers, but merely a matter of definition. Both differentiation and integration operators anticommute with Grassmann variables.

[1] In this appendix we shall stick to a common notation, where Grassmann variables are denoted by Greek letters and conventional numbers by Latin ones. The also common use of Greek letters as angles (e.g. $e^{i\theta}$) has made this convention impractical in the rest of the thesis.

Supermathematics

The name supermathematics refers to mathematics containing both Grassmann variables and conventional numbers. The main concern in this part is to ensure a consistent structure of our linear algebra. Consider a so-called supervector with the structure

$$\Psi = \begin{pmatrix} \vec{\xi} \\ \vec{A} \end{pmatrix}, \tag{A.7}$$

where $\vec{\xi}$ contains the Grassmann numbers of the vector and $\vec{A}$ the conventional ones. We want any supervector to retain this structure of separated commuting and anticommuting variables (remember that a pair of Grassmann numbers are a commuting variable). This requires supermatrices to have the structure

$$M = \begin{pmatrix} X & \sigma \\ \rho & Y \end{pmatrix} \tag{A.8}$$

where X, Y contain commuting variables and ρ, σ contain anticommuting ones. Notice that the cross-terms switch the type of number.

We want the mechanics of the supermatrices to be similar to conventional linear algebra. If we, for instance, want the trace to be cyclic, we must define our supertrace as

$$\mathrm{Str}(M) \equiv \mathrm{Tr}(X) - \mathrm{Tr}(Y). \tag{A.9}$$

The corresponding superdeterminant is often defined through the relation

$$\ln\left(\mathrm{Sdet}(M)\right) \equiv \mathrm{Str}\left(\ln(M)\right), \tag{A.10}$$

which means

$$\mathrm{Sdet}(M) = \det(X - \sigma Y^{-1}\rho)\det(Y^{-1}). \tag{A.11}$$

It should be noted that, although the motivation for the definition varies in the literature, the definition themselves are standard.

A.1 Gaussian Grassmann Integral

We use the rewriting of a Gaussian Grassmann integral as a determinant. We therefore briefly show the derivation of this. This may also be found in most textbooks on the subject.

Given an integral of the form

$$\int \prod_{ij}^{N} d\theta_i^* d\theta_j e^{-\theta_i^* A_{ij} \theta_j} \tag{A.12}$$

where θ, θ^* are Grassmann variables, we may write

$$\begin{aligned} \int \prod_{ij}^{N} d\theta_i^* d\theta_j e^{-\theta_i^* A_{ij} \theta_j} &= \int d\theta_1^* d\theta_1 ... d\theta_N^* d\theta_N \frac{1}{N!}(-\theta_{i_1}^* A_{i_1 j_1} \theta_{j_1}) ... (-\theta_{i_N}^* A_{i_N j_N} \theta_{j_N}) \\ &= \frac{1}{N!} \int d\theta_1^* ... d\theta_N^* \int d\theta_1 ... d\theta_N \theta_{i_1}^* .. \theta_{i_N}^* \theta_{j_1} ... \theta_{j_N} (-A_{i_1 j_1}) ... (-A_{i_N j_N}) \\ &= \frac{1}{N!} \int d\theta_1^* ... d\theta_N^* \theta_{i_1}^* ... \theta_{i_N}^* \int d\theta_1 ... d\theta_N \theta_{j_1} ... \theta_{j_N} A_{i_1 j_1} ... A_{i_N j_N} \end{aligned} \tag{A.13}$$

The sign in the second and third line is a little subtle. Rearrange the integrals and the variables on their own. This must give the same sign. If N is even (odd), the signs from the exponentials gives a plus (minus), and moving the θ^* through the $d\theta$ gives a plus (minus). So either way the overall sign is a plus.

Exchanging two indices i_n or j_n gives a sign. If any of the indices are the same, the integrals give 0. Otherwise they give 1 or -1. From this we can deduce that they are Levi-Civita symbols. So our Gaussian integral is

$$\begin{aligned} \int \prod_{ij}^{N} d\theta_i^* d\theta_j e^{-\theta_i^* A_{ij} \theta_j} &= \frac{1}{N!} \epsilon^{i_1 \ldots i_N} \epsilon^{j_1 \ldots j_N} A_{i_1 j_1} \ldots A_{i_N j_N} \\ &= \det(A) \end{aligned} \tag{A.14}$$

where we have used one of the definitions of the determinant.

We use this when analysing the eigenvalues of the Dirac operator. Given the partition function of QCD for a single topology

$$Z^\nu = \int_\nu D\bar{q} D q D A \exp\left\{ i \int d^4x \bar{q} (i \not{D} - m) q - \frac{1}{4} G^a_{\alpha\beta} G^a_{\alpha\beta} \right\} \tag{A.15}$$

we can integrate out the quark fields and get

$$Z^\nu = \int_\nu D A \det(i \not{D} - m) e^{S_{YM}} \tag{A.16}$$

where $S_{YM} = -i \int d^4x \frac{1}{4} G^a_{\alpha\beta} G^a_{\alpha\beta}$.

Appendix B

Various Calculation Tricks

B.1 Hubbard-Stratanovitch Transformation

The Hubbard-Stratanvitch transformation is the introduction of an auxiliary matrix to linearise an integral

$$e^{c^2\mathrm{Tr}(Q^2)} \sim \int d\sigma e^{-\mathrm{Tr}\frac{\sigma^2}{4c^2}+\mathrm{Tr}(Q\sigma)} \tag{B.1}$$

$$e^{-c^2\mathrm{Tr}(\bar{Q}^2)} \sim \int d\bar{\sigma} e^{-\mathrm{Tr}\frac{\bar{\sigma}^2}{4c^2}+i\mathrm{Tr}(\bar{Q}\bar{\sigma})}. \tag{B.2}$$

We ignore an overall constant when making this transformation. Notice that the Hubbard-Stratanovitch transformation is a Gaussian integral for matrices in reverse. The difficult part of the transformation is to determine the structure of the auxiliary matrix.

In Chapter 3, all transformation matrices are arbitrary real matrices [7].

When $Q \in \Sigma(2|2)$, we have [8]

$$\sigma = \mathrm{diag}(\mathbf{1}_2, \tilde{O}) \begin{pmatrix} iu & 0 & \eta^* & \chi^* \\ 0 & iu & -\eta & -\chi \\ \eta & \eta^* & v & 0 \\ \chi & \chi^* & 0 & w \end{pmatrix} \mathrm{diag}(\mathbf{1}_2, \tilde{O}^T) \tag{B.3}$$

where $\tilde{O} \in O(2)$ and $u, v, w \in \mathbb{R}$.

For $Q \in Gl(1|1)$, we may parametrise σ as

$$\sigma = \begin{pmatrix} a & \chi \\ \eta & ib \end{pmatrix} \tag{B.4}$$

where $a, b \in \mathbb{R}$. This can be realised by inserting Q and σ in (B.2) and performing the Grassmann integrals. The real parameters of σ then follow as ordinary Gaussian integrals.

B.2 Saddle Point Approximation

The saddle point approximation works as follows: Given an integral of the form[1]

$$I = \int_{-\infty}^{\infty} f(x) e^{-Ng(x)} dx \tag{B.5}$$

[1]This explanation of the saddle point approximation is based on [50], but alternatives can be found elsewhere.

we expand $g(x)$ to second order. If N is large, and if the second order derivative exists, the integral will be dominated by the maximum of $e^{-Ng(x)}$, because the function will decrease as $\frac{1}{\sqrt{N}}$ away from the maximum x_0.

Expanding $g(x)$ to quadratic order around the maximum, the contribution from $f(x)$ will disappear very quickly away from the maximum, so we may just expand it to constant order

$$I \approx f(x_0) \int_{-\infty}^{\infty} e^{-N(g(x_0)+\frac{g''(x_0)}{2}(x-x_0)^2)} dx = f(x_0) e^{-Ng(x_0)} \sqrt{\frac{2\pi}{g''(x_0)}}. \tag{B.6}$$

This is the saddle point approximation.

Appendix C

Various Calculations

C.1 Majorana Zero Modes in RMT

In Section 2.6, investigated the differences between high energy and solid state Majorana modes. Now we might ask the question: How to make the zero modes special? Let us revisit the differences between Dirac modes and Majorana modes and the conditions of the random matrix theory.

At the time of writing, this is not finished work, and we can therefore only sketch possible approaches to this. The main idea is to establish the properties of the eigenvectors associated with the zero modes.

Chiral Basis

This is the usual basis for chUE. Both conditions (2.65) are automatically satisfied by

$$i\not{D} = \begin{pmatrix} 0 & iW \\ iW^\dagger & 0 \end{pmatrix}, \tag{C.1}$$

with W being general matrices with complex entries. If we want to make Majorana zero modes, we require the Majorana eigenvectors to have the substructure of (2.85), corresponding to

$$\Psi = \begin{pmatrix} \psi_1 \\ \psi_2 \\ -{\psi_2}^* \\ {\psi_1}^* \end{pmatrix} \tag{C.2}$$

where ψ_1, ψ_2 are general column vectors with complex entries. Dirac modes can have any substructure.

Majorana Basis

One might also approach this in Majorana basis. Here it is less clear what the matrix should be if we require the conditions (2.65) to hold, but identification of the Majorana modes will be easier. Let us consider a matrix of the form

$$\begin{pmatrix} \tilde{A} & \tilde{W} \\ -\tilde{W}^\dagger & \tilde{B} \end{pmatrix} \tag{C.3}$$

with $\tilde{A}, \tilde{B}$ antisymmetric and all entries real. This satisfies both antihermicity and the condition that $i\not{D}$ must be real (Majorana basis).

If we require the anticommutation relation to hold, we must have

$$\begin{aligned} 0 &= \begin{pmatrix} -\sigma_2 & 0 \\ 0 & \sigma_2 \end{pmatrix} \begin{pmatrix} \tilde{A} & \tilde{W} \\ -\tilde{W}^\dagger & \tilde{B} \end{pmatrix} + \begin{pmatrix} \tilde{A} & \tilde{W} \\ -\tilde{W}^\dagger & \tilde{B} \end{pmatrix} \begin{pmatrix} -\sigma_2 & 0 \\ 0 & \sigma_2 \end{pmatrix} \\ &= \begin{pmatrix} -\sigma_2\tilde{A} & -\sigma_2\tilde{W} \\ -\sigma_2\tilde{W}^\dagger & \sigma_2\tilde{B} \end{pmatrix} + \begin{pmatrix} -\tilde{A}\sigma_2 & \sigma_2\tilde{W} \\ \tilde{W}^\dagger\sigma_2 & \tilde{B}\sigma_2 \end{pmatrix} \end{aligned} \tag{C.4}$$

with $\tilde{A}, \tilde{B}$ antihermitian.

This is equivalent to

$$\{\tilde{A}, \sigma_2\} = \{\tilde{B}, \sigma_2\} = [\tilde{W}, \sigma_2] = 0 \tag{C.5}$$

which requires the substructure

$$\tilde{W} = a \otimes \mathbf{1} + b \otimes i\sigma_2 \tag{C.6}$$

where a and b are general matrices with real entries acting in a subspace. We also find $\tilde{A} = \tilde{B} = 0$, because no antisymmetric matrix anticommutes with σ_2 (which makes the substructure irrelevant).

The structure of $\tilde{\not{D}}$ is more complicated than $\not{D}$, but the identification of Majorana modes is significantly simpler. Majorana modes are purely real, whereas Dirac modes are complex.

C.2 EFT of Flavour Coupling for Two-Flavour RMT

This result can also be obtained through random matrix theory. Consider the theory corresponding to 3.3:

$$Z^{n,\nu}_{chGUE,2} = \int dW \det \begin{pmatrix} m_R & iW & 0 & ic_R \\ iW^\dagger & m_R & ic_R & 0 \\ 0 & ic_R & m_R & iW \\ ic_R & 0 & iW^\dagger & m_R \end{pmatrix} e^{-n\mathrm{Tr}(WW^\dagger)} \tag{C.7}$$

where W are complex $(n+\nu) \times n$ matrices, and m_R, c_R are dimensionless parameters with implicit identity matrices of appropriate sizes padded with zeros where necessary. We express the determinant as fermionic integrals

$$\begin{aligned} Z^{n,\nu}_{chGUE,2} &= \int dW d\phi^1 d\phi^2 d\psi^1 d\psi^2 e^{-n\mathrm{Tr}(WW^\dagger)} \\ &\quad \times \exp\left\{ \begin{pmatrix} \psi^1 \\ \phi^1 \\ \psi^2 \\ \phi^2 \end{pmatrix}^\dagger \begin{pmatrix} m_R & iW & 0 & ic_R \\ iW^\dagger & m_R & ic_R & 0 \\ 0 & ic_R & m_R & iW \\ ic_R & 0 & iW^\dagger & m_R \end{pmatrix} \begin{pmatrix} \psi^1 \\ \phi^1 \\ \psi^2 \\ \phi^2 \end{pmatrix} \right\}. \end{aligned} \tag{C.8}$$

We write W_j as $a_j + ib_j$ and do the integrals over these.

$$
\begin{aligned}
Z^{n,\nu}_{chGUE,2} &= \int dadbd\phi^1 d\phi^2 d\psi^1 d\psi^2 \exp\Big\{ -n\left({a^2}_{ij} + {b^2}_{ij}\right) \\
&\quad +ia_{ij}(\psi_i^{1*}\phi_j^1 - \psi_i^1\phi_j^{1*} + \psi_i^{2*}\phi_j^2 - \psi_i^2\phi_j^{2*}) \\
&\quad -b_{ij}(\psi_i^{1*}\phi_j^1 + \psi_i^1\phi_j^{1*} + \psi_i^{2*}\phi_j^2 + \psi_i^2\phi_j^{2*}) \\
&\quad +m_R\big(\psi_i^{1*}\psi_i^1 + \phi_i^{1*}\phi_i^1 + \psi_i^{2*}\psi_i^2 + \phi_i^{2*}\phi_i^2\big) \\
&\quad +ic_R(\phi_i^{1*}\psi_i^2 + \psi_i^{1*}\phi_i^2 + \phi_i^{2*}\psi_i^1 + \psi_i^{2*}\phi_i^1)\Big\} \\
&= \int d\phi^1 d\phi^2 d\psi^1 d\psi^2 \exp\Big\{\frac{1}{n}\big(\psi_i^{1*}\psi_i^1\phi_j^{1*}\phi_j^1 + \psi_i^{2*}\psi_i^2\phi_j^{2*}\phi_j^2 \\
&\quad +\psi_i^{1*}\psi_i^2\phi_j^{2*}\phi_j^1 + \psi_i^{2*}\psi_i^1\phi_j^{1*}\phi_j^2\big) \\
&\quad +m_R\big(\psi_i^{1*}\psi_i^1 + \phi_i^{1*}\phi_i^1 + \psi_i^{2*}\psi_i^2 + \phi_i^{2*}\phi_i^2\big) \\
&\quad +ic_R(\phi_i^{1*}\psi_i^2 + \psi_i^{1*}\phi_i^2 + \phi_i^{2*}\psi_i^1 + \psi_i^{2*}\phi_i^1)\Big\} \\
&= \int d\phi^1 d\phi^2 d\psi^1 d\psi^2 \exp\Big\{\frac{1}{4n}\Big(\qquad\qquad (C.9) \\
&\quad (\psi_i^{1*}\psi_i^1 + \phi_i^{1*}\phi_i^1)(\psi_j^{1*}\psi_j^1 + \phi_j^{1*}\phi_j^1) - (\psi_i^{1*}\psi_i^1 - \phi_i^{1*}\phi_i^1)(\psi_j^{1*}\psi_j^1 - \phi_j^{1*}\phi_j^1) \\
&\quad +(\psi_i^{2*}\psi_i^2 + \phi_i^{2*}\phi_i^2)(\psi_j^{2*}\psi_j^2 + \phi_j^{2*}\phi_j^2) - (\psi_i^{2*}\psi_i^2 - \phi_i^{2*}\phi_i^2)(\psi_j^{2*}\psi_j^2 - \phi_j^{2*}\phi_j^2) \\
&\quad +2(\psi_i^{1*}\psi_i^2 + \phi_i^{1*}\phi_i^2)(\psi_j^{2*}\psi_j^1 + \phi_j^{2*}\phi_j^1) - 2(\psi_i^{1*}\psi_i^2 - \phi_i^{1*}\phi_i^2)(\psi_j^{2*}\psi_j^1 - \phi_j^{2*}\phi_j^1) \\
&\quad +m_R\big(\psi_i^{1*}\psi_i^1 + \phi_i^{1*}\phi_i^1 + \psi_i^{2*}\psi_i^2 + \phi_i^{2*}\phi_i^2\big) \\
&\quad +ic_R(\phi_i^{1*}\psi_i^2 + \psi_i^{1*}\phi_i^2 + \phi_i^{2*}\psi_i^1 + \psi_i^{2*}\phi_i^1)\Big)\Big\}.
\end{aligned}
$$

Again we must be careful about the length of the vector in the coupling term. We make four Hubbard-Stratanovitch transformations and get

$$
\begin{aligned}
Z^{n,\nu}_{chGUE,2} &= \int d\sigma_{ij} d\bar{\sigma}_{ij} d\phi^1 d\phi^2 d\psi^1 d\psi^2 \exp\Big\{ -n\mathrm{Tr}(\sigma_{ij}^2 + \bar{\sigma}_{ij}^2) \qquad (C.10) \\
&\quad +\sigma_{11}(\psi_i^{1*}\psi_i^1 + \phi_j^{1*}\phi_j^1) + i\bar{\sigma}_{11}(\psi_i^{1*}\psi_i^1 - \phi_j^{1*}\phi_j^1) \\
&\quad +\sigma_{22}(\psi_i^{2*}\psi_i^2 + \phi_j^{2*}\phi_j^2) + i\bar{\sigma}_{22}(\psi_i^{2*}\psi_i^2 - \phi_j^{2*}\phi_j^2) \\
&\quad +\sigma_{21}(\psi_i^{2*}\psi_i^1 + \phi_j^{2*}\phi_j^1) + i\bar{\sigma}_{21}(\psi_i^{2*}\psi_i^1 - \phi_j^{2*}\phi_j^1) \\
&\quad +\sigma_{12}(\psi_i^{1*}\psi_i^2 + \phi_j^{1*}\phi_j^2) + i\bar{\sigma}_{12}(\psi_i^{1*}\psi_i^2 - \phi_j^{1*}\phi_j^2) \\
&\quad +m_R\big(\psi_i^{1*}\psi_i^1 + \phi_i^{1*}\phi_i^1 + \psi_i^{2*}\psi_i^2 + \phi_i^{2*}\phi_i^2\big) \\
&\quad +ic_R(\phi_i^{1*}\psi_i^2 + \psi_i^{1*}\phi_i^2 + \phi_i^{2*}\psi_i^1 + \psi_i^{2*}\phi_i^1)\Big\},
\end{aligned}
$$

where σ are arbitrary real matrices [7]. Defining $A_{ij} = \sigma_{ij} + i\bar{\sigma}_{ij}$, $A^\dagger_{ij} = \sigma_{ij} - i\bar{\sigma}_{ij}$, and $M_R = \mathrm{diag}(m_R, m_R)$, we get

$$\begin{aligned} Z^{n,\nu}_{chGUE,2} &= \int dA d\phi^1 d\phi^2 d\psi^1 d\psi^2 \exp\Big\{ -n\mathrm{Tr}(AA^\dagger) \\ &\quad + \begin{pmatrix}\psi^1_i \\ \psi^2_i\end{pmatrix}^\dagger (A + M_R) \begin{pmatrix}\psi^1_i \\ \psi^2_i\end{pmatrix} + \begin{pmatrix}\phi^1_i \\ \phi^2_i\end{pmatrix}^\dagger (A^\dagger + M_R) \begin{pmatrix}\phi^1_i \\ \phi^2_i\end{pmatrix} \\ &\quad + ic_R \left(\begin{pmatrix}\psi^1_i \\ \psi^2_i\end{pmatrix}^\dagger \tau_1 \begin{pmatrix}\phi^1_i \\ \phi^2_i\end{pmatrix} + \begin{pmatrix}\phi^1_i \\ \phi^2_i\end{pmatrix}^\dagger \tau_1 \begin{pmatrix}\psi^1_i \\ \psi^2_i\end{pmatrix} \right) \Big\}. \end{aligned} \tag{C.11}$$

We first do the $n + \nu$ integrals over ψ^1 and ψ^2, and thereafter the n integrals over ϕ^1 and ϕ^2. Again the coupling part only has n integrals.

$$\begin{aligned} Z^{n,\nu}_{chGUE,2} &= \int dA d\phi^1 d\phi^2 \det{}^{n+\nu}(A + m_R) \exp\Big\{ -n\mathrm{Tr}(AA^\dagger) \\ &\quad + \begin{pmatrix}\phi^1_i \\ \phi^2_i\end{pmatrix}^\dagger (A^\dagger + M_R) \begin{pmatrix}\phi^1_i \\ \phi^2_i\end{pmatrix} + c_R^2 \begin{pmatrix}\phi^1_i \\ \phi^2_i\end{pmatrix}^\dagger \tau_1 (A + M_R)^{-1} \tau_1 \begin{pmatrix}\phi^1_i \\ \phi^2_i\end{pmatrix} \Big\} \\ &= \int dA \exp\Big\{ -n\mathrm{Tr}(AA^\dagger) \Big\} \det{}^{n+\nu}(A + M_R) \det{}^n\big(A^\dagger + M_R + c_R^2 \tau_1 (A + M_R)^{-1} \tau_1\big) \\ &= -\int dA \exp\Big\{ -n\mathrm{Tr}(AA^\dagger) \Big\} \det{}^{\nu}(A + M_R) \det{}^n\big((A + M_R)\tau_1 (A^\dagger + M_R) + c_R^2 \tau_1\big) \\ &= -\int dA \exp\Big\{ -n\mathrm{Tr}(AA^\dagger) \Big\} \det{}^{\nu}(A + M_R) \det{}^n\big(A\tau_1 A^\dagger + M_R A \tau_1 + M_R \tau_1 A^\dagger + c_R^2 \tau_1\big). \end{aligned} \tag{C.12}$$

where we have ignored terms of $\mathcal{O}(m_R^2)$. We have also multiplied by $1 = -\det(\tau_1)$ in the third line.

We diagonalise $A = U\Lambda V$. Using a saddle point approximation we find that the Gaussian term sets $\Lambda \propto \mathbf{1}$. The Gaussian term is dominant, since it is $\mathcal{O}(n)$, whereas all other terms are no higher than $\mathcal{O}(1)$. We then absorb V in U and multiply by $1 = \pm\det{}^n(U\tau_1 U^\dagger)$. We ignore the overall sign.

$$\begin{aligned} Z^{n,\nu}_{chGUE,2} &= \int dU \det{}^{\nu}(U + M) \det{}^n\big(U\tau_1 U^\dagger + M_R U \tau_1 + M_R \tau_1 U^\dagger + c_R^2 \tau_1\big) \det{}^n(U\tau_1 U^\dagger \tau) \\ &= \int dU \det{}^{\nu}(U + M_R) \det{}^n\big(1 + M_R U \tau_1 U \tau_1 U^\dagger + M_R U^\dagger + c_R^2 \tau_1 U \tau_1 U^\dagger\big) \\ &= \int dU \det{}^{\nu}(U + M_R) \exp\Big\{ n\mathrm{Tr}\big[\ln(1 + M_R U \tau_1 U \tau_1 U^\dagger + M_R U^\dagger + c_R^2 \tau_1 U \tau_1 U^\dagger)\big] \Big\}. \end{aligned} \tag{C.13}$$

We then expand the logarithm.

$$\begin{aligned} Z^{n,\nu}_{chGUE,2} &= \int dU \det{}^{\nu}(U + M_R) \exp\Big\{ n\mathrm{Tr}\big[M_R U \tau_1 U \tau_1 U^\dagger + M_R U^\dagger + c_R^2 \tau_1 U \tau_1 U^\dagger\big] \Big\} \\ &= \int dU \det{}^{\nu}(U + M_R) \exp\Big\{ n\mathrm{Tr}\big[M_R U + M_R U^\dagger + c_R^2 \tau_1 U \tau_1 U^\dagger\big] \Big\}. \end{aligned} \tag{C.14}$$

Letting $n \to \infty$ while keeping $m = 2nm_R$ and $c^2 = nc_R^2$ constant yields our final effective partition function.

$$Z^{\nu}_{chUE,2} = \int dU \det{}^{\nu}(U) \exp\left\{\frac{1}{2}\mathrm{Tr}\left[MU + MU^\dagger\right] + c^2 \mathrm{Tr}\left[\tau_1 U \tau_1 U^\dagger\right]\right\}. \tag{C.15}$$

C.3 Full Derivation of the Coupled chUE Partition Function

We start from the partition function

$$\begin{aligned} & Z^{\nu_1,\nu_2}_{chUE,1|1+1|1}(m,m',c) \\ = & \int_{Gl(1|1)} dU_1 dU_2 \ \mathrm{Sdet}^{\nu_1}(U_1)\ \mathrm{Sdet}^{\nu_2}(U_2) \\ & \times \exp\left\{\frac{1}{2}\mathrm{Str}\left[M^\dagger U_1 + M U_1^{-1} + M^\dagger U_2 + M U_2^{-1}\right] + c^2 \mathrm{Str}\left[U_1 U_2^{-1} + U_2 U_1^{-1}\right]\right\} \end{aligned} \tag{C.16}$$

where $M = \mathrm{diag}(m, m')$ and Str and Sdet are graded trace and determinant, and use the parametrisation [12]

$$U_j = \begin{pmatrix} e^{i\theta_j} & 0 \\ 0 & e^{s_j} \end{pmatrix} \exp\begin{pmatrix} 0 & \alpha_j \\ \beta_j & 0 \end{pmatrix} = \begin{pmatrix} e^{i\theta_j}(1+\frac{1}{2}\alpha_j\beta_j) & e^{i\theta_j}\alpha_j \\ e^{s_j}\beta_j & e^{s_j}(1-\frac{1}{2}\alpha_j\beta_j) \end{pmatrix} \tag{C.17}$$

and

$$U_j^{-1} = \begin{pmatrix} e^{-i\theta_j}(1+\frac{1}{2}\alpha_j\beta_j) & -e^{-i\theta_j}\alpha_j \\ e^{-s_j}\beta_j & e^{-s_j}(1-\frac{1}{2}\alpha_j\beta_j) \end{pmatrix}, \tag{C.18}$$

where α and β are Grassmann variables and the angular variable θ extends over $[-\pi : \pi]$, while $s \in [-\infty : \infty]$ is non-compact. The change of variables is calculated with the Berezinian (a generalisation of the Jacobian for supermatrices)[1]

$$\begin{aligned} dU_j &= |\mathrm{Sdet}(B_j)| d\theta_j ds_j d\beta_j d\alpha_j \ , \\ \mathrm{Sdet}(B_j) &= \mathrm{Sdet}\begin{pmatrix} \frac{\partial U_{j\,11}}{\partial s_j} & \frac{\partial U_{j\,11}}{\partial \theta_j} & \frac{\partial U_{j\,11}}{\partial \alpha_j} & \frac{\partial U_{j\,11}}{\partial \beta_j} \\ \frac{\partial U_{j\,22}}{\partial s_j} & \frac{\partial U_{j\,22}}{\partial \theta_j} & \frac{\partial U_{j\,22}}{\partial \alpha_j} & \frac{\partial U_{j\,22}}{\partial \beta_j} \\ \frac{\partial U_{j\,12}}{\partial s_j} & \frac{\partial U_{j\,12}}{\partial \theta_j} & \frac{\partial U_{j\,12}}{\partial \alpha_j} & \frac{\partial U_{j\,12}}{\partial \beta_j} \\ \frac{\partial U_{j\,21}}{\partial s_j} & \frac{\partial U_{j\,21}}{\partial \theta_j} & \frac{\partial U_{j\,21}}{\partial \alpha_j} & \frac{\partial U_{j\,21}}{\partial \beta} \end{pmatrix} \\ &= \mathrm{Sdet}\begin{pmatrix} 0 & i(1+\frac{1}{2}\alpha_j\beta_j)e^{i\theta_j} & \frac{1}{2}\beta_j e^{i\theta_j} & -\frac{1}{2}\alpha_j e^{i\theta_j} \\ (1-\frac{1}{2}\alpha_j\beta_j)e^{s_j} & 0 & -\frac{1}{2}\beta_j e^{s_j} & \frac{1}{2}\alpha_j e^{s_j} \\ 0 & i\alpha_j e^{i\theta_j} & e^{i\theta_j} & 0 \\ \beta_j e^{s_j} & 0 & 0 & e^{s_j} \end{pmatrix} \\ &= \det\left[\begin{pmatrix} 0 & i(1+\frac{1}{2}\alpha_j\beta_j)e^{i\theta_j} \\ (1-\frac{1}{2}\alpha_j\beta_j)e^{s_j} & 0 \end{pmatrix}\right. \\ &\quad \left. - \begin{pmatrix} -\frac{1}{2}\alpha_j e^{i\theta_j} & \frac{1}{2}\beta_j e^{i\theta_j} \\ \frac{1}{2}\alpha_j e^{s_j} & -\frac{1}{2}\beta_j e^{s_j} \end{pmatrix}\begin{pmatrix} e^{-i\theta_j} & 0 \\ 0 & e^{-s_j} \end{pmatrix}\begin{pmatrix} \beta_j e^{s_j} & 0 \\ 0 & i\alpha_j e^{i\theta_j} \end{pmatrix}\right] \det\left[\begin{pmatrix} e^{-i\theta_j} & 0 \\ 0 & e^{-s_j} \end{pmatrix}\right] \\ &= -i(1+\alpha_j\beta_j)e^{i\theta_j}(1-\alpha_j\beta_j)e^{s_j}e^{-i\theta_j}e^{-s_j} \\ &= -i. \end{aligned} \tag{C.19}$$

[1] This is also calculated in [12].

We calculate parts of (C.16) one at a time

$$\begin{aligned}
\mathrm{Sdet}^{\nu_j}(U_j) &= e^{\nu_j \,\mathrm{Str}(\ln(U_j))} \\
&= \exp\left\{\nu_j \,\mathrm{Str}\left(\ln\left(\begin{pmatrix} e^{i\theta_j} & 0 \\ 0 & e^{s_j}\end{pmatrix}\right) + \begin{pmatrix} 0 & \alpha_j \\ \beta_j & 0\end{pmatrix}\right)\right\} \\
&= e^{\nu_j(i\theta_j - s_j)} \qquad \text{(C.20)} \\
\frac{1}{2}\mathrm{Str}(MU_j + MU_j^{-1}) &= \frac{1}{2}\mathrm{Str}\left(\begin{pmatrix} m & 0 \\ 0 & m'\end{pmatrix}\begin{pmatrix} 2(1+\frac{1}{2}\alpha_j\beta_j)\cos(\theta_j) & \alpha_j(e^{i\theta_j} - e^{s_j}) \\ -\beta_j(e^{s_j} - e^{-i\theta_j}) & 2(1-\frac{1}{2}\alpha_j\beta_j)\cosh(s_j)\end{pmatrix}\right) \\
&= m(1+\frac{1}{2}\alpha_j\beta_j)\cos(\theta_j) - m'(1-\frac{1}{2}\alpha_j\beta_j)\cosh(s_j) \qquad \text{(C.21)} \\
c^2\mathrm{Str}\left(U_iU_j^{-1}\right) &= c^2\mathrm{Str}\left(\begin{pmatrix} e^{i\theta_i}(1+\frac{1}{2}\alpha_i\beta_i) & e^{i\theta_i}\alpha_i \\ e^{s_i}\beta_i & e^{s_i}(1-\frac{1}{2}\alpha_i\beta_i)\end{pmatrix}\right. \\
&\quad \left.\times\begin{pmatrix} e^{-i\theta_j}(1+\frac{1}{2}\alpha_j\beta_j) & -e^{-i\theta_j}\alpha_j \\ e^{-s_j}\beta_j & e^{-s_j}(1-\frac{1}{2}\alpha_j\beta_j)\end{pmatrix}\right) \\
&= c^2\Big(e^{i(\theta_i-\theta_j)}(1+\frac{1}{2}\alpha_i\beta_i)(1+\frac{1}{2}\alpha_j\beta_j) + e^{i\theta_i - s_j}\alpha_i\beta_j \qquad \text{(C.22)} \\
&\quad -e^{s_i-s_j}(1-\frac{1}{2}\alpha_i\beta_i)(1-\frac{1}{2}\alpha_j\beta_j) - e^{s_j-i\theta_i}\alpha_j\beta_i\Big).
\end{aligned}$$

Inserting this in (C.16), we find

$$\begin{aligned}
& Z^{\nu_1,\nu_2}_{chUE,1|1+1|1}(m,m',c) \\
= & \int ds_1 ds_2 d\theta_1 d\theta_2 d\alpha_1 d\alpha_2 d\beta_1 d\beta_2 \; e^{\nu_1(i\theta_1 - s_1)} \; e^{\nu_2(i\theta_2 - s_2)} \\
\times & \exp\Big\{m(1+\frac{1}{2}\alpha_1\beta_1)\cos(\theta_1) - m'(1-\frac{1}{2}\alpha_1\beta_1)\cosh(s_1) \qquad \text{(C.23)} \\
& + m(1+\frac{1}{2}\alpha_2\beta_2)\cos(\theta_2) - m'(1-\frac{1}{2}\alpha_2\beta_2)\cosh(s_2) \\
& + c^2\Big(2\cos(\theta_1-\theta_2)(1+\frac{1}{2}\alpha_1\beta_1)(1+\frac{1}{2}\alpha_2\beta_2) + e^{i\theta_1 - s_2}\alpha_1\beta_2 + e^{i\theta_2 - s_1}\alpha_2\beta_1 \\
& - 2\cosh(s_1-s_2)(1-\frac{1}{2}\alpha_1\beta_1)(1-\frac{1}{2}\alpha_2\beta_2) - e^{s_2 - i\theta_1}\alpha_2\beta_1 - e^{s_1 - i\theta_2}\alpha_1\beta_2\Big)\Big\}.
\end{aligned}$$

From here we expand the Grassmann part of the exponential. Only the terms that contain all four Grassmann variables survive

$$\begin{aligned}
& Z^{\nu_1,\nu_2}_{chUE,1|1+1|1}(m,m',c) \\
= & \frac{1}{(2\pi)^2}\int ds_1 ds_2 d\theta_1 d\theta_2 \, e^{\nu_1(i\theta_1 - s_1)} e^{\nu_2(i\theta_2 - s_2)} \qquad \text{(C.24)} \\
& \times \exp\Big[m\cos(\theta_1) + m\cos(\theta_2) - m'\cosh(s_1) - m'\cosh(s_2) + 2c^2(\cos(\theta_1-\theta_2) - \cosh(s_1-s_2))\Big] \\
& \times\Big(1/4(m\cos(\theta_1) + m'\cosh(s_1))(m\cos(\theta_2) + m'\cosh(s_2)) + c^2/2(\cos(\theta_1-\theta_2) - \cosh(s_1-s_2)) \\
& + c^2/2(\cos(\theta_1-\theta_2) + \cosh(s_1-s_2))(m\cos(\theta_1) + m\cos(\theta_2) + m'\cosh(s_1) + m'\cosh(s_2)) \\
& - c^4(\sin(\theta_1-\theta_2) + i\sinh(s_2-s_1))^2\Big),
\end{aligned}$$

where the prefactor comes from normalisation. Remember that it should be 1 for $m = m'$, which we check explicitly.

Differentiation with respect to m yields the chiral condensate

$$\begin{aligned}
&\Sigma^{\nu_1,\nu_2}_{chUE,1|1+1|1}(m,c)\\
=\;& \frac{1}{(2\pi)^2}\int ds_1 ds_2 d\theta_1 d\theta_2\, e^{\nu_1(i\theta_1-s_1)}e^{\nu_2(i\theta_2-s_2)} \qquad \text{(C.25)}\\
&\times\exp\Big[m_1\cos(\theta_1)+m_2\cos(\theta_2)-m_1\cosh(s_1)-m_2\cosh(s_2)+2c^2(\cos(\theta_1-\theta_2)-\cosh(s_1-s_2))\Big]\\
&\times\Big[1/4\cos(\theta_1)(m_2\cos(\theta_2)+m_2\cosh(s_2))+1/4(m_1\cos(\theta_1)+m_1\cosh(s_1))\cos(\theta_2)\\
&+(\cos(\theta_1)+\cos(\theta_2))\Big(1/4(m_1\cos(\theta_1)+m_1\cosh(s_1))(m_2\cos(\theta_2)+m_2\cosh(s_2))\\
&\quad+c^2\cos(\theta_1-\theta_2)\\
&\quad+c^2/2(\cos(\theta_1-\theta_2)+\cosh(s_1-s_2))(m_1\cos(\theta_1)+m_2\cos(\theta_2)+m_1\cosh(s_1)+m_2\cosh(s_2))\\
&\quad-c^4(\sin(\theta_1-\theta_2)+i\sinh(s_2-s_1))^2\Big)\Big].
\end{aligned}$$

From here we show the issues that arise when trying to evaluate the spectral density.

Numerical Evaluation of Spectral Density

The integrand of Equation (C.25) is highly oscillating along the imaginary axis, and we therefore require numerical regularisation

$$\Re(\Sigma^{\nu_1,\nu_2}_{chUE,1|1+1|1}(i\lambda,c))\to\lim_{\epsilon\to 0}\Re(\Sigma^{\nu_1,\nu_2}_{chUE,1|1+1|1}(i\lambda+\epsilon,c)), \qquad \text{(C.26)}$$

where $\epsilon\to 0$ is a numerical limit rather than an analytical one. The smaller ϵ, the smaller the discrepancy until a certain point. By fitting a curve to the points in the reliable regime, we may deduce the value in $\epsilon=0$. However, this value fluctuates heavily with the cut-off of the fit even with the cut-off in the reliable regime. This is why the limiting cases are considered.

C.4 Different Cases of ν_1 and ν_2

For $\nu_1,\nu_2<0$ we have:

$$\begin{aligned}
Z^{\nu_1,\nu_2}_{chUE,1|1+1|1}(M) &= \int_{Gl(1|1)} dA\exp\Big[-\mathrm{Str}\Big(\frac{AA^\dagger}{4c^2}\Big)\Big]\mathrm{Sdet}^{-\nu_1-\nu_2}(M^\dagger+A)\\
&\quad\times Z^{(\nu_1),nz}_{chUE}([M+A^\dagger][M^\dagger+A])Z^{(\nu_2),nz}_{chUE}([M+A^\dagger][M^\dagger+A]) \qquad \text{(C.27)}
\end{aligned}$$

which for $c\ll 1$ becomes

$$\begin{aligned}
Z^{\nu_1,\nu_2}_{chUE,1|1+1|1}(M) &= \int_{Gl(1|1)} dA\exp\Big[-\mathrm{Str}\Big(\frac{AA^\dagger}{4c^2}\Big)\Big]\mathrm{Sdet}^{-\nu_1-\nu_2}(M^\dagger+A)\\
&\quad\times Z^{(\nu_1),nz}_{chUE}(MM^\dagger)Z^{(\nu_2),nz}_{chUE}(MM^\dagger) \qquad \text{(C.28)}
\end{aligned}$$

Since $\nu_1+\nu_2<0$, we can again directly identify $n=0$ and $\nu=\nu_1+\nu_2$ from equation (2.67).

For $\nu_1 \geq 0$ and $\nu_2 < 0$ we have:

$$\begin{aligned} Z^{\nu_1,\nu_2}_{chUE,1|1+1|1}(M) &= \int_{Gl(1|1)} dA \exp\Big[-\mathrm{Str}\Big(\frac{AA^\dagger}{4c^2}\Big)\Big] \mathrm{Sdet}^{\nu_1}(M+A^\dagger)\mathrm{Sdet}^{-\nu_2}(M^\dagger+A) \\ &\times Z^{(\nu_1),nz}_{chUE}([M+A^\dagger][M^\dagger+A]) Z^{(\nu_2),nz}_{chUE}([M+A^\dagger][M^\dagger+A]) \end{aligned} \tag{C.29}$$

which for $c \ll 1$ becomes

$$\begin{aligned} Z^{\nu_1,\nu_2}_{chUE,1|1+1|1}(M) &= \int_{Gl(1|1)} dA \exp\Big[-\mathrm{Str}\Big(\frac{AA^\dagger}{4c^2}\Big)\Big] \mathrm{Sdet}^{\nu_1}(M+A^\dagger)\mathrm{Sdet}^{-\nu_2}(M^\dagger+A) \\ &\times Z^{(\nu_1),nz}_{chUE}(MM^\dagger) Z^{(\nu_2),nz}_{chUE}(MM^\dagger) \end{aligned} \tag{C.30}$$

Assuming $\nu_1 + \nu_2 \geq 0$:
We compare this to equation (2.67) and find $n = -\nu_2$ and $n + \nu = \nu_1$, which is consistent with $n' = \frac{|\nu_1|+|\nu_2|-|\nu_1+\nu_2|}{2}$.

Assuming $\nu_1 + \nu_2 < 0$:
We compare this to equation (2.67) and find $n = \nu_1$ and $n - \nu = -\nu_2$, which is also consistent with $n' = \frac{|\nu_1|+|\nu_2|-|\nu_1+\nu_2|}{2}$.

We can let $\nu_1 \leftrightarrow \nu_2$ and repeat the arguments.

C.5 Special Cases of Eigenvalue Spectrum for Quenched chGOE

In all cases the eigenvalue spectrum is

$$\rho(\lambda_R) = \sum_k \langle \delta(\lambda_R - \lambda_k) \rangle \tag{C.31}$$

where λ_k are the eigenvalues of our system, which all appear along the imaginary axis.

For $n = 1$ and $\nu = 0$

The special case $n = 1$ and $\nu = 0$ has matrices of the form

$$\begin{pmatrix} 0 & ix \\ ix & 0 \end{pmatrix} \tag{C.32}$$

for $m_R = 0$, making the eigenvalues

$$i\lambda_\pm = \pm ix. \tag{C.33}$$

The quenched partition function is

$$Z^{n=1,\nu=0}_{chGOE,2|2}(m_R) = \frac{1}{\sigma\sqrt{2\pi}} \int dx \; e^{-\frac{x^2}{2\sigma^2}} \tag{C.34}$$

which makes the quenched spectrum

$$\begin{aligned} \rho(\lambda_R) &= \frac{1}{\sigma\sqrt{2\pi}} \int dx \, [\delta(\lambda_R + x) + \delta(\lambda_R - x)] \, e^{-\frac{x^2}{2\sigma^2}} \\ &= \frac{2}{\sigma\sqrt{2\pi}} e^{-\frac{\lambda_R^2}{2\sigma^2}}. \end{aligned} \tag{C.35}$$

For $n = 1$ and $\nu = 1$

The special case $n = 1$ and $\nu = 1$ has matrices of the form

$$\begin{pmatrix} 0 & 0 & ix \\ 0 & 0 & iy \\ ix & iy & 0 \end{pmatrix} \tag{C.36}$$

for $m_R = 0$, making the eigenvalues

$$\lambda_0 = 0 \quad , \quad i\lambda_\pm = \pm i\sqrt{x^2 + y^2} \tag{C.37}$$

The quenched partition function is

$$Z^{n=1,\nu=1}_{chGOE,2|2}(m_R) \;=\; \frac{1}{2\pi\sigma}\int dxdy\; e^{-\frac{x^2+y^2}{2\sigma^2}} \tag{C.38}$$

which makes the quenched spectrum

$$\rho(\lambda_R) \;=\; \delta(\lambda_R) + \frac{1}{2\pi\sigma^2}\int dxdy\left[\delta(\lambda_R + \sqrt{x^2+y^2}) + \delta(\lambda_R - \sqrt{x^2+y^2})\right] e^{-\frac{x^2+y^2}{2\sigma^2}} \tag{C.39}$$

We switch to polar coordinates $r = \sqrt{x^2+y^2}$ and $\theta = \arctan\left(\frac{y}{x}\right)$ with the Jacobian r. The angular integral gives 2π, and we arrive at

$$\begin{aligned} \rho(\lambda_R) \;&=\; \frac{1}{\sigma^2}\int dr\;\; r\left[\delta(\lambda_R + r) + \delta(\lambda_R - r)\right] e^{-\frac{r^2}{2\sigma^2}} \\ &=\; \frac{2}{\sigma^2}\lambda_R e^{-\frac{\lambda_R^2}{2\sigma^2}}. \end{aligned} \tag{C.40}$$

Appendix D

Statistical Test of Numerics versus Theoretical Distribution

In this appendix, we make proper statistical comparisons between the numerical and analytical curves. They are in obvious visual agreement in Chapter 6, so this should just be considered a jovial addition for the single chUE ensemble to underline the comparison. We perform this analysis for $n = 40$ and 10^5 matrices. For an introduction to the statistical tests used here, we recommend [51].

χ^2 Calculation

To estimate the error on the numerical results, we assume the numerical distribution to be a continuous one and fit a third degree polynomial to a small section of it, see Figure D.1. The root mean square error of the fit is used to estimate the χ^2 error of the analytical curve, see Figure D.2. We find the reduced χ^2 to be

$$\chi^2_{red} \quad = \quad 0.54. \tag{D.1}$$

The reduced χ^2 should be around 1, which means the numerical and analytical distributions are in very good agreement (or that we have overestimated our errors).

Kolmogorov-Smirnov Test

The Kolmogorow-Smirnow test is estimation of how much two cumulative distributions differ. We use standard statistical packages from Matlab to calculate the associated probability that the two curves are the same. We find the probability of the numerical and analytical distributions being the same to be 79.3%. This is lower than we would have expected, given that the cumulative curves are indistinguishable when plotted together, but is still good agreement.

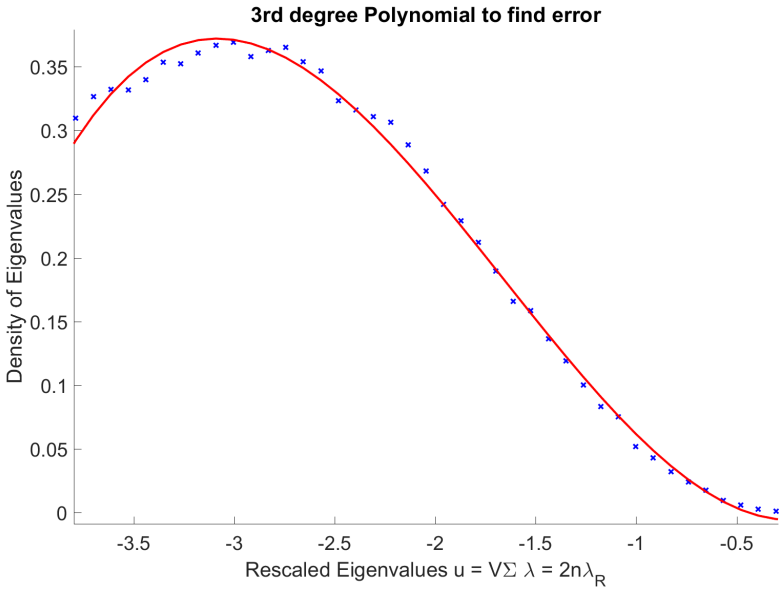

Figure D.1: Estimation of the numerical error by polynomial fit of small section. Plotted is a small section of the eigenvalue density of a single chUE for $n = 40$ and $\nu = 1$. We find the error to be ± 0.0081.

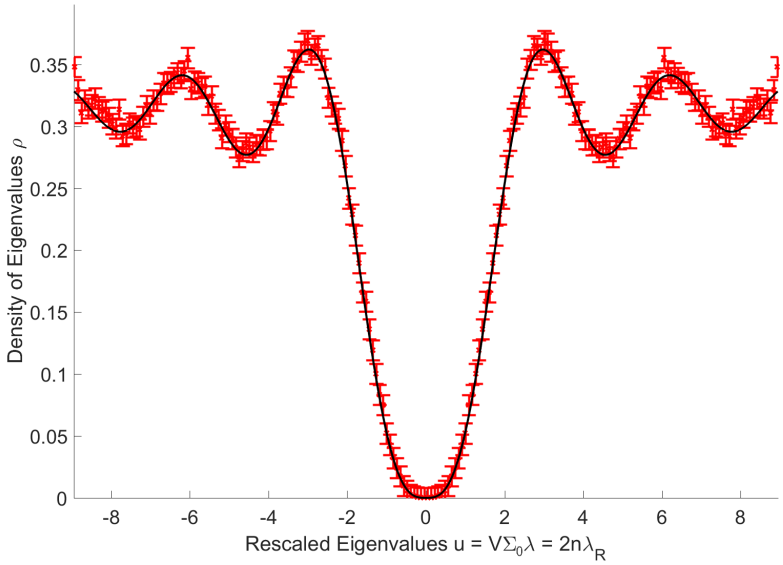

Figure D.2: Eigenvalue density of random matrix simulation for single chUE with $n = 40$ and $\nu = 1$ plotted with estimated error bars. Plotted on top is the analytical distribution. We see that it is well within the errors bars, which suggests that we may have overestimated our uncertainties. However, we still find $\chi^2_{red} = 0.54$, which is good agreement.